REPUBLIC OF TÜRKİYE

ALTINBAŞ UNIVERSITY

Institute of Graduate Studies

Mechanical Engineering

MODELING AND SIMULATING AIRCRAFT TAKEOFF PERFORMANCE ON AIRCRAFT CARRIERS

Mihriban Miraç YILMAZ

Master's Thesis

Supervisor

Asst. Prof. Dr. Yaser ALAIWI

İstanbul, 2024

MODELING AND SIMULATING AIRCRAFT TAKEOFF PERFORMANCE ON AIRCRAFT CARRIERS

Mihriban Miraç YILMAZ

Mechanical Engineering

Master’s Thesis

ALTINBAŞ UNIVERSITY

2024

The thesis titled MODELING AND SIMULATING AIRCRAFT TAKE-OFF PERFORMANCE ON AIRCRAFT CARRIERS prepared by MİRAÇ YILMAZ and submitted on 04.06.2024 has been **by majority of votes** for the degree of Master of Science in Mechanical Engineering.

Dr. Öğr. Üyesi Yaser ALAIWI

Supervisor

Thesis Defense Committee Members:

Dr. Öğr. Üyesi Yaser ALAIWI	Department of Mechanical Engineering Altınbaş University	_____
Dr. Öğr. Üyesi Serdar AY	Department of Mechanical Engineering Altınbaş University	_____
Dr. Öğr. Üyesi Haydar İzzettin KEPEKÇİ	Department of Mechatronics Engineering İstanbul Gelişim University	_____

I hereby declare that this thesis/dissertation meets all format and submission requirements for a (Master's) thesis.

I hereby declare that all information/data presented in this graduation project has been obtained in full accordance with academic rules and ethical conduct. I also declare all unoriginal materials and conclusions have been cited in the text and all references mentioned in the Reference List have been cited in the text, and vice versa as required by the abovementioned rules and conduct.

Miraç YILMAZ

Signature

DEDICATION

I would like to express my gratitude to the many individuals who have guided, supported, and encouraged me throughout this thesis. First and foremost, I extend my sincere thanks to my thesis advisor, Dr. Yaser ALAIWI, for his invaluable guidance and vision in every meeting we had.

I would also like to extend my thanks to Assoc. Prof. Dr. Süleyman BAŞTÜRK, the Head of the Department of Mechanical Engineering, for his guidance and support throughout my academic journey.

I would also like to thank my fiancee, who helped me at every stage of writing my thesis. Furthermore, the love and faith of my parents and sisters and brother, who have always been by my side in overcoming the challenges encountered while writing the thesis, have made this process even more meaningful. Therefore, I sincerely thank them for their support and for always being there for me.

PREFACE

This thesis is the culmination of the work conducted as a graduate student in the Department of Mechanical Engineering at Altınbaş University. The focus of this thesis is on the ground effect during the take-off of aircraft launched from aircraft carriers.

In order to understand and analyse the effects of wind speed and ship speed on the take-off process, a model was developed using MATLAB Simulink, and this topic was examined in detail. This study aims to comprehend the aerodynamic and physical challenges faced by aircraft during take-off from aircraft carriers and to provide valuable insights for future aircraft carrier designs and operations.

ABSTRACT

MODELING AND SIMULATING AIRCRAFT TAKEOFF PERFORMANCE ON AIRCRAFT CARRIERS

YILMAZ, Miraç

M.Sc. Mechanical Engineering, Altınbaş University,

Supervisor: Asst. Prof. Dr. Yaser ALAIWI

Date: 06/2024

Pages: 119

Aircraft carriers are strategically significant military platforms in today's world and constitute crucial elements that bolster the strength of naval forces. They provide maritime mobility, enabling the execution of various missions, particularly playing critical roles in tasks such as air defense, sea control, attack operations, and humanitarian aid. Aircraft carriers contribute to the achievement of strategic objectives such as ensuring air superiority and controlling maritime regions.

Catapult systems, a significant component of aircraft carriers, are utilized to accelerate the takeoff of aircraft and ensure their safe ascent from the vessel. These systems facilitate operational flexibility and efficiency by enabling aircraft to accelerate and take off over short distances. Catapult systems enhance the operational capacity of aircraft carriers by enabling aircraft to take off with heavier loads and over shorter distances.

In line with this, within the scope of the thesis, suitable aerial vehicles for aircraft carriers have been modelled using MATLAB Simulink, and the accuracy of theoretical information has been observed. This research represents an important step in understanding the effects of catapult systems, a critical aspect of aircraft carriers, and aims to provide valuable contributions to future aircraft carrier designs.

Keywords: Aircraft Carriers, Catapult System, MATLAB, Modelling, CFD.

ÖZET

UÇAK GEMİLERİNDE UÇAK KALKIŞ PERFORMANSININ MODELLENMESI VE SİMÜLASYONU

YILMAZ, Miraç

M.Sc. Makine Mühendisliği, Altınbaş Üniversitesi,

Tez Danışmanı: Dr. Öğr. Üyesi Yaser ALAIWI

Tarih: 06/2024

Sayfa Sayısı: 119

Günümüz dünyasında uçak gemileri stratejik olarak önemli askeri platformlardır ve deniz kuvvetlerinin gücünü artıran kritik unsurlar arasında yer alır. Deniz hareketliliği sağlarlar ve özellikle hava savunması, deniz kontrolü, saldırı operasyonları ve insani yardım gibi çeşitli görevlerin icrasında önemli roller üstlenirler. Uçak gemileri, hava üstünlüğünün sağlanması ve deniz bölgelerinin kontrolü gibi stratejik hedeflerin gerçekleştirilmesine katkıda bulunur.

Mancınık sistemleri, uçakların daha ağır yüklerle ve daha kısa mesafelerden kalkış yapabilmesini sağlayarak uçak gemilerinin operasyonel kapasitesini artırır ve gemiden güvenli bir şekilde havalanmalarını sağlamak için kullanılır. Bu sistemler, uçakların kısa mesafelerde hızlanarak kalkış yapmalarına olanak tanıyarak operasyonel esneklik ve verimlilik sağlar.

Bu doğrultuda, tez kapsamında uçak gemileri için uygun hava araçları MATLAB Simulink kullanılarak modellenmiş ve teorik bilgilerin doğruluğu gözlemlenmiştir. Bu araştırma, uçak gemilerinin kritik bir yönü olan mancınık sistemlerinin etkilerini anlamada önemli bir adımı temsil etmekte olup, gelecekteki uçak gemisi tasarımlarına değerli katkılar sağlamayı amaçlamaktadır.

Anahtar Kelimeler: Uçak Gemileri, Mancınık Sistemi, MATLAB, Modelleme, CFD.

TABLE OF CONTENTS

Pages

LIST OF TABLES

Pages

LIST OF FIGURES

Pages

ABBREVIATIONS

CATOBAR	:	Catapult Assisted Take-Off Barrier Arrested Recovery
CFD	:	Computational Fluid Dynamics
Cl	:	Lift Coefficient
EGPWS	:	Enhanced Ground Proximity Warning System
EM	:	Electromagnetic
EMALS	:	Electromagnetic Aircraft Launch System
EPR	:	Engine Pressure Ratio
GPWS	:	Ground Proximity Warning System
LCA	:	Light Combat Aircraft
MATLAB	:	Matrix Laboratory
STOBAR	:	Short Take-Off Barrier Assisted Recovery
STOVL	:	Short Take-Off Vertical Landing
TCAS	:	Traffic Alert and Collision Avoidance System
TOW	:	Takeoff weight
VTOL	:	Vertical Take-Off and Landing

LIST OF SYMBOLS

a	:	Acceleration Vector
b	:	Span
c_D	:	Air Foil Drag Coefficient
c_L	:	Air Foil Lift Coefficient
C_D	:	Drag Coefficient
C_L	:	Lift Coefficient
D	:	Drag
e	:	Oswald's Efficiency Factor
g	:	Acceleration Of Gravity
F	:	Force
h	:	Altitude Above Sea Level
L	:	Lift
m	:	Mass
M	:	Molar Mass
R_0	:	Specific Gas Constant for Air.
p	:	Atmospheric Pressure
ρ_0	:	Density Of Air at Sea Level.
S	:	Wing Area
T_0	:	Temperature At Sea Level

V : Velocity

W : Weight

1. INTRODUCTION

1.1 PURPOSE OF THIS RESEARCH

This thesis aims to investigate the phenomenon of ground effect during aircraft take offs on aircraft carriers. Specifically, it will conduct detailed analyses of the effects of ground effect on the take-off of the light combat aircraft (LCA) under different speeds and catapult lengths when taking off from an aircraft carrier.

This study endeavors to contribute to a better understanding of ground effect, which is a critical element in the safety and efficiency of aircraft carrier operations. The findings may have a significant impact on future aircraft carrier design and operational strategies, while also providing valuable insights to enhance the operational capabilities. This thesis aims to contribute to the body of knowledge in military aviation by offering design recommendations and engineering solutions for optimizing ground effect in aircraft carrier take offs.

1.2 GENERAL INFORMATION ABOUT AIRPLANES

An airplane is a powered air vehicle and aircraft that can stay aloft and ascend in the air by creating a pressure difference between the upper and lower surfaces of wing-profiled components, primarily the wings, thanks to the airflow [1], [2]. Airplanes operate based on aerodynamic principles. They generate lift by creating low pressure on the upper surface of the wings and high pressure on the lower surface. Many types of aircraft, whether powered by piston engines or jet engines and featuring fixed wings, belong to the category of airplanes. In today's context, the fundamental airplane types are known as passenger aircraft, fighter aircraft, and cargo aircraft, with specialized aircraft customized for various geographic conditions also existing.

Passenger Aircraft: These are aircraft used for transporting passengers and are typically employed by commercial airlines.
Cargo Aircraft: These planes are used for carrying cargo and freight and play a significant role in commerce and logistics.

Military Aircraft: They are used for defense purposes. Various types fall under this category, including fighter aircraft, bomber aircraft, and transport aircraft.

Private Aircraft: These are aircraft used for individual purposes, such as personal use or business jets.

The main components of an aircraft are the wings, which provide lift to keep it airborne, the tail that stabilizes the wings, flight controls that alter the aircraft's attitude and position, and the propulsion system, including the aircraft's engines and propellers, which provide the necessary thrust [3]. The fuselage houses passengers and cargo, while the cockpit accommodates the flight crew and flight systems.

1.2.1 Parts of the Aircraft and Their Functions

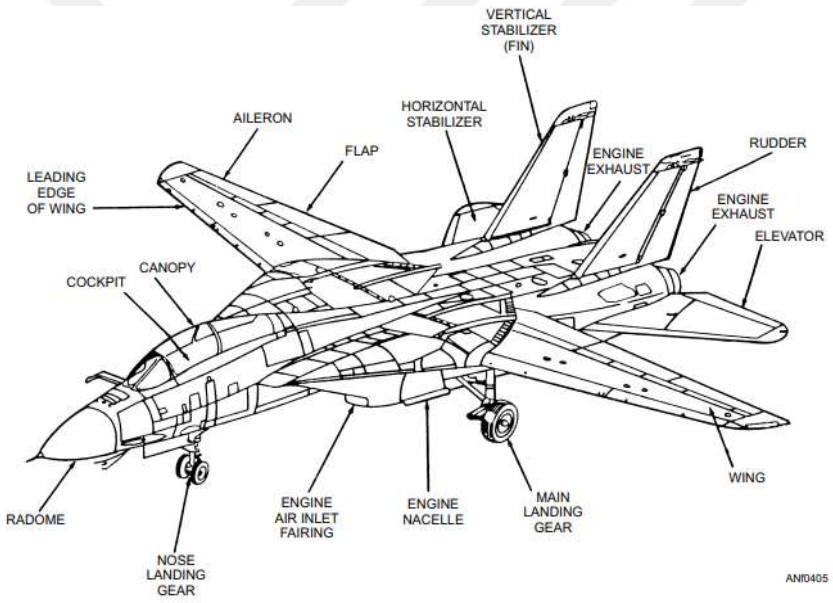

Figure 1.1: Principal Structural Units on an F-14 Aircraft [1].

1.2.1.1 Fuselage

The fuselage is the main structure of an aircraft, typically cylindrical in shape, that houses the crew, passengers, cargo, and other essential components of the aircraft. It is essentially the body of the aircraft and serves as the central structure to which the wings, tail assembly, and engines are attached. The fuselage plays a crucial role in aerodynamics, structural integrity, and overall performance of the aircraft. It is usually designed to be streamlined to reduce drag and optimize flight efficiency.

1.2.1.2 Engine

The primary role of the engine in an aircraft is to generate power to propel the aircraft forward. For an aircraft to maintain straight and level flight, it requires thrust equal and opposite to the drag force acting on it. This thrust, or thrust force, is provided by an appropriate type of aircraft propulsion engine. This thrust force enables the aircraft to progress through the air and move in the desired speeds and directions. Additionally, engines typically also power the aircraft's electrical and hydraulic systems. Aircraft engines typically burn fuel, converting it into energy to propel the aircraft [2].

1.2.1.3 Radome

A radome serves as a protective covering or structure for an antenna, shielding it from the elements of its surroundings [3]. The radar antenna located at the aircraft's nose serves two primary functions: detecting precipitation for weather radar and operating the Ground Proximity Warning System (GPWS). Notable advancements in aviation technology include Traffic Alert and Collision Avoidance System (TCAS) for tracking nearby aircraft, Enhanced Ground Proximity Warning System (EGPWS) for terrain and obstacle awareness, satellite-based navigation systems for precise runway localization, real-time air-ground messaging systems, and cockpit camera systems for monitoring wings and landing gear [4].

1.2.1.4 Cockpit

The cockpit, also known as the Flight Deck, is the area where pilots are seated. It houses the flight controls responsible for manoeuvring the aircraft, along with the array of buttons and switches necessary for operating its systems [5].

1.2.1.5 Canopy

Canopies, transparent components in aircraft, are used to enclose the cockpit and provide visibility and protection to the pilot. Canopies can be produced in various sizes, shapes, or functionalities [6], [7]. For instance, canopies can be hinged or removable for rapid entry and exit by the pilot [8]. They are preferred especially in aerobatic and fighter aircraft for isolating noise and meteorological effects, enhancing visibility, and reducing friction. They began to be widely used particularly after World War II.

1.2.1.6 Ailerons

Ailerons constitute essential control surfaces within the wing structure of an aircraft. They are movable segments typically attached to the aileron spar or rear wing spar and are activated either by lateral movement of the control stick or by turning the wheel on the yoke [9]. Positioned at the trailing edge of the wing, typically one on each side, they operate in opposition to each other: as one is raised, the other lowers. For example, during a left turn initiation, the left aileron rises to reduce lift, while the right aileron descends to increase lift, causing the aircraft to bank left and execute the turn. This mechanism remains fundamental in steering fixed-wing aircraft [5].

1.2.1.7 Flaps

Trailing-edge flaps, including plain flaps like ailerons and elevators, cover the rear portion of the wing [10]. These flaps adjust their position by moving up or down to alter the wing's camber, thereby influencing lift [11]. Wing flaps are used to provide extra lift to the aircraft. By reducing the landing speed, they shorten the landing distance, which facilitates landing in small or obstructed areas by allowing an increase in the glide angle without the need for a significant increase in approach speed. Moreover, deploying flaps during take-off decreases the required take-off distance [9]. It's not surprising that increasing the size of flaps has been demonstrated to result in greater alterations in lift [12].

1.2.1.8 Wing

The wing is primarily responsible for generating the majority of the lift needed for aircraft flight. Its design is tailored specifically to the aircraft it serves. In many aircraft, the interior space of the wing is utilized for storing the fuel necessary to operate the engines [10].

1.2.1.9 Winglet

Certain aircraft wings incorporate an extra feature known as a winglet, situated at the wing's extremity. Its function is to diminish the drag encountered as the wing moves through the air. Consequently, this enables the aircraft to achieve higher speeds and consume less fuel, thereby extending its range between refuelling stops [5].

1.2.1.10 Rudder

The rudder is responsible for controlling the aircraft's movement along its vertical axis, known as yaw. Its operation is managed by the left and right rudder pedals. When the rudder is angled into the airflow, it generates a horizontal force in the opposite direction. Depressing the left pedal, for instance, causes the rudder to move left, altering the airflow around the vertical stabilizer/rudder and producing a lateral lift that shifts the tail to the right, resulting in a leftward yaw of the aircraft's nose. In propeller-driven aircraft, the slipstream passing over the rudder enhances its effectiveness [13].

1.2.1.11 Elevator

The fundamental principle of the elevator is to change the pitching moment of the horizontal tail. Due to the deflection of the elevator up or down, the lift coefficient (Cl) of the horizontal tail will decrease or increase, respectively. Therefore, the two main objectives of the elevator are longitudinal control and longitudinal trim [14].

1.2.1.12 Stabilizer

An aircraft's stabilizing surfaces consist of vertical and horizontal wing profiles. These are called vertical stabilizer (or fin) and horizontal stabilizer. These two wing profiles, along with the rudder and elevator, form the tail section [1].

The horizontal stabilizer functions as an inverted wing, serving to apply downward thrust on the tail. Historically, aircraft have tended toward a nose-heavy layout, necessitating this downward force to maintain alignment with the remainder of the aircraft. Conversely, the vertical stabilizer is engineered to stabilize the lateral movement of the aircraft [9].

1.2.2 Flight Principles

Bernoulli's Principle: As the air accelerates over the top surface of the wings, the pressure decreases, causing the aircraft to lift.
Thrust: Engines create thrust to propel the aircraft forward.
Weight and Altitude: The aircraft counteracts the force of gravity due to its mass and velocity.

1.3 WHAT IS AN AIRCRAFT CARRIER?

An aircraft carrier is a type of warship whose primary mission is to deploy and recover aircraft, serving as a floating airbase at sea. Aircraft carriers are typically considered the flagship of a fleet [15]. Aircraft carriers are typically ships that are larger, faster, and more maneuverable compared to large, heavily armored battleships. An aircraft carrier is the largest and most complex of all warships [16]. Aircraft carriers come in a wide range of sizes, costs, and capabilities [17]. Its construction is extremely expensive, and its protection is paramount [15].

Throughout history, it has been proven that the technological advancements, new tactical capabilities, and versatility developed by aircraft carriers have changed the face of warfare and contributed to wartime situations [18]. With their capabilities, aircraft carriers have been the most powerful military and political tools for a century since 1918. The purpose of aircraft carriers is to enable the overseas deployment of aircraft operations without the need for a domestic airbase to control and organize them. In addition to providing air support, aircraft carriers also serve as naval forces [19].

Aircraft carriers are designed as platforms to deploy aircraft that can detect the enemy fleet's position before it reaches the horizon, thus allowing for maneuvering the carrier and its own battle line to the best advantage. The carrier will move to position its fleet's battle line between itself and the enemy and cannot be exposed to risk without its own substantial defense. Thus, aircraft carriers have become nests for combat aircraft that can fulfill the roles of scouts, engage in combat against enemy fleets, and achieve air superiority [16]. Additionally, aircraft carriers can be utilized in peacetime missions such as humanitarian aid operations [20]. Speed holds immense importance for aircraft carriers as they require swift deployment to various global locations and must possess the agility to avoid detection and targeting by hostile forces. These vessels boast speeds of up to 31 knots. Historically, prior to the advent of arrester gear and "accelerators," such high speeds were indispensable for aircraft carriers. This was necessary because, in calm or light wind conditions, they had to travel swiftly enough to generate the requisite wind speed over the deck for launching and recovering aircraft [21].

One advantage of aircraft carriers is their ability to sail in international waters due to their vast range of vision, thus avoiding interference with any territorial sovereignty. As a result, this obviates the necessity of securing overflight clearances from external nations, diminishes flight durations and transit distances for aircraft, and notably prolongs the duration spent within the operational theater [18].

1.4 WHAT IS A CATAPULT SYSTEM?

The catapult, or trebuchet, is a simple war machine used to hurl projectiles over long distances. It served as a fundamental siege engine, particularly during the Ancient and Medieval periods [22]. Initially developed as a large bowl, the catapult was employed to launch massive arrows at enemies. Throughout history, it has been utilized for military purposes, notably in castle sieges and naval warfare. Despite significant variations from its historical predecessors, the catapult continues to find utility in contemporary contexts [23].

The catapult system, commonly employed for accelerating the take-off of aircraft carriers and certain military aircraft, plays a pivotal role in sea-based air operations, augmenting the strategic importance of modern warships. Its primary objective is to facilitate aircraft in achieving faster take-off speeds over shorter distances. By providing the necessary speed and acceleration during take-off, catapults enable aircraft to lift off with heavier payloads and within reduced take-off distances. This method propels aircraft to speeds of approximately 270 km/h in less than 3 seconds over a distance of fewer than 100 meters. Particularly crucial for military aircraft operating in confined spaces like aircraft carriers, the catapult system can also be mounted on land-based runways in rare instances [24].

Catapult-assisted takeoff is a versatile and dynamic process with various interconnected systems and degrees of freedom [25]. Traditionally, the launch process encompasses the movements of the sea, ship, aircraft, atmosphere, and all associated interactions. Additionally, considering the influences of the pilot and/or commander, it involves human-machine collaboration. Specifically, concerning the ship, deck motion, catapult force, and deck effects are involved, while regarding the aircraft, factors include the movement distance of landing gear, engine power, and pilot control. Special wind effects are also pertinent concerning the atmosphere [26], [27].

Consequently, the catapult launch of ship-based aircraft exemplifies a typical instance of multiple-body dynamics with different natural frequencies. Deck motion, landing gear characteristics, engine power, and wind effects are the primary influencers on the process.

Catapults must meet exceptionally high standards of design and construction to operate efficiently. As expressed by an American specialist, even a 99 percent performance rate is considered inadequate. Additionally, aircraft carriers must possess substantial power capabilities to generate the energy required for catapult operations, especially when navigating against the wind for flight operations [28].

2. LITERATURE REVIEW

2.1 AIRCRAFT ENGINE

Aircraft engines are the propulsion systems responsible for the movement of aircraft and generating thrust during flight. Aircraft engines are designed and selected based on a variety of factors including power, efficiency, noise levels, and aircraft type. The choice of which type of engine to use depends on the intended use and performance requirements of the aircraft. Aircraft engines are categorized into two main types based on their operating principles: piston engines and jet engines. Each type of engine has different characteristics and operating principles.

Piston engines, also known as internal combustion engines, operate based on the four-stroke principle and convert mechanical energy into motion, powering vehicles. These engines can be categorized into diesel or gasoline-powered, V-type, inline, or radial in piston arrangement, and water-cooled or air-cooled in cooling system. Piston aircraft engines are commonly found in small general aviation planes like training and agricultural aircraft, chosen for their cost-effectiveness, especially for speeds below 400 km/h. However, they can be affected by atmospheric conditions during cruise flight due to their operating principles.

Jet engines, also referred to as turbine engines, are widely utilized in long-distance commercial aviation. They are a subset of internal combustion engines, operating on the principle of converting heat energy into mechanical energy. These engines adhere to Newton's third law of motion, which dictates action and reaction. Gas turbine engines, following the Brayton Cycle, compress air, combust it with fuel, and utilize turbines to convert the resulting high-energy gases into mechanical power. Jet engines deliver substantial power and velocity, facilitating aircraft in reaching high altitudes and cruising speeds. They are used in various types of aircraft such as airplanes, helicopters, rockets, and other aerial vehicles. Jet engines are fuel-efficient and are used in large passenger aircraft like the Boeing 747 or Airbus A380. They operate based on a fundamental working principle that includes intake, compression, combustion, and exhaust stages.

The main components common to all jet engines include a gas compressor at the inlet, a combustion chamber, and a turbine at the outlet, which is on the same shaft as the compressor.

Gas turbine engines can be categorized into four main groups based on their purposes: Turbojet, Turboprop, Turbofan, and Turboshaft. Each type has different applications and design features, selected based on the aircraft's purposes, sizes, and design requirements.

Turbojet engines represent a basic form of gas turbine engine [29], initially crafted for military aircraft during World War II. The inception of the first centrifugal-flow turbojet can be credited to Frank Whittle of the Royal Air Force in 1930, while a parallel engine design was patented by Hans von Ohain in Germany in 1935 [30]. Apart from their superior speed compared to piston engines, turbojets are recognized for their enhanced reliability. As the oldest form of jet engines, turbojets are classified as reaction engines. Their operation follows Newton's third law of motion, which dictates that every action results in an equal and opposite reaction [31]. Turbojet engines generate significant thrust, enabling aircraft equipped with them to rapidly attain supersonic velocities. However, their efficiency diminishes at lower speeds due to the high velocity of the exhaust jet. Consequently, turbojet gas turbines exhibit reduced effectiveness and higher fuel consumption during subsonic flight [32]. Because of the fast jet, turbojet gas turbines produce a high level of noise, limiting their utility [33]. In contrast to turboprop engines, turbojets feature a smaller frontal area and emit higher exhaust velocities. This characteristic enables turbojet-equipped aircraft to operate at elevated altitudes, achieving superior speed and fuel efficiency [34]. Turbojet engines comprise several components, including an inlet for air intake, a compressor for pressurizing the incoming air, a combustion chamber for fuel ignition, a gas turbine that powers the compressor, and a nozzle for directing the exhaust gases [31].

Turbojet engines are internal combustion engines that utilize fuel combustion to heat air directly. The resulting hot gases are then expelled through an exhaust nozzle to generate propulsion [35], [36]. The operating principle of turbojet engines involves intake, compression, combustion, and thrust stages.

Turbojet engines consist of a thrust-nozzle gas turbine. Within the gas turbine, there exists an air inlet, a compressor, a combustion chamber, and a turbine (which drives the compressor) [37]. The air, pressurized and consequently heated within the compressor, progresses towards the combustion chamber. Fuel is injected into the pressurized and heated air through various means, promoting combustion.

As a result, the combustion gases, reaching high temperatures, pass through the turbine, generating power. The power produced here is sufficient to meet the needs of the compressor and mechanical components. The combustion gases exiting the turbine are accelerated through the exhaust nozzle and expelled into the surrounding environment. Thus, the thrust required for the aircraft's motion is achieved [38], [39].

Turbofan engines are internal combustion engines that belong to the jet engine family and are commonly used in commercial passenger aircraft. Turbofan engines offer many advantages over other types of aircraft engines, such as higher efficiency, lower noise levels, and lower emissions. Additionally, they are generally easier to maintain due to having fewer moving parts compared to other jet engine types [40].

Turbofan engines feature a large fan at the front that replaces the propeller found in turboprop engines. This fan serves a critical role in the air intake process and is typically measured by its diameter. Similar to a propeller, the fan's function is to enhance air pressure before it reaches the compressor and to augment the volume of air entering the engine per unit of time [38], [39]. A significant portion of the air bypasses the engine externally, making the engine quieter and providing more thrust at lower speeds.

A turbofan engine, a variant of the turbojet engine, incorporates a sizable, enclosed fan positioned on a shaft ahead of the compressor [11], [41]. In a turbojet engine, every bit of air that enters through the intake travels through a gas generator comprising a compressor, combustion chamber, and turbine [42]. In turbofan engines, only a portion of the incoming air goes to the combustion chamber. The high-pressure and hot gases resulting from combustion are expelled through a jet exhaust nozzle to produce thrust. At the same time, the fan creates a mixture of compressed air with external air, and a portion of this mixture is used to straighten the airflow around the fan. This feature contributes to turbofan engines

being quieter and more fuel-efficient. When energy is added, the air remains at a relatively constant pressure but increases in volume, increasing its velocity as it exits the engine [43]. The rest of the air is directed through a fan or a low-pressure compressor, where it is either expelled directly as a "cold" jet or combined with the exhaust from the gas generator to create a "hot" jet. This bypass system aims to enhance thrust without escalating fuel consumption. Turbofan engines are manufactured in two types: low-bypass and high-bypass.

The total thrust produced by a turbofan engine is the sum of the thrust generated by the fan blades and the jet expelled from the exhaust nozzle. Consequently, the efficiency of a turbofan engine surpasses that of a turbojet engine [11].

Turbofan engines with a large frontal area are most suitable for commercial aircraft, as they generate the highest thrust at low (takeoff) speeds [44].

Turboprop engines are a type of jet engine commonly utilized in aircraft designed for short-distance flights. These engines are created by integrating a propeller into a basic gas turbine aircraft engine. The propeller's function is to pressurize the air prior to its entry into the engine, thereby augmenting the airflow. They are categorized as single-shaft or two-shaft engines. In single-shaft turboprop engines, akin to turbojets, power from the combustion gases is transmitted by the turbine to both the compressor and the propeller via a single shaft. In two-shaft turboprop engines, an additional turbine known as the free turbine or power turbine is present. While one shaft turbine channels power to the compressor, the second shaft directly conveys power generated by the free turbine to the propeller [38], [45].

In turboprop engines, approximately 85% of the thrust comes from the propeller, while the remaining 15% comes from the jet exhaust. Turboprops are efficient powerplants operating in the range of 300 to 500 miles per hour; one of the prime examples of this application is the Lockheed Electra transportation in the 1950s [11].

Turboprop engines do not possess a high capacity for generating energy; thus, most of the produced energy is utilized to rotate the propellers [46]. Turboprop engines exhibit optimal efficiency at speeds below 725 km/h due to the moderate speed of the propeller. In contrast to piston engines, turboprops boast a superior power-to-weight ratio, enhancing reliability and reducing take off durations [34].

In advanced turboprop engines, there are two independently controlled variables: fuel flow and propeller blade angle, which enable the propeller to rotate at variable speeds while maintaining a constant pitch. Therefore, turboprop engines can generate more power with less fuel consumption [47]. Over time, as advancements have occurred, turboprops have replaced turbojets in slower aircraft due to their lower fuel consumption [33].

a. Air Intake: The engine draws in ambient air from its surroundings, a process involving the intake of external air, typically filtered to remove contaminants.

b. Compression: The incoming air is compressed by a compressor, increasing the density of air molecules, and thereby elevating the oxygen content for enhanced combustion efficiency.

c. Fuel Injection and Combustion: The compressed air is mixed with fuel injected by a fuel injector and subsequently ignited by an ignition system. This combustion process yields high-temperature gases.

d. Expansion: The high-pressure and high-temperature gases resulting from combustion are utilized to drive a turbine, generating energy in the process.

e. Propeller Drive: The energy produced by the turbine is transmitted via a shaft to drive a propeller. The propeller generates thrust, propelling the aircraft forward.

f. Thrust Generation: The thrust generated by the propeller facilitates the forward movement of the aircraft. Simultaneously, the rotational motion produced by the propeller is transferred to another shaft via a gearbox, facilitating energy transmission.

Turboprop engines possess the capability to regulate thrust levels based on the aircraft's speed and flight conditions. This enables effective maneuvering at low speeds and ensures optimal performance during takeoff and landing procedures.

Turboshaft engines are small turbojet engines designed to take advantage of the high-speed capabilities of jet engines [48]. They exhibit characteristics such as high-power output, high reliability, small size, and light weight. The operating principles of turboshaft and turboprop engines are similar. The difference between turboprops and turboshafts lies in the

mechanical part that transfers energy [49]. The fundamental distinction is that turboshaft engines do not produce thrust from the exhaust section, whereas turboprop engines utilize the remaining thrust from the expansion gases in the exhaust [50]. Unlike turbojets, turboshaft engines feature a transmission-like power transfer system that rotates the rotor blades. Through this transmission, it converts the mechanical energy obtained from the turbine into rotating the rotor blades. Efficiency for turboshaft engines is defined by the ratio of the obtained output to the shaft power.

The energy obtained in turboshaft engines is used to rotate the shaft. The rotation of the propellers and blades connected to the shaft generates thrust [38]. Turboshaft engines can operate at low speeds and high power, thus exhibiting good fuel economy.

Turboshaft engines are utilized in various applications such as helicopters, ships, trains, tanks, pumping units, and various industrial gas turbine applications [51]. One notable distinction of turboshaft engines is the inclusion of a reduction gearbox, which is powered by the compressor front shaft. This gearbox not only reduces speed but also converts horizontal motion into vertical motion to rotate the propeller. Additionally, turboshaft engines feature two separate turbine groups rotating in opposite directions, unlike other engines where turbines rotate in the same direction. The first turbine operates the compressor for engine function, while the second turbine drives the gearbox. Through the gearbox, motion is proportionally reduced and transferred to the helicopter's rotor blades via a vertical shaft. Unlike jet engines, turboshaft engines cannot utilize jet engine thrust. Instead, the rotation of the blades controls the helicopter's axial movement, while the tail rotor prevents the helicopter from rotating in place [48].

2.2 HISTORY OF AIRCRAFT CARRIERS

In 1909, six years after the Wright brothers' historic flights, a group of officers began advocating for the Navy to invest in aircraft. By 1910, Glenn Curtiss, a civilian aircraft builder, and Eugene Ely, a civilian pilot, demonstrated to the Navy and the world the feasibility of aviation at sea. On November 14, Ely accomplished the first successful take-off from a specially constructed platform on the cruiser Birmingham.

He further solidified this feat on January 18, 1911, by executing the first successful landing on the armoured cruiser Pennsylvania in San Francisco Bay before returning safely to shore [52].

Thus, November 14, 1910, is recorded as the date when the first aircraft took off from a ship. The first successful landing of an aircraft on a ship occurred on January 18, 1911. Both endeavors were undertaken by the United States Navy. The USS Birmingham cruiser, with its deck converted into a makeshift runway, was used in the initial attempt. In the second attempt, the USS Pennsylvania armored cruiser was equipped with the necessary arresting gear [53].

While these attempts did not directly initiate the construction of aircraft carriers, they were significant in demonstrating the capability of an aircraft to take off and land on a ship [54] Moreover, it is noteworthy that in both attempts, the ships were observed to be anchored in port. Indeed, the first flight from a moving ship took place on May 2, 1912, carried out by the British Royal Navy. The HMS Hibernia, a battleship, served as the platform hosting this historic flight [53]. One of the first platforms designed as an aircraft carrier was HMS Argus, which entered service in 1918. HMS Argus was designed for the British Royal Navy and was the first ship specifically equipped to carry aircraft. The conversion of HMS Argus was completed in September. Subsequently, HMS Hermes was designed as an aircraft carrier and entered service in 1924 [55].

The Ark Royal marked the Royal Navy's inaugural modern aircraft carrier. In contrast to other carriers in the Fleet, which were converted from existing warships, the Ark Royal was meticulously designed from the outset to serve as an aircraft carrier. Built in Birkenhead, England, from 1935 to 1938, the newly constructed carrier boasted an impressive overall length of 244 meters and a displacement exceeding 23,000 tons upon its commissioning in November 1938. It possessed a maximum speed of 31 knots and had the capacity to accommodate up to seventy-two attack aircraft [56]. The name of Ark Royal, which was also used in testing systems for the loading and unloading of seaplanes onto the ship, was changed to "Pegasus" in 1934 [57].

The development of aircraft carriers continued in the period between World War I and World War II [58]. Unlike their relatively limited role in World War I, aircraft carriers played a crucial role in World War II. It is widely accepted that aircraft carriers completely altered the course of World War II. The Second World War witnessed a series of naval battles that prominently featured aircraft carriers [59].

One of the most significant changes in the naval forces of major world powers in the 20th century was the displacement of battleships by aircraft carriers. Particularly, developments in the Pacific theater during the 1944-45 period played a crucial role in this shift [60]. Emerging as the primary capital ship during World War II, the aircraft carrier continued its development in the subsequent era, incorporating innovations such as angled flight decks and steam catapults [58].

Ships with Decks Capable of Landing Wheeled Aircraft [18] ;

In England, the deck of the ship named HMS Argus was converted into a large runway where aircraft could take off and land, and it joined the navy in 1918.

Japan's aircraft carrier named "Hosho" is the world's first purpose-built aircraft carrier and entered service in 1922.

The US aircraft carriers USS Saratoga and USS Lexington were commissioned in 1927.

2.3 AIRCRAFT CARRIERS

An aircraft carrier can be defined as a warship capable of facilitating the takeoff and landing of aircraft. Various design features characterize aircraft carriers across the world's navies. While classifications based on size and propulsion systems exist, emphasis today primarily revolves around the takeoff and landing configurations [58]. As delineated by methods of aircraft launch and recovery, there exist four main types of aircraft carriers operational worldwide [17]. Accordingly, aircraft carriers are categorized into four types: Catapult Assisted Take-Off Barrier Arrested Recovery (CATOBAR), Short Take-Off Barrier Assisted Recovery (STOBAR), Short Take-Off Vertical Landing (STOVL), and Vertical Take-Off and Landing (VTOL).

CATOBAR (Catapult Assisted Take-Off Barrier Arrested Recovery) is a non-traditional horizontal takeoff technique commonly employed on aircraft carriers with limited space for acceleration on the deck. Most modern CATOBAR systems incorporate steam catapults, which have been widely used since World War II [61].

Contemporary catapult systems are employed for launching aircraft from aircraft carrier decks. These catapults utilize steam as a power source to drive a piston along a linear path on the carrier deck. The piston accelerates the aircraft, enabling it to reach take-off speed within a minimal distance [23]. The primary challenge in launching the aircraft is to provide sufficient steam pressure. As the aircraft accelerates, valves of the catapult pressure tank, filled with high-pressure steam beneath the short runway, are opened, supporting a piston with the force necessary to accelerate the aircraft to takeoff speed [61]. This method involves aiding the aircraft in take off by pulling it with a high-speed sled. Catapults are mounted on the flight deck surface of the ship and are powered by either nuclear reactors or steam boilers [62]. Landing occurs when the aircraft's tailhook catches the wire on the deck of the runway.

The CATOBAR category necessitates immense vessels. Indeed, the United States Navy currently restricts the term "carrier" for CATOBAR ships only. All other smaller carriers are considered assault ships [17].

In the STOBAR configuration, another configuration, no catapult system is used for assisted takeoff from the deck [63]. In STOBAR, the aircraft takes off under its own thrust. The inclined ramp at the bow of the ship serves to facilitate takeoff. The aircraft is launched by its own power using a ski-jump at the end of the runway to assist in takeoff [64]. Landing on these types of ships occurs similarly to CATOBAR, with the aircraft's tailhook catching the wire on the runway [58]. As of 2015, only Indian, Russian, and Chinese aircraft carriers regularly employ this system [64]. Comparatively, maintenance and development of STOBAR are more cost-effective due to the absence of any moving parts and thus requiring fewer operators for successful launches. Moreover, STOBAR is easier to operate as it does not require any additional power systems to generate force for initiating launches, unlike CATOBAR configurations which may necessitate high-power equipment such as nuclear reactors to support the launch mechanism.

The launch sequence starts with the aircraft accelerating normally on the flat deck and ramp, culminating in reaching the ideal take-off angle toward the end of the ramp. As the aircraft takes off from the carrier via the ramp, it may not have attained enough speed for level flight, but it does achieve a positive climb rate due to the ski-jump [58].

Technically, the construction and installation of the STOBAR system are simpler compared to the CATOBAR system. On the other hand, the main disadvantage of this configuration is the requirement for a high power-to-weight ratio for takeoff, which prevents aircraft from taking off with their full payload [65]. Consequently, they are considered more suitable for missions involving air defense or attacking ground targets that do not require long-range or heavy weapon payloads [28].

The third type is the Vertical Take-Off and Landing (VTOL) carrier. A Vertical Take-Off and Landing (VTOL) aircraft is capable of both vertical takeoff and landing, eliminating the need for a runway. The VTOL aircraft achieves this by generating lifting force directly upward using its engines, rather than gradually tilting the aircraft's nose upward [66]. VTOL aircraft have simple requirements for takeoff and landing areas, can hover precisely in the air, provide good maneuverability, and are highly flexible [67].

In rotary-wing aircraft, the fundamental principle of vertical takeoff remains consistent: Due to the rotating wings, there is a decrease in pressure above the rotor and an increase in pressure below it, resulting in the generation of thrust. To move forward, the aircraft slightly tilts to direct a portion of its thrust forward. In the case of directed jet thrust, the aircraft's jet engine and thus the thrust vector are vertically aligned to generate vertical lift but can later change direction to move horizontally [68].

VTOL encompasses various types of aircraft, including fixed-wing aircraft as well as other aircraft with motorized rotors such as helicopters, gyrocopters, and tiltrotors [69]. VTOL fundamentally comprises three configurations: wing-type configuration, helicopter-type configuration, and ducted-fan configuration. In the wing-type configuration, there are fixed wings or movable wings with vector thrust engines, in the ducted-fan type, there is a ducted rotor that assists in providing lift, and in the helicopter type, there is a rotor mounted on top to provide lift [70].

The most well-known type of VTOL aircraft is the helicopter, which utilizes rotor blades to generate vertical lift [71]. One of its earliest significant applications occurred during World War II, where helicopters swiftly transported soldiers from battlefronts with limited runways. The success of VTOL aircraft during this period prompted major aircraft companies such as McDonnell Douglas, Boeing, and Lockheed Martin to begin producing and engineering VTOL aircraft [66].

The general characteristics include ease of use, rapid response time, and high engine stability [72]. A significant advantage is that the aircraft can take off and land in almost any location and requires very little space [61]. Compared to STOVL, the VTOL design sacrifices more of the aircraft's operational capacity and allows for a slower ship. Opting for VTOL instead of STOVL typically indicates that the ship is primarily intended for helicopter operations, tailored for a specific purpose that restricts performance, or exclusively designed for non-combat or general support tasks. The difference between STOVL and VTOL for fixed-wing aircraft typically involves the presence of a ski-jump ramp at the front of the flight deck and the ability to generate enough wind over the deck for takeoff [17].

In the fourth design, "Short Takeoff Vertical Landing" (STOVL), the aircraft takes off using its own thrust, typically from a sloped ramp, like STOBAR. The difference with these types of ships lies in the vertical landing instead of using arresting gear for landing. Theoretically, STOVL aircraft can also perform vertical takeoff. However, this is not practically preferred due to the reduction in weapon payload and fuel quantity it entails [58].

The Short Take-off Vertical Landing (STOVL) aircraft's exhaust and lift fan generate two thrust jets upon the landing surface. While these jets aid in take-off, hovering, and landing manoeuvres, they also result in elevated structural loads, considerable acoustic emissions, and surface abrasion on the landing surface [72]. Such aircraft are typically designed to operate from confined spaces like aircraft carriers. The most common examples of STOVL aircraft include the Harrier and the F-35B. The Short Takeoff Vertical Landing (STOVL) variant of the F-35 Joint Strike Fighter (JSF) is a multi-role combat aircraft that provides the capability to establish forward bases in challenging terrains and on small carriers [73]. The use of STOVL aircraft on carriers offers advantages due to their smaller footprint on the carrier's deck or in its hangar.

STOVL aircraft utilize speed as an additional weapon to reach a greater number of targets in a shorter amount of time [74]. STOVL aircraft enhance the flexibility of aircraft carriers and can perform safe landings in confined spaces and on decks, as well as easier and safer landings at night and in adverse weather conditions due to the lack of traditional arresting gear systems [75]. One of the most significant advantages of STOVL is its low construction and maintenance costs. However, the disadvantage lies in the relatively shorter range of STOVL aircraft, which particularly reduces their effectiveness in attack missions [17]. Understanding that the combat radius of the F-35 in its STOVL version (F-35B) is 833 km, while in its CATOBAR version (F-35C) it is 1,111 km, helps clarify the difference [76].

Historically, the origins of catapults date back to ancient times. In ancient Greek and Roman periods, there were simple catapults used as stone-throwing machines for military purposes. However, the development and use of modern catapult systems emerged in the early 20th century. The first aircraft carriers and catapult systems appeared during World War I. During this period, landing and takeoff of aircraft from ships were quite challenging and time-consuming. Therefore, the use of catapult systems on aircraft carriers enabled aircraft to take off more quickly and increased operational flexibility. The initial catapult systems were piston-based systems powered by hydraulic or steam power.

The selection of the ship's hull for the placement of the catapult system is associated with two main reasons. Firstly, the ship's cranes were unable to lift aircraft at both ends. In this case, it became necessary to place a temporary boom on the barrel of the turret gun and use it as a crane. It was considered the most suitable option to place the catapult at the rear of the towers according to the designers' plans. Additionally, it was a significant design requirement for the catapult to be mounted forward and pass directly over the bow. Lastly, it was anticipated that the risk of crushing the pilot and aircraft in case of failure to catch air at the end of the run was an undesirable situation [77].

The importance and usage of catapult systems further increased during World War II. Following World War II, with the development of jet-powered aircraft, more powerful and sophisticated catapult systems were developed.

Samuel Langley, a prominent figure in aviation and the Secretary of the Smithsonian Institution, developed successful flight models and, in 1903, introduced a type of spring-loaded catapult system to showcase his Aerodrome project, which, however, ended in failure [78]. Similarly, in 1904, the Wright Brothers used a weight and crane-style catapult system to assist their aircraft in taking off over a limited distance [79]. Subsequently, on July 31, 1912, Theodore Gordon Ellyson was recorded as the first person to be launched with the Navy's catapult system, installing the improved compressed-air catapult system at the Santee Pier in Annapolis, Maryland. On November 12, 1912, Lieutenant Ellyson successfully conducted the Navy's first successful catapult flight, launched from a stationary coal ship. Additionally, on November 5, 1915, Colonel Henry C. Mustin also took off from a ship using a catapult system [80].

Steam catapults were developed by the British Royal Navy in 1952, utilizing pressurized steam power derived from the carrier's engines. The shuttle, connected directly to two pistons, propels along the rail and attaches to the aircraft's arresting cable. These catapults are capable of launching jet-powered and heavy aircraft within the fleet, boasting a superior maximum capacity compared to pneumatic and hydraulic counterparts. Utilizing steam from the ship's boilers and water from the steam system, they generate the required pressure to launch aircraft from the flight deck [64].

The operational principle of the system is briefly outlined below:

Steam catapults are installed on the flight deck surface of a ship. A tow bar attached to the catapult moves within a holder located inside the nose wheel of the aircraft. Upon activation, the tow bar pulls the aircraft along the catapult track, ensuring it reaches the necessary speed for takeoff by the end of the runway. During this process, the aircraft is set to full throttle, and the carrier is oriented as much as possible into the wind to aid takeoff. Additionally, various control surfaces are adjusted to ensure the aircraft achieves a balanced takeoff.

During the launch process, if the force exerted on the aircraft by the shuttle surpasses the tow bar's capacity, the aircraft is released to begin the take-off run. At this stage, the speed of the aircraft and its readiness for takeoff are monitored.

Subsequently, as the operation nears completion, the piston approaches the water cutoff point. The piston is utilized to stop the shuttle, and a key is operated to close the launch valves, halting the steam flow into the cylinder. Simultaneously, exhaust valves are opened to expel spent steam. Throughout these procedures, a retraction motor is engaged to return the shuttle and piston to the cocked position.

Hydraulically powered catapults utilize pressurized fluid to release energy and propel the aircraft attached to the tow bar. However, due to unreliability and operational issues, this system was quickly decommissioned [64]. Particularly, in May 1954, a catastrophic hydraulic catapult explosion aboard the USS Bennington resulted in the loss of approximately 100 crew members [81]. Following this incident, the utilization of hydraulic catapults was abandoned due to the technical challenges and associated risks involved.

Hydraulic catapults are systems that operate using hydraulic fluids. Typically, fluids such as hydraulic oil are employed, and hydraulic pressure, by pushing the pistons during launch, rapidly propels the aircraft. These systems can be installed with less complexity and at lower costs. On the other hand, steam catapults operate using steam pressure. Steam is usually generated from steam boilers and kept under high pressure. During launch, this steam propels the aircraft by pushing the pistons in the cylinders. While steam catapults may offer higher launching power, their installation and operational costs are typically higher. Therefore, hydraulic catapults are generally preferred as a simpler and more economical option, whereas steam catapults can provide higher performance albeit at a higher cost.

EMALS is an innovative technology utilized on modern aircraft carriers to launch aircraft, serving as a replacement for the long-standing steam-powered catapult system [82]. The Electromagnetic Aircraft Launch System was first developed by the United States during World War II and successfully launched a 4.5-ton aircraft [83]. Implemented on the USS Gerald R. Ford, the Navy's latest and most advanced carrier, the EMALS was incorporated from the ground up. The vessel was specifically designed to integrate this new launch system, featuring four EMALS catapults capable of launching aircraft weighing up to 100,000 pounds each [82]. While the typical cruising altitudes of conventional aircraft range from 5000 to 6000 feet, on aircraft carriers, this altitude drops significantly to as low as 300 feet. This necessitates rapid acceleration for takeoff over a very short distance.

The launch system is determined by factors such as the weight of the aircraft, its performance characteristics, and various external conditions. These conditions can be effectively managed on an aircraft carrier through electromagnetic launch systems [83]. EMALS provided a launch energy of 122 MJ in conducted tests, representing a 29% increase over the operational limit of traditional steam catapults, which typically stand at 95 MJ [64]. The significant launch power demonstrated by EMALS underscores its capability to significantly enhance aircraft carrier capabilities by efficiently launching larger and heavier aircraft. Another notable advantage of EMALS is its potential to extend the service life of carrier-based aircraft, reduce maintenance requirements, and decrease the frequency of aircraft body inspections. This could improve operational efficiency by strengthening the durability of carrier-based aircraft and reducing long-term maintenance costs. Additionally, reduced stress on aircraft bodies may result in fewer inspections, further enhancing operational reliability.

Achieving uniform acceleration along the catapult track will effectively provide a smoother launch. This implies that pilots will experience a gradual increase in speed rather than the initial jolt experienced with traditional catapult launches. This smoother acceleration will also limit the initial stresses applied to the aircraft [84].

EMALS eliminates complex components such as the intricate tube network, water brakes, and auxiliary units used in traditional steam systems, thereby reducing the need for steam, valves, pumps, hydraulic systems, motors, steam boilers, and gallons of sweet water for hydraulic fluid transportation. Instead, EMALS simplifies the system by utilizing the launch motor itself and reducing the number of auxiliary units, offering a less complex solution for the launch process of carrier-based aircraft. Carriers equipped with EMALS will require significant amounts of electrical power compared to the steam pressure required by steam catapults [82]. All electromagnetic catapults employ four linear motors with individual power exceeding 30 MW, and the total power can reach 100 MW. This is equivalent to the amount of electricity used by a small town simultaneously [85]. The ability of an Electromagnetic (EM) launch system to adjust speed and thrust to meet the requirements of the launched vehicle makes a single catapult suitable for a wide range of manned and unmanned aircraft bodies.

This feature represents a significant advantage of EMALS in terms of flexibility and versatility [86]. EMALS utilizes a method similar to an electromagnetic railgun to accelerate the aircraft-holding shuttle. It derives power from the ship's enhanced electrical system, comprising six primary subsystems: the launch motor, main power interface, power conversion system, advanced launch control system, energy storage, and power distribution system [87].

2.4 FACTORS AFFECTING AIRCRAFT TAKEOFF

Performance refers to an aircraft's capacity to fulfil specific objectives, making it functional. For example, the ability to execute short take-offs and landings is vital for pilots operating in constrained airfields. Airliners and executive aircraft rely on capabilities such as carrying heavy loads, high-speed and high-altitude flight, and covering long distances. Key factors influencing performance include take-off and landing distance, climb rate, ceiling, payload, range, speed, manoeuvrability, stability, and fuel efficiency [88], [89]. The required takeoff runway distance for an aircraft depends on its takeoff weight, air density, and the aircraft's takeoff performance [89].

Aircraft design: Factors such as the aircraft model, wing design, engine power, aerodynamic characteristics, and payload capacity directly influence takeoff performance. For instance, large commercial aircraft require more thrust and may necessitate longer runways. The shape and size of the wings determine the aircraft's ability to generate lift in the air. A well-designed wing can lead to more efficient takeoffs. Additionally, the aircraft's aerodynamic properties can reduce resistance during takeoff, facilitating the process. Furthermore, the aircraft's fuselage structure and landing gear also impact takeoff performance. The size and capacity of the aircraft are crucial factors to consider in designing the fuselage aerodynamics since it should minimize drag depending on its size [90]. An optimized fuselage structure and appropriate landing gear make takeoffs safer. All these factors underscore the significant role of aircraft design in determining takeoff performance.

Aircraft weight: The takeoff weight of an aircraft is a crucial aspect of aircraft performance [91]. Takeoff weight (TOW) is an important parameter for modeling or estimating other aircraft performance characteristics such as climb/descent rate, range, endurance, ceiling, and takeoff distance, in addition to the aircraft's orbit and fuel consumption [92]. Any item that would increase the overall weight of the aircraft is undesirable from a performance perspective. An aircraft that is overloaded may face difficulties during take-off and may exhibit unexpectedly poor flight characteristics if it manages to take off. Excessive weight negatively impacts flight performance in nearly every aspect. This includes higher take-off speed, longer take-off distances, lower climb rate and angle, reduced maximum altitude, decreased range, slower cruise speed, diminished manoeuvrability, higher stall speed, extended approach and landing speed, longer landing roll, and excessive weight on nose or tail wheels. The presence of excessive weight diminishes the safety margins available to the pilot, posing greater danger when combined with other factors that impair performance [93].

Pilot skills and experience: Pilot experience is one of the most critical factors influencing aircraft takeoff. Pilot skill is crucial for managing the dynamic and sometimes unpredictable nature of takeoff and landing [88]. For aircraft to take off safely, pilots must consider these factors and make appropriate decisions. Unfortunately, these factors are immeasurable, and mathematical corrections are impossible.

Some factors that can significantly affect takeoff performance include [94]: the speed and sequence of releasing brakes and applying power, the utilization of nose wheel steering, differential braking, or rudder deflection for directional control, the frequency and extent of directional control inputs, the positions of flaps and elevators during acceleration, airspeed during turns, bank rate during turns, and angle of attack during take-off. Hence, it is essential for the pilot to comprehend all factors influencing the aircraft's take-off and landing performance and adhere to meticulous, professional operational procedures during these phases of flight [95].

Air density: Aircraft performance is directly affected by air density, which influences lift and drag forces, engine power, and propeller efficiency. Air density has significant effects on aircraft performance [88]. As air becomes less dense, both engine and aerodynamic efficiency decrease. Conversely, as air density increases (resulting in lower density altitude),

aircraft performance improves. On the contrary, when air density decreases (leading to higher density altitude), aircraft performance diminishes. A decrease in air density signifies higher density altitude, while an increase in air density signifies lower density altitude. Density altitude serves as a measure in determining aircraft performance. In standard atmospheric conditions, each level of the atmosphere contains air with a specific density; thus, pressure altitude and density altitude denote the same level under standard conditions. Consequently, density altitude represents the vertical distance from sea level in the standard atmosphere where a specific density is encountered [88].

There are three significant factors contributing to high-density altitude [96]:

a. Altitude: The effect of pressure on density diminishes with altitude as atmospheric pressure decreases with altitude due to compression of air near the Earth's surface by the air above it [88]. The higher the elevation, the lower the barometric pressure, and consequently, the lower the air density [97]. In such situations, operations between morning and afternoon can become extremely hazardous [96]. As altitude increases, the decrease in pressure has a more dominant effect on density compared to the influence of temperature [88].

b. Temperature: Temperature is a significant meteorological factor affecting the takeoff and landing performance of aircraft [98]. Air density shows an inverse correlation with temperature and a direct correlation with pressure. When temperature rises, density decreases to uphold a constant pressure; conversely, when pressure rises, density increases to maintain a constant temperature [99]. This results in the aircraft wing producing less lift force at a given airspeed, potentially imposing a weight restriction on a departing aircraft [100]. Low-density air conditions result in decreased lift force for aircraft, significantly affecting an aircraft's maximum takeoff weight [101]. Higher air temperatures will also decrease aircraft and engine performance. Since all aircraft performances are compared and evaluated in a standard atmospheric environment, all aircraft performance instrumentation is calibrated to the standard atmosphere [99]. Therefore, when it comes to performance, it is recommended to schedule operations during the cooler hours of the day when unexpected temperature rises above normal are not expected [96].

c. Humidity: As humidity increases, there is a slight decrease in air pressure. When air carries water vapor, its density is less than that of dry air because dry air is denser than water vapor [94]. This means there are fewer air molecules passing over the wings, resulting in less lift force compared to dry air. Similarly, moist air passing through a jet engine will produce slightly less power as there will be less air available for combustion [95]. Therefore, as the air's water content increases, the air density decreases, density altitude increases, and performance decreases [88].

Wind: An aircraft's flight relies on airspeed, which can notably deviate from ground speed in strong winds [88]. The presence of headwind enables the aircraft to achieve take-off speed with a lower ground speed, whereas tailwind necessitates a higher ground speed to reach take-off speed [94]. Departing into the wind results in a considerably longer climb distance and a decrease in climb angle [88]. A headwind of up to 10% of the take-off speed reduces the take-off distance by roughly 19%. Conversely, a tailwind of up to 10% of the take-off speed increases the take-off distance by about 21% [94].

Runway length, slope and surface: The takeoff phase of flight involves various critical factors that must be considered to ensure a successful departure. One of the most significant factors is the length of the runway [102]. The required takeoff distance for an aircraft depends on its takeoff weight, air density, and takeoff performance [89]. The runway length must be sufficient to allow the aircraft to reach takeoff speed. Takeoff speed varies depending on the size and weight of the aircraft, with larger aircraft potentially exceeding speeds of 200 miles per hour. Runway conditions, including surface type and slope, significantly influence aircraft take-off and landing performance. The runway's slope denotes the degree of elevation change over its length and is typically expressed as a percentage, like a three percent gradient.

A positive slope signifies an elevation increase along the runway, whereas a negative slope indicates a decline in elevation. An uphill slope hinders acceleration, resulting in an extended ground roll during take-off. Conversely, a downhill slope aids in acceleration, leading to shorter take-off distances [94]. A two percent slope increases takeoff distance by approximately 15 percent, while a two percent slope decreases takeoff distance by approximately 10 percent [88]. Performance charts typically assume optimal runway

conditions, such as smooth, flat, and dry surfaces. However, actual runways vary widely in characteristics like slope and material composition, ranging from concrete and asphalt to gravel, dirt, or grass. Uneven or soft surfaces increase rolling resistance during take-off, impeding smooth tire movement. Although wet or muddy conditions may decrease friction between the runway and tires, they can also create obstacles that may affect landing distances [94].

Takeoff speed and angle: Takeoff speed is typically about 15 percent higher than the stall speed, so an increase in weight will result in a higher takeoff speed. As the weight changes, the airspeed required to fly at that CL will also change. In addition to the required high speed, acceleration of a heavy aircraft is slower. Therefore, a longer takeoff distance will be required. As a rule, a 10 percent increase in takeoff weight has an approximately 20 percent increase effect on takeoff distance [88].

Elevating the angle of attack results in a heightened pressure disparity between the upper and lower wing surfaces, consequently amplifying the lift force. At lower angles of attack, lift force is primarily generated by the pressure drop on the upper surface. However, at higher angles, both the pressure decreases on the upper surface and the pressure increase on the lower surface contribute to the lift force [103].

Wing surface: The presence of frost, ice, or snow on the surface affects any type of wing profile, including propellers. Small hangar dents or dents on lifting surfaces or propellers will also decrease performance [88].

Engine power and efficiency: The aircraft's engine power generates the thrust required to accelerate takeoff. Efficient engine operation positively affects takeoff performance. Engine Pressure Ratio (EPR) represents the ratio between the exhaust pressure (jet output) and the inlet (static) pressure within turbojet or turbofan engines. Pilots rely on the EPR indicator to gauge engine power output, with higher EPR values indicating greater engine thrust. EPR serves to prevent engine overspeed and allows for adjustments to take-off and climb power as needed. This data is crucial pre-take-off as it influences the aircraft's performance assessment [94].

3. METHODOLOGY

In the methodology section of this study, a model of an aircraft taking off from an aircraft carrier has been developed using MATLAB Simulink software. In the created model, three different catapult types, namely C13-0, C13-1, and C13-2, have been investigated. The lengths and launch weights of these catapult types have been researched and integrated into the model according to the relevant formulas. Additionally, various factors affecting the aircraft's takeoff have been incorporated into the model, and the accuracy of these values has been emphasized. Subsequently, different configurations have been created for the three different catapult types, and the values of the aircraft dependent on the wind speed and ship velocity have been calculated. Thus, the takeoff distance and takeoff velocity of aircraft with different weights have been examined, considering the wind speed and ship velocity.

3.1 AN INVESTIGATION INTO THE AERODYNAMIC PRINCIPLES GOVERNING AIRCRAFT FLIGHT

The four primary factors affecting an aircraft in cruise flight (weight, lift, drag, and engine thrust) are illustrated in Figure 3.1. Throughout this phase, the aircraft maintains equilibrium. Air pressure and friction strains contribute to a unique aerodynamic force, comprising two components: lift and drag. As the aircraft advances, lift, perpendicular to the direction of flight, compensates for its weight. Conversely, drag, the tangential component of this aerodynamic force, opposes the aircraft's motion.

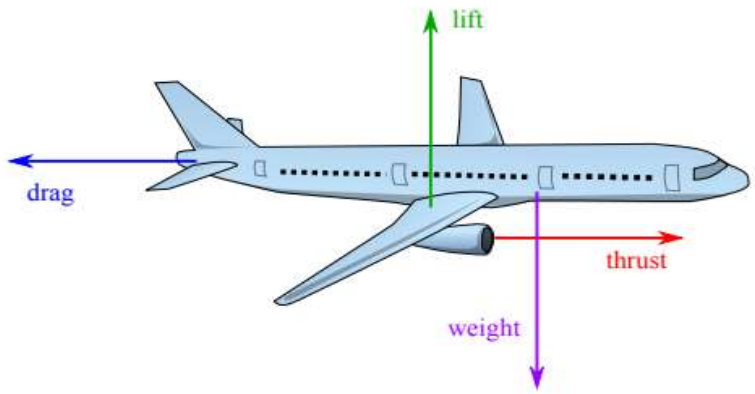

Figure 3. 1: Representing the Four Main Forces Acting on An Aircraft [104].

These two aerodynamic forces, lift $\vec{L}$ and drag $\vec{D}$, can be expressed via the equations (3.1) and (3.2):

$$\vec{L} = \frac{1}{2}\rho S V^2 C_L \overrightarrow{e_z} \tag{3.1}$$

$$\vec{D} = \frac{1}{2}\rho S V^2 C_D \overrightarrow{e_x} \tag{3.2}$$

In this equation, ρ represents the air density at the flight level, S denotes the wing surface area of the aircraft, V signifies the true airspeed of the aircraft, and C_L and C_D are two dimensionless coefficients influenced by the wing's geometry, angle of attack, and flight conditions. By applying Newton's second law of motion, the total sum of these forces balances out to zero during the cruise phase, characterized by a steady speed and altitude. Thus, the thrust generated by the engines plays a pivotal role in sustaining a consistent aircraft speed, ensuring the generation of lift to counteract its weight, and offsetting the drag force [104]. There are four forces that affect a plane: thrust**,** drag**,** gravity**,** and lift**.** Each of these forces act on the airplane in different directions [105].

3.1.1 Lift

Lift, the primary force enabling an aircraft to ascend and remain airborne, is generated by the wings and acts perpendicularly to the aircraft's motion. Its magnitude varies based on factors like wing shape, size, and speed. The pressure disparity on the wings' upper and lower surfaces generates lift. Lower pressure atop the wings and higher pressure beneath them create this difference, facilitating lift. Overall, lift empowers the aircraft to take off, climb, and execute maneuvers [106].

Bernoulli's principle was important in the Wright brothers' success in gaining flying in the air with their heavier-than airplane. It's because of the wing's upper curved curvature. As the plane flies forward, the airflow on the upper side of the wing differs from that on the bottom side. The lower side, on the other hand, is flatter, therefore airflow speed is unaffected, resulting in higher pressure. Lift is created by pressure differences above and below the wing, which allows the plane to fly [107].

It's worth noting that Bernoulli's principle can also be derived directly from Newton's second law. If a small volume of fluid is moving horizontally from a high-pressure area to a low-pressure area, there is more pressure behind it than in front of it. This causes a net force on the fluid, accelerating it along the flow path [108], [109].

3.1.2 Weight

Weight is the force pulling the aircraft downward due to gravity. All of the aircraft's mass is affected by gravity, and this force prevents the aircraft from falling to the ground. The lift force is the balancing force of weight. For the aircraft to stay airborne, the lift force must balance the weight. [110].

3.1.3 Thrust

Thrust, the force propelling an object, changes its speed or direction. Newton's third law of motion dictates that every action results in an equal and opposite reaction. In aviation, thrust, often from aircraft engines, is crucial. Engines intake, compress, and heat air, then mix it with jet fuel, producing temperatures up to three thousand degrees. This heated air turns turbines, eventually expelling backward and propelling the engine forward, as per Newton's law. Thrust is vital for various flight manoeuvres in aviation [110].

3.1.4 Drag

Drag is the aerodynamic force that opposes the forward motion of the aircraft. It acts in the opposite direction of the aircraft's motion. During the aircraft's movement, air molecules frictionally interact with the aircraft's surfaces, creating this frictional force known as drag. Drag slows down the aircraft's speed and acts against the thrust generated by the engines.

3.1.4.1 Aerodynamic

Aerodynamics is the study of the interaction of forces that propel an object through the air. When we examine a cross-section of an airplane wing, we can observe that the upper surface is more curved than the lower surface. Let's take a closer look at two air particles, one passing over the upper edge of the wing and the other passing beneath it.

The air surrounding the upper edge has a higher velocity compared to the air passing beneath the wing [111]. According to proponents of fluid mechanics, the wing's curved shape causes the air flowing horizontally over the upper part of the wing to have a higher velocity compared to the airflow beneath the wing. This variance in velocity results in reduced air pressure on the upper wing surface and elevated pressure beneath it, giving rise to the creation of upward vertical lift force. Consequently, the aircraft is raised upwards due to the pressure contrast between the upper and lower wing surfaces, particularly the decreased pressure on the upper side of the wing [112].

The traditional Newtonian theories of 'momentum' and 'downwash' lift suggest that wings alter the direction of relative airflow by redirecting it downward, resulting in the transfer of momentum from the aircraft to the surrounding air. This leads to equal and opposing forces that push the aircraft upwards [112].

In order to create lift force, a wing must interact with the air in some way. The action performed by the wing on the air is what generates lift, and the lift itself is the response or reaction to this action [113].

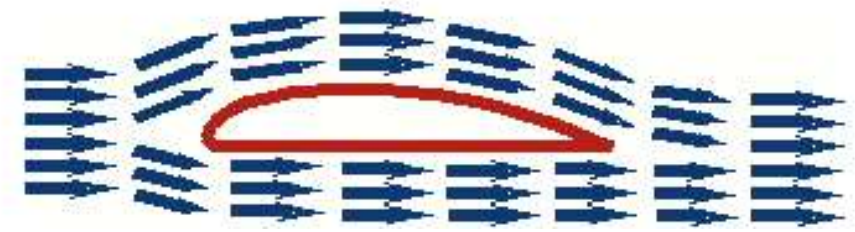

Figure 3. 2: Common Depiction of Airflow Overa Wing. This Wing Has No Lift [113].

Let's compare two illustrations used to depict the airflow (streamlines) over a wing. In Figure 3.2, the air approaches the wing directly, bends around it, and then separates directly behind the wing. In Figure 3.3, the streamlines are shown as they should be. The air flows over the wing and is bent downward. The bending of the air is the action, and the reaction is the lift force on the wing [113].

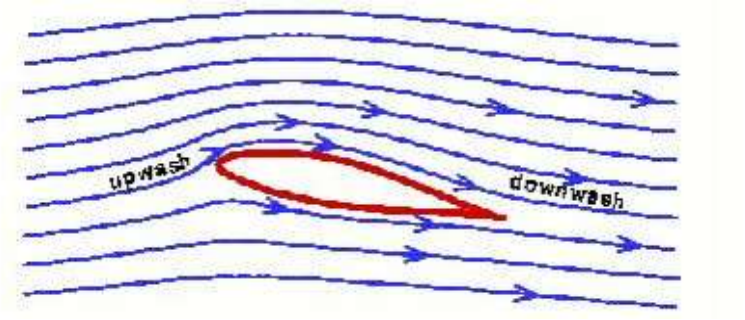

Figure 3. 3: True Airflow Showing Upwash and Downwash [113].

3.2 FORMULAS USED IN MATLAB SIMULINK MODEL

The calculations within the Equations of Motion block are illustrated by the following formulas. Initially, the computation of Lift Force is derived from Equation 3.1 as presented above. Subsequently, the computations within the Drag block are performed according to the formula outlined in Equation 3.2. The Total Drag calculation is the aggregate of parasitic drag and induced drag formulas. Following this, for the calculations within the mass/weight block, the formulas provided in Equation 3.5 and Equation 3.6 are employed to ascertain the weight/mass values.

Parasitic Drag;

$$D = c_d \times \frac{V^2 \times \rho}{2} \times \mathrm{A} \tag{3.3}$$

Induced Drag;

$$Cd_i = \frac{Cl^2}{\Pi \times AR \times e} \tag{3.4}$$

$$W = m \times g \tag{3.5}$$

$$F = m \times a \tag{3.6}$$

The Catapult Acceleration Calculations block initially computes the aircraft's acceleration. Subsequently, the lift required for the total weight is determined. Finally, the required acceleration for the catapult is derived by subtracting the aircraft's acceleration from the total required acceleration. Following this, to determine the catapult force, the masses of the aircraft and the catapult are summed, and then multiplied by the acceleration of the catapult. Then, the catapult force is calculated by multiplying this result by the selected distance value corresponding to the catapult type.

$$Catapult\ Force = Catapult\ Acceleration \times (Shuttle\ Mass + Jet\ Mass) \quad (3.7)$$

The Distance-Velocity calculation block computes ground speed, airspeed, and distance. Initially, distance is calculated according to Formula 3.8, where it is observed that the integral of acceleration yields distance. The resulting value is then multiplied by 1.94 to convert it to Knots. Subsequently, airspeed is calculated based on Formula 3.9, where wind speed, ship speed, and the integral of acceleration are utilized to determine airspeed. The resulting value is then multiplied by 1.94 to convert it to Knots. Finally, as indicated in Formula 3.10, distance is determined by integrating airspeed.

$$\int Air\ Speed = Distance \quad (3.8)$$

$$Air\ Speed = Wind\ Speed + Carrier\ Speed + \int Acceleration \quad (3.9)$$

$$\int Acceleration = Ground\ Speed \quad (3.10)$$

The Atmosphere Calculations block conducts computations according to the following formulas. Initially, pressure is computed using Formula 3.11, followed by the calculation of air density using Formula 3.12 derived from the calculated pressure formula.

$$P = \rho_0 \times \left(1 - \frac{g \times h}{c_p \times T_0}\right)^{\frac{C_p.M}{R_0}} \quad (3.11)$$

$$\rho = \frac{P}{R \times T} \quad (3.12)$$

3.3 MODELING OF AN AIRCRAFT TAKING OFF FROM AN AIRCRAFT CARRIER IN MATLAB SIMULINK

In this section, the modeling of an aircraft taking off from an aircraft carrier using MATLAB Simulink will be examined. The purpose of this study is to determine the takeoff speed of a light attack aircraft with an unknown takeoff speed and to investigate the effect of the catapult distance on the aircraft's takeoff performance.

The formulas described above have been used to create a model using MATLAB Simulink. In the process of creating the MATLAB Simulink model, the specified formulas are step-by-step applied, and calculations are performed to ensure the accurate estimation of the aircraft's takeoff speed. This model enables the accurate simulation of the aircraft's takeoff speed through the proper adjustment of input values and the implementation of specific mathematical operations based on scientific principles.

Thus, this model created using MATLAB Simulink represents the mathematical foundation of certain formulas and the principles of flight dynamics. It allows for the analysis and prediction of the aircraft's takeoff speed and the effect of the catapult distance on the aircraft's takeoff performance using a scientific approach.

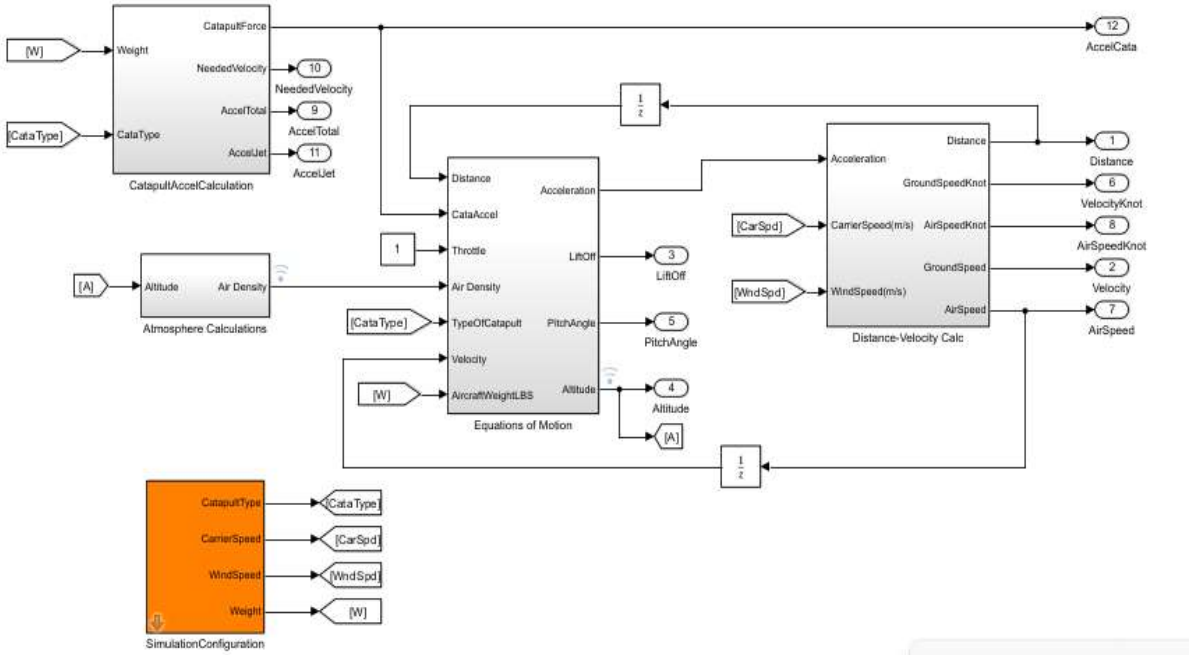

Figure 3. 4: Main Diagram of the MATLAB Model.

The main diagram of the model, depicted above, provides a comprehensive representation of the various factors influencing the aircraft's takeoff performance. These factors encompass a range of aerodynamic, mechanical, and environmental variables crucial for accurately simulating the aircraft's behavior during takeoff. Additionally, the diagram incorporates the main formulas utilized within the model, which govern the calculations and interactions among these factors. These formulas encapsulate fundamental principles of physics, aerodynamics, and engineering, ensuring a rigorous and precise simulation of the aircraft's performance. Together, the factors and formulas depicted in the diagram form the backbone of the model, enabling detailed analysis and prediction of the aircraft's takeoff dynamics under different conditions.

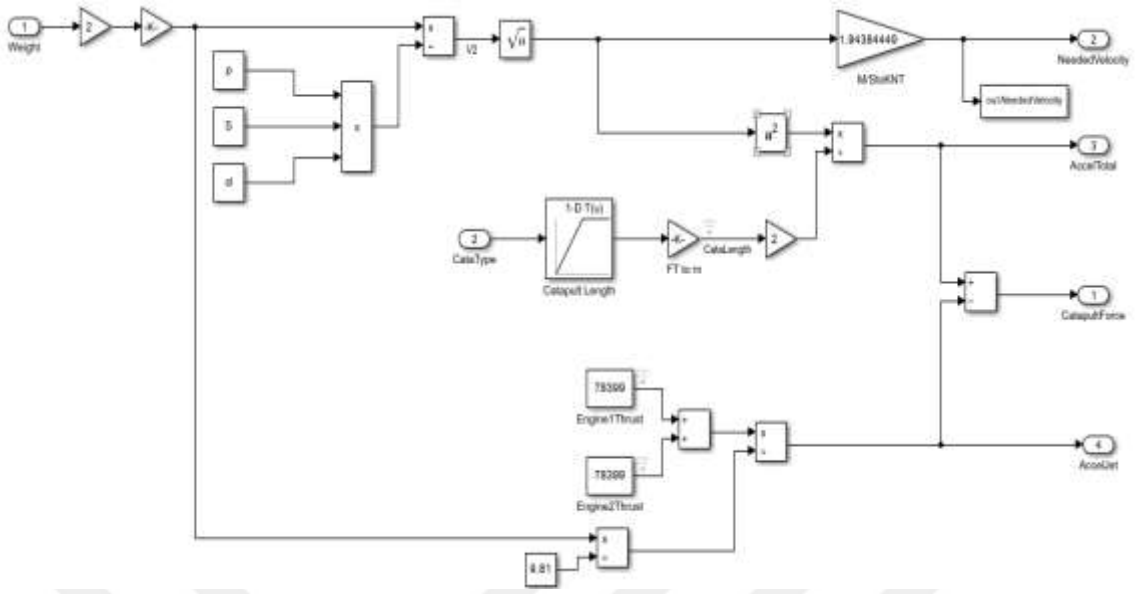

Figure 3. 5: Inside of the Catapult Acceleration Calculation.

In this section, the required acceleration for the catapult is determined. Initially, modeling is conducted for three different catapult types. The characteristics of the catapult types are researched, and based on the gathered information, the lengths of the catapult types are inputted. Subsequently, we calculate the acceleration of the aircraft along the distance covered by the catapult, thus determining the necessary total acceleration. Next, to ascertain the catapult's acceleration, we first determine the acceleration of the aircraft. Then, by subtracting the obtained acceleration from the total acceleration, we find the required acceleration for the catapult.

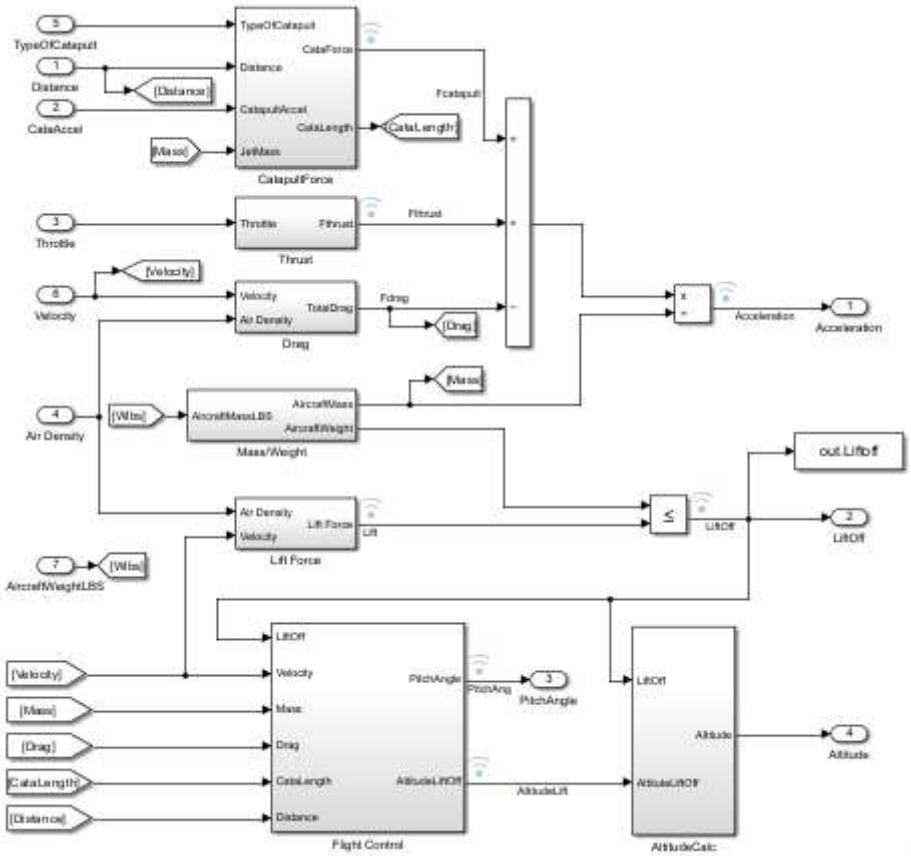

Figure 3. 6: Inside Equation of Motion Block.

The detailed version of the 'Equation of Motion' block depicted in Figure 3.5 is presented. This block encapsulates the key parameters influencing the aircraft's take-off performance. Specifically, the force exerted by the catapult and the thrust contribute positively to the aircraft's take-off. A higher catapult force results in an increased take-off speed of the aircraft. Additionally, the calculation of drag, representing the resistance experienced by the aircraft, is considered. Another significant factor impacting take-off is air density, extensively discussed in the literature review section. Figure 3.6 illustrates the impact of air density on lift and drag forces, demonstrating their variations with changes in density. Furthermore, the flight control block is designed to simulate the vertical movement of the aircraft, involving estimation of the aircraft's altitude during the simulation.

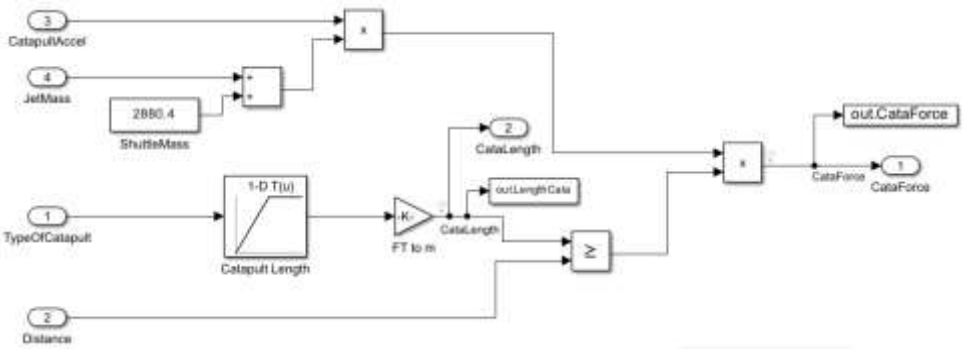

Figure 3. 7: Inside the Catapult Force Block.

In this section, the force required for the catapult and the distance at which this force will be applied are calculated. The required catapult acceleration, obtained from a different block, along with the masses of the aircraft and the shuttle, are utilized to determine the force to be exerted by the catapult. Calculations are conducted for three different catapult types: C/13-0, C/13-1, and C/13-2, with lengths of 76.1492m, 94.4m, and 93.5m, respectively. In the current simulation, the catapult type is selected, and the distance at which the force will be applied is determined using a Look-Up Table (LUT).

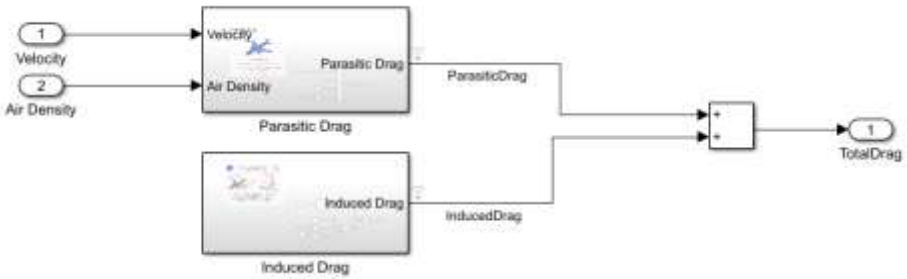

Figure 3. 8: Inside the Drag Block.

Drag force is a force that acts in the opposite direction to the direction of motion of the aircraft and is an obstacle that the aircraft must overcome during takeoff. Total drag is the sum of parasitic drag and induced drag forces. Parasitic drag is the resistance caused by the shape, surfaces, or assembly of the aircraft that acts in the opposite direction to the aircraft's motion. This type of drag is associated with the external surface of the aircraft and arises from non-aerodynamic elements. Induced drag is a consequence of the lift force generated on the wings of the aircraft. While wings produce lift force by directing the airflow, they also create induced drag, which is a type of opposing force.

This drag occurs due to the turning and swirling effects at the tips of the wings. This force slows down the aircraft and requires the engine to produce more thrust, negatively affecting takeoff performance. Therefore, it plays a significant role in MATLAB calculations. The drag force has been calculated using the relevant formula.

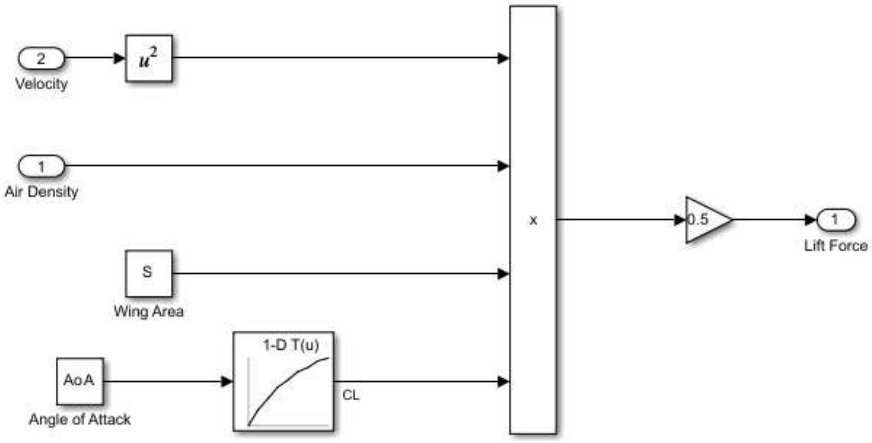

Figure 3. 9: Inside of Lift Force Block.

The lift force is the force generated by the wings of the aircraft, which enables the aircraft to be lifted upward. The pressure difference between the low pressure on the upper surface of the wings and the high pressure on the lower surface creates the lift force. The CL value (lift coefficient) is a measure of the lift force that an aircraft's wings can generate. Depending on the characteristics of the wing profile and aerodynamic structure, the CL value varies under different air conditions and flight situations. In the model shown in figure four, the calculation of the lift force has been performed in Simulink. CL values for the F/A-18 aircraft have been researched, and the obtained values have been used in the calculations. The lift force has been calculated using the relevant formula.

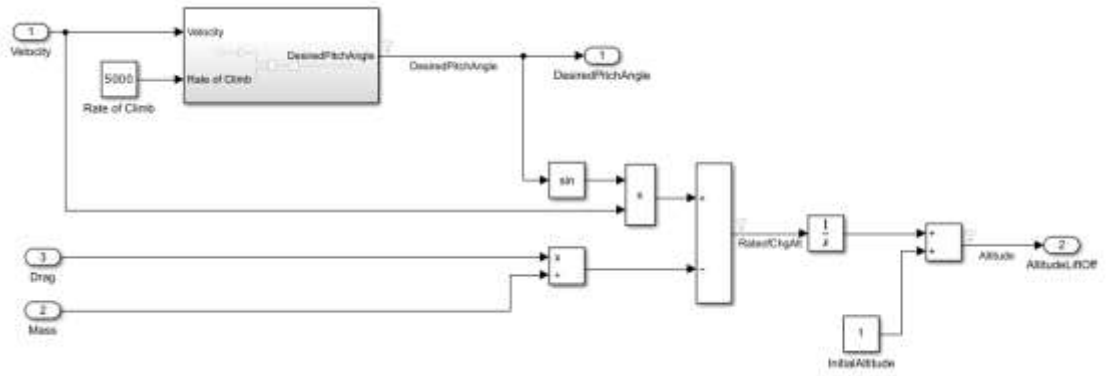

Figure 3. 10: Inside the Flight Control Block.

In Figure 3.10, the interior of the flight control block is depicted. In this section, the desired climb angle is primarily calculated. During this calculation, the rate of climb value is assumed to be an average of 5000 ft/min for jet aircraft. The desired climb angle is calculated using the relevant formula.

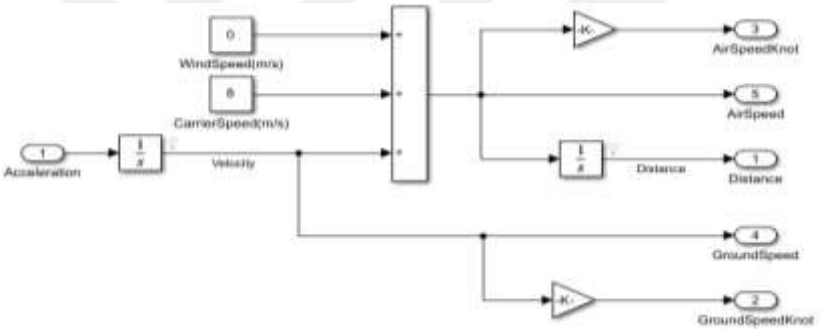

Figure 3.11: Inside the Distance-Velocity Calculation Block.

In this section, calculations for Air speed, Ground speed, and distance are performed. The acceleration calculated by the dynamics of the aircraft is utilized here. Acceleration represents the rate of change of velocity of an object. Integrating acceleration yields velocity in meters per second (m/s). Simultaneously, integrating velocity yields distance in meters. Two different speeds are obtained in this section. Ground speed indicates the speed of the aircraft relative to the ground, while Air speed represents the speed of the aircraft relative to the air. Ground speed is obtained by integrating acceleration. Other factors affecting the aircraft include ship speed and wind speed. Ship speed and wind speed, acting in the opposite direction to the aircraft's direction, positively affect the aircraft. Incorporating these into the current speed yields airspeed.

4. ANALYSIS AND MATLAB RESULTS

4.1 CFD ANALYSIS MODEL OF THE F/A-18 AIRCRAFT

In this section, a comprehensive analysis was conducted using Ansys software to calculate the lift coefficient values of an aircraft at different angles of attack. Determining the aerodynamic performance of aircraft and understanding their flight characteristics is a crucial research area within the aviation industry. Therefore, accurately calculating fundamental aerodynamic concepts such as lift holds critical importance in both the design process and flight operations. In this study, the Ansys Fluent software was utilized to analyze the aerodynamic behavior of the aircraft and determine the lift force.

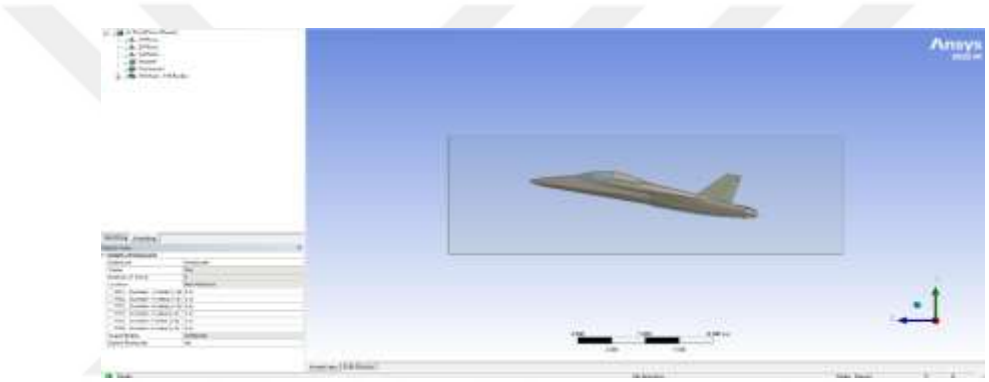

Figure 4. 1: The Wind Tunnel Created in Ansys Fluent.

Initially, a 10-degree angle of attack is applied to the component under analysis using the Solidworks program. Subsequently, the component is transferred to the Ansys Fluent program to commence the analysis. Within the program's geometry section, upon generating the model, pertinent parameters are inputted into the Enclosure section to facilitate the creation of a wind tunnel surrounding the component. Increasing the values within the Enclosure section offers the advantage of enhancing the precision of the analysis outcomes. For this analysis, the dimensions along the x and y axes are designated as 3m each, while the z-axis dimension is set at 6m to establish the wind tunnel. This decision stems from the default behavior of the Enclosure command, which initially generates a cubic enclosure with 1m dimensions along each axis.

To bolster accuracy and better simulate the airflow, dimensions of 3m along the x and y axes are chosen, while dimensions of +z and -z are set at 6m to represent the direction of airflow.

Details View	
Details of Enclosure1	
Enclosure	Enclosure1
Shape	Box
Number of Planes	0
Cushion	Non-Uniform
FD1, Cushion +X value (>0)	3 m
FD2, Cushion +Y value (>0)	3 m
FD3, Cushion +Z value (>0)	6 m
FD4, Cushion -X value (>0)	3 m
FD5, Cushion -Y value (>0)	3 m
FD6, Cushion -Z value (>0)	6 m
Target Bodies	All Bodies
Export Enclosure	Yes

Figure 4. 2: Showing the Values Inputted for The Reference Set in Ansys Fluent.

In Computational Fluid Dynamics (CFD) analysis, a crucial step involves partitioning the flow domain into distinct regions to determine the aerodynamic interactions of the aircraft. For this purpose, the front and rear surfaces of the airflow domain surrounding the aircraft are designated as "inlet" and "outlet," respectively. The "inlet" region serves as the point of entry for the airflow into the domain, facilitating its ingress, while the "outlet" region represents the exit point where the airflow exits the domain. The lateral surfaces are named "walls" to delineate the boundaries of the airflow domain. To identify the aircraft within this domain, the faces of the airflow domain are concealed, and the entire surface of the aircraft is selected using the bulk selection command within the software, subsequently named as "plane." This naming process enables better definition of specific regions during the analysis process and facilitates a more accurate interpretation of the analysis results.

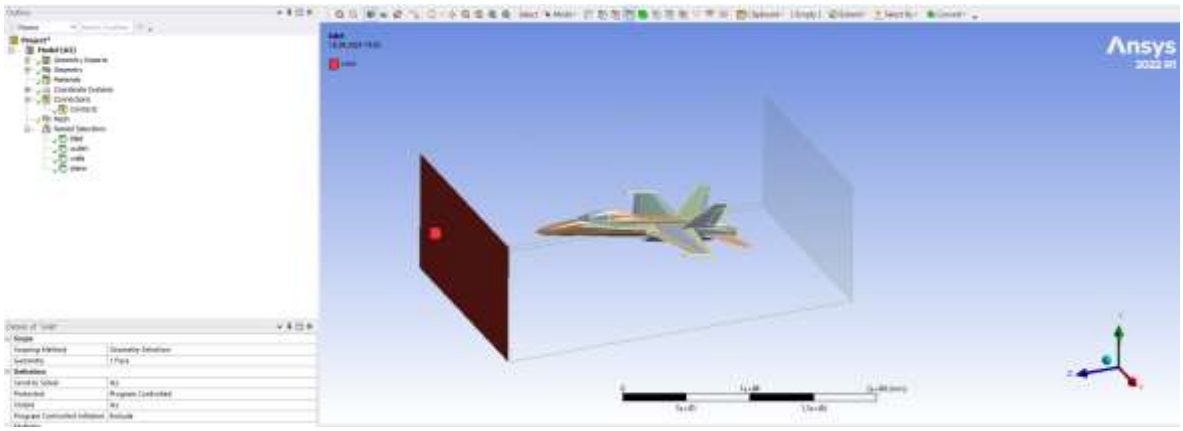

Figure 4. 3: The Part Called the Inlet Region.

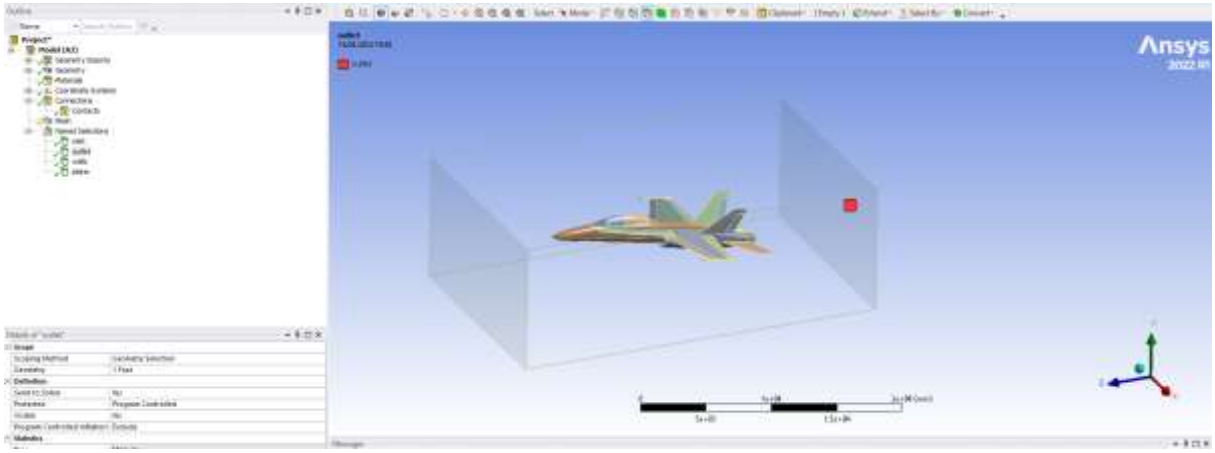

Figure 4. 4: The Part Called the Outlet Region.

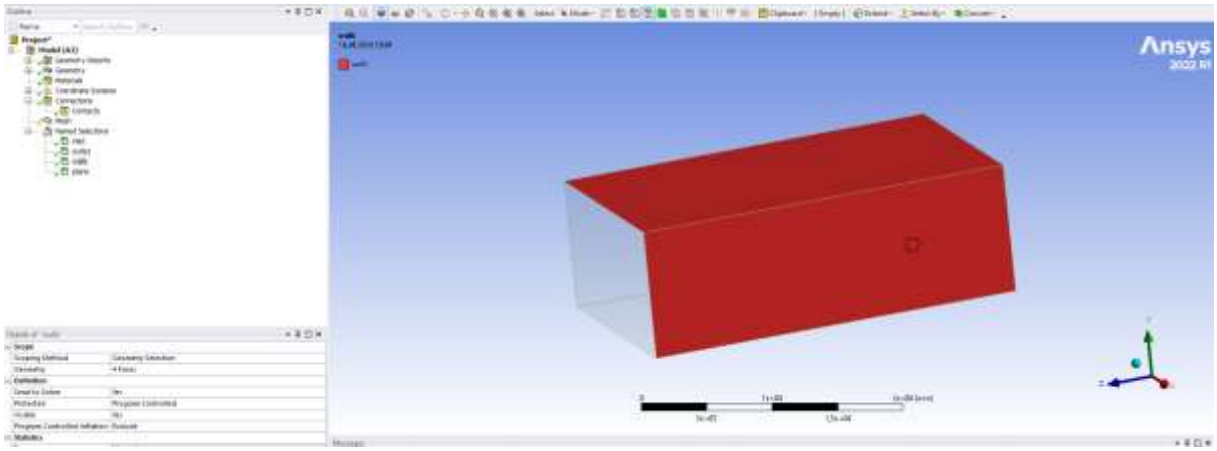

Figure 4. 5: The Part Called the Walls Region.

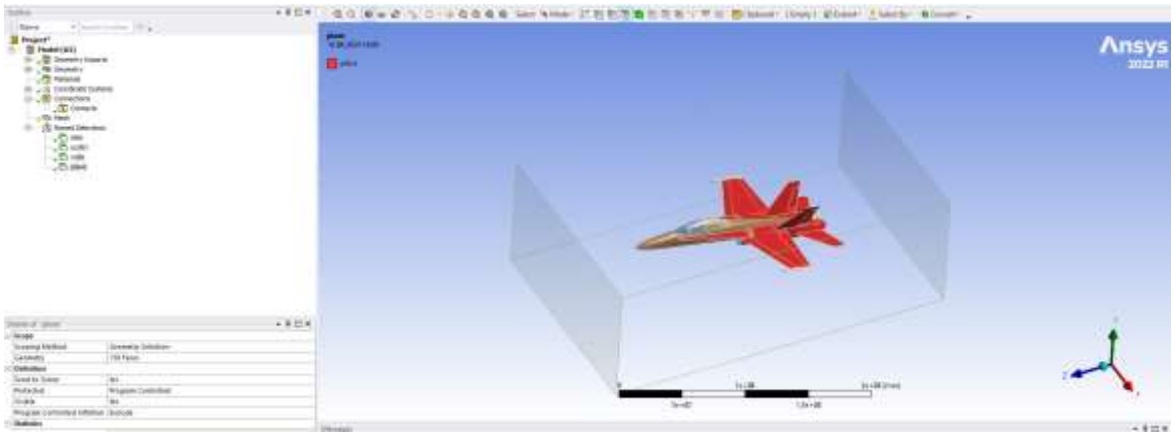

Figure 4. 6: The Part Called the Plane Region.

During the mesh generation phase, creating a mesh structure that aligns with the geometry of the aircraft is a critical step. The quality and detail of the mesh directly impact the accuracy and reliability of the resulting analysis. Initially, a mesh was applied using the default settings recommended by the Ansys software but encountered errors during this process. Consequently, mesh settings were adjusted to predominantly use tetrahedral elements, with multi/zone mesh types assigned to specific regions of the aircraft's geometry, and the process was reattempted. Upon completion of the mesh generation process, the quality of the generated mesh was evaluated. In Computational Fluid Dynamics (CFD) analyses, mesh quality is typically assessed by examining orthogonal quality values. These values provide insights into the homogeneity and geometric suitability of the mesh, thereby enhancing the reliability of the analysis results. Orthogonal quality values are presented in Figure 4.7. Subsequently, the aircraft's mesh generation was completed in accordance with these values.

Orthogonal Quality mesh metrics spectrum:

Unacceptable	Bad	Acceptable	Good	Very good	Excellent
0-0.001	0.001-0.14	0.15-0.20	0.20-0.69	0.70-0.95	0.95-1.00

Figure 4. 7: Orthogonal Quality Reference Values.

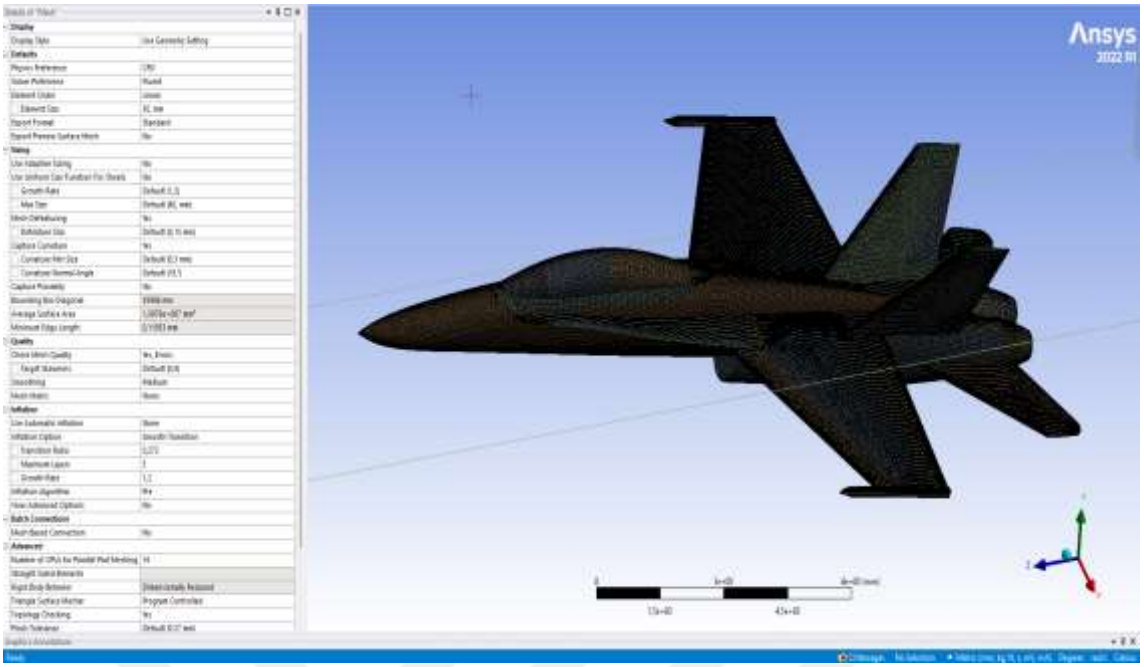

Figure 4. 8: Mesh Visualization of Ansys Analysis.

Multiple combinations were attempted during the mesh generation for the aircraft. As a result of these trials, the mesh with the best quality was achieved with an element size of 30mm. Due to the presence of curved regions in the aircraft's geometry, "capture curvature" was enabled, while "capture proximity" was initially tested as enabled in previous attempts. However, due to errors encountered during mesh generation, "capture proximity" was disabled, and the mesh generation process was completed. When attempting mesh generation using the default settings recommended by Ansys, the element size and adaptive size values were excessively high, leading to the disabling of adaptive sizing and using a smaller element size. The "check mesh quality" command was used with the option "Yes with errors" to better visualize errors in the generated mesh. Additionally, to ensure higher orthogonal quality values for the mesh, the target skewness value was left at the default setting of 0.9 (very good). The detailed table of the generated mesh is provided in Figure 4.9.

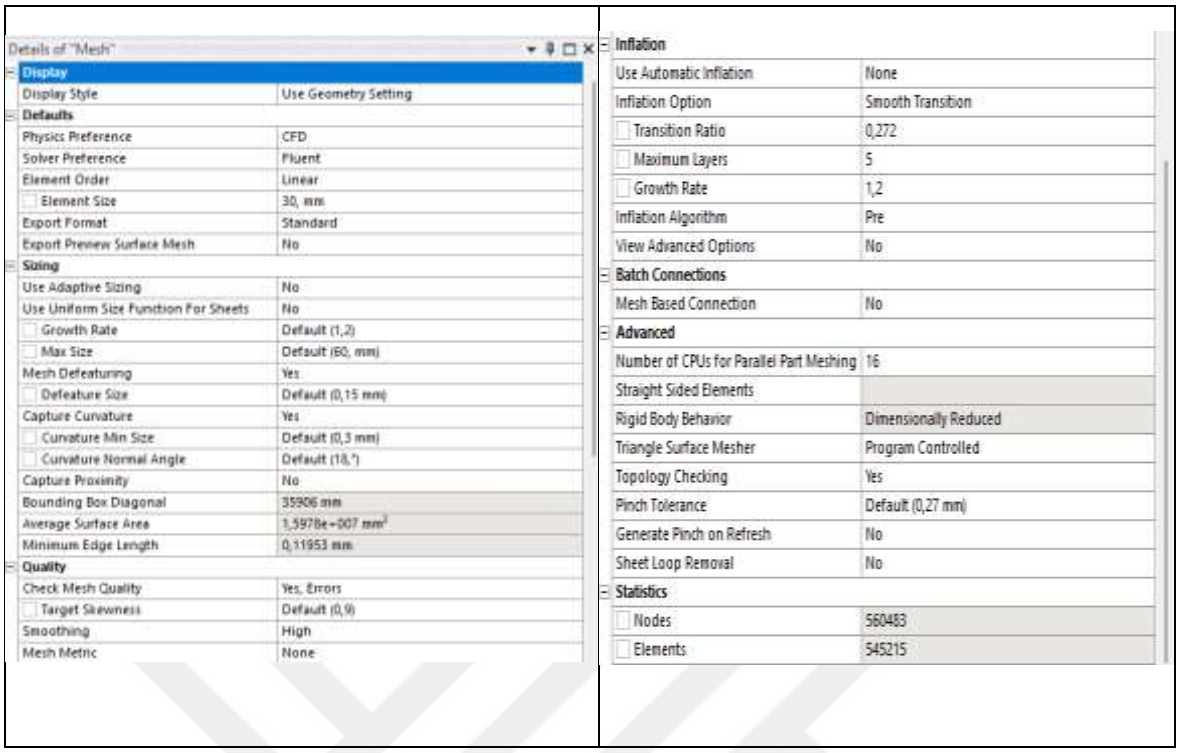

Details of "Mesh"	
Display	
Display Style	Use Geometry Setting
Defaults	
Physics Preference	CFD
Solver Preference	Fluent
Element Order	Linear
Element Size	30, mm
Export Format	Standard
Export Preview Surface Mesh	No
Sizing	
Use Adaptive Sizing	No
Use Uniform Size Function For Sheets	No
Growth Rate	Default (1,2)
Max Size	Default (60, mm)
Mesh Defeaturing	Yes
Defeature Size	Default (0,15 mm)
Capture Curvature	Yes
Curvature Min Size	Default (0,3 mm)
Curvature Normal Angle	Default (18,°)
Capture Proximity	No
Bounding Box Diagonal	35906 mm
Average Surface Area	1,5978e+007 mm²
Minimum Edge Length	0,11953 mm
Quality	
Check Mesh Quality	Yes, Errors
Target Skewness	Default (0,9)
Smoothing	High
Mesh Metric	None

Inflation	
Use Automatic Inflation	None
Inflation Option	Smooth Transition
Transition Ratio	0,272
Maximum Layers	5
Growth Rate	1,2
Inflation Algorithm	Pre
View Advanced Options	No
Batch Connections	
Mesh Based Connection	No
Advanced	
Number of CPUs for Parallel Part Meshing	16
Straight Sided Elements	
Rigid Body Behavior	Dimensionally Reduced
Triangle Surface Mesher	Program Controlled
Topology Checking	Yes
Pinch Tolerance	Default (0,27 mm)
Generate Pinch on Refresh	No
Sheet Loop Removal	No
Statistics	
Nodes	560483
Elements	545215

Figure 4. 9: Details of Mesh.

During the analysis, a velocity value corresponding to 180 knots, which is 92.6 m/s, was assigned at the inlet of the wind tunnel to calculate the lift coefficient of the aircraft. Reference values and solution methods were determined based on research conducted for the analysis. Figures 4.10 and 4.11 below respectively provide the velocity assigned to the wind tunnel, solution methods, and reference values.

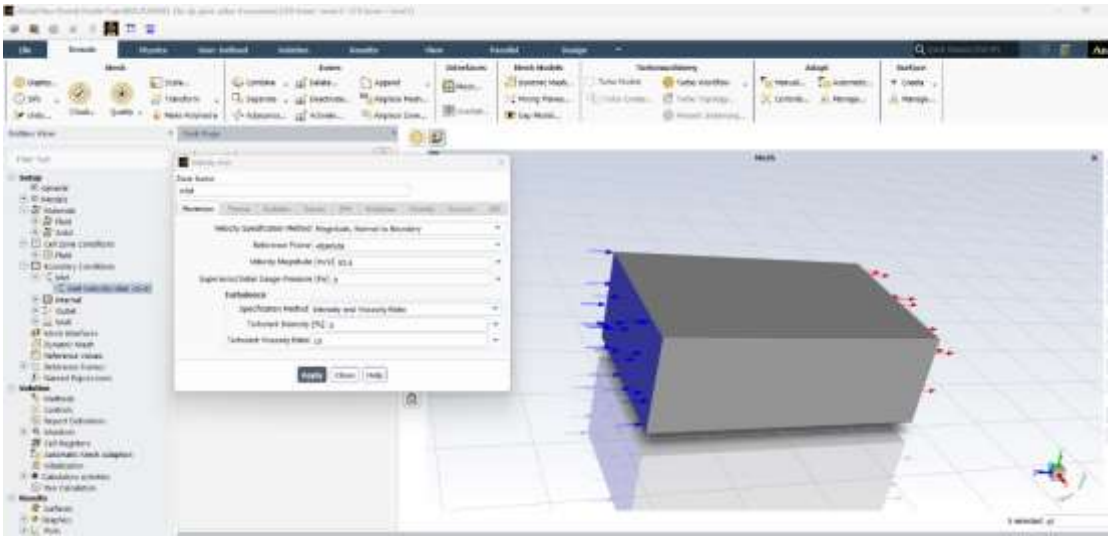

Figure 4. 10: Velocity Magnitude.

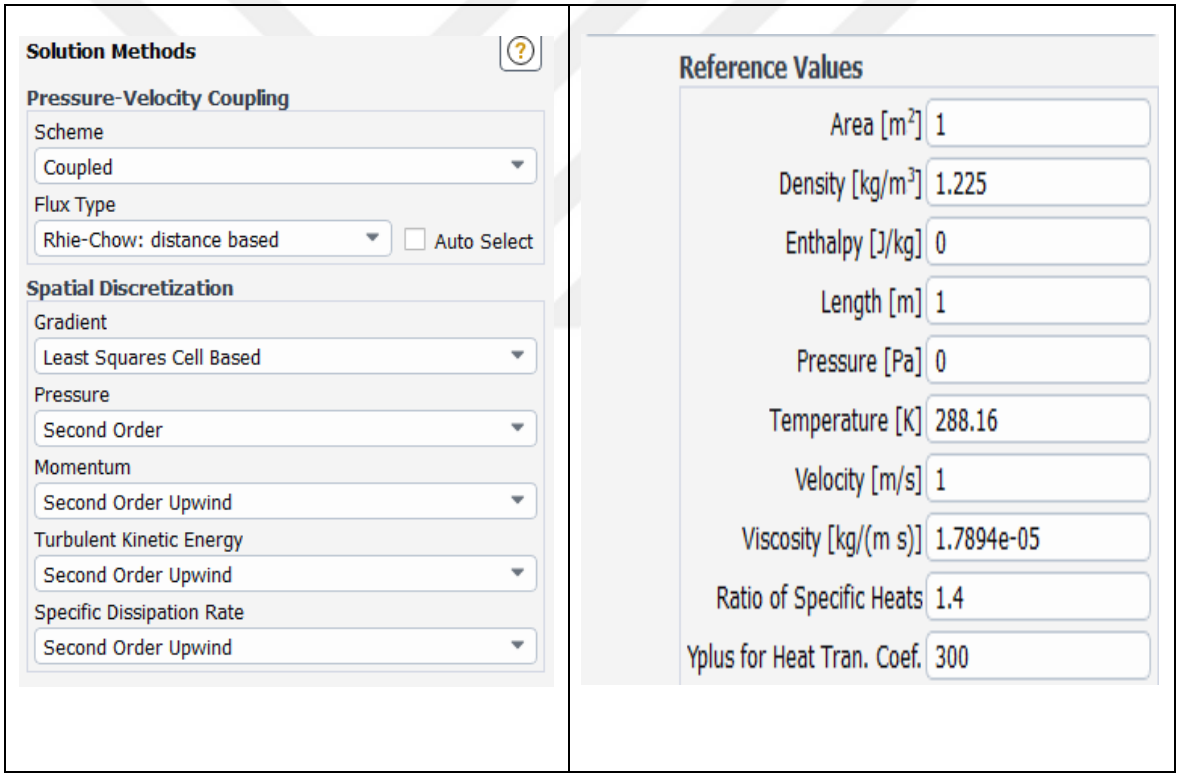

Figure 4. 11: Details of Solution Methods and Reference Values.

The lift coefficient of the aircraft was found to be between 0.850 and 0.910 as a result of the analysis. The graph of the lift coefficient, depicted in Figure 4.12 below, illustrates this variation.

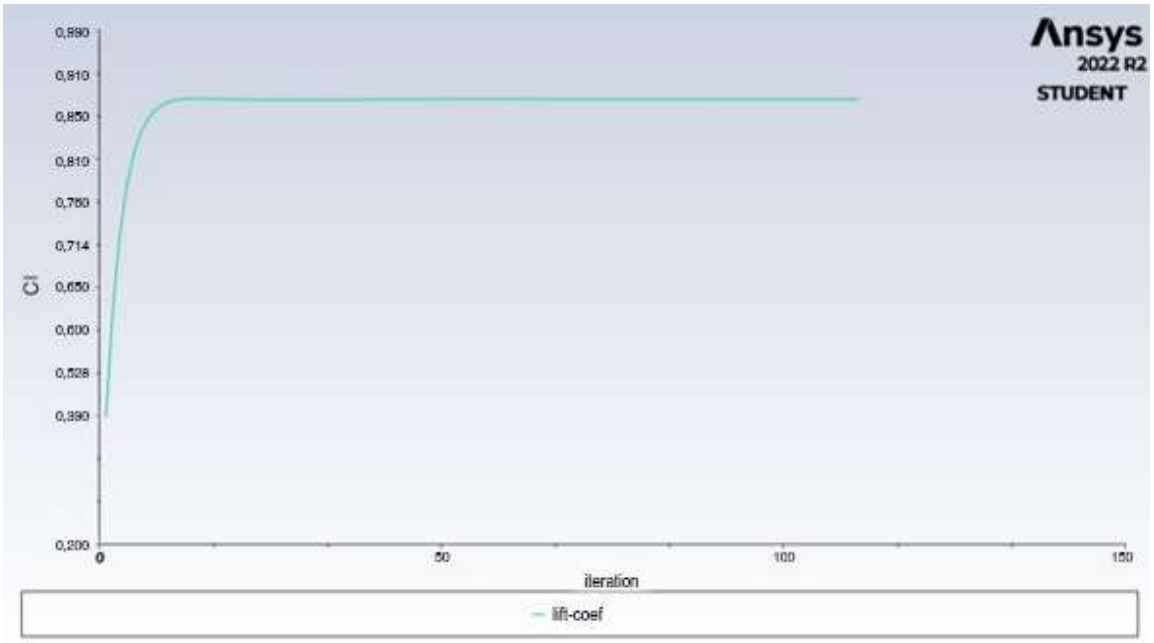

Figure 4. 12: Lift Coefficient Value According To 10-Degree Angle of Attack.

Analysis results according to 4-degree angle of attack

In this section, in addition to the lift values of the aircraft calculated at a 10-degree angle of attack, the lift values at a 4-degree angle of attack were also examined. Thus, in order to evaluate the accuracy of our analyzes and increase the reliability of our results, a detailed analysis was carried out by comparing the lift values obtained at different angles of attack. This additional analysis will provide a more comprehensive view to understand and optimize the performance of the aircraft. The lift coefficient of the aircraft was found to be between 0.390 and 0.514 as a result of the analysis. The graph of the lift coefficient, depicted in Figure 4.13 below, illustrates this variation.

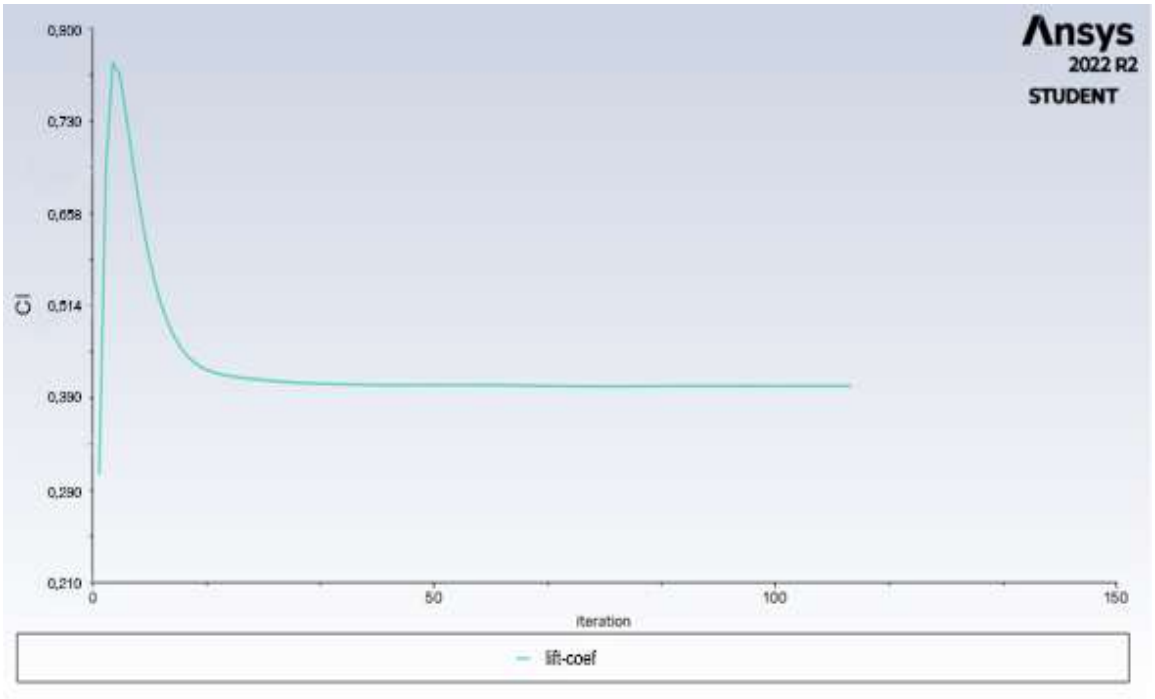

Figure 4. 13: Lift Coefficient Value According To 4-Degree Angle of Attack.

4.2 MATLAB SIMULINK RESULTS OF THE F/A-18 AIRCRAFT

C-13-1 Catapult: The C-13-1 catapult is commonly found on more modern aircraft carriers. It boasts a more advanced design compared to the C-13-0, providing a higher takeoff velocity. These catapults offer a faster and safer takeoff process by utilizing hydraulic systems and more sophisticated technologies.

C-13-2 Catapult: The C-13-2 serves as an enhanced version of the C-13-1 and is typically utilized on aircraft carriers equipped with the latest technologies. This catapult type features advanced systems to ensure higher takeoff speeds and precise takeoff control. Additionally, it delivers more reliable and efficient performance.

Which type is best suited for a particular application or aircraft carrier may depend on a number of factors, such as the size, weight and performance requirements of the aircraft to be used.

Power stroke (in feet) and bITrack length (in feet) values of C-13-0, C-13-1 and C-13-2 catapult types shown in Table 4.1 below are referenced and used in the MATLAB Simulink model.

Table 4.1: Steam Catapult Data [114].

Item	C-13-0	C-13-1	C-13-2
Power stroke (in feet)	249-10”	309-8 3/4”	306-9”
bITrack length (in feet)	264-10”	324-10”	324-10”
Weight of shuttle and pistons (in pounds)	6,350	6,350	6,350
Cylinder bore (in inches)	18	18	18
Power stroke displacement (in cubic feet)	910	1,148	1,527

Table 4.2: Values of the FA-18 Hornet Aircraft [115].

Empty weight	23,000 lbs
Loaded weight	36,970 lbs
Max. takeoff weight	51,900 lbs
Wing Area	46.45 m^2
Wingspan	13.62 m
Angle of attack	10°
Coefficient of Drag	0.02
Length	18.31 m

Table 4.3: Parameters of C/13-0 Type Catapult MATLAB Simulink Model.

Aircraft-Environmental Conditions				**Simulation Results**				
ID	Carrier Speed (Knots)	Wind Speed (m/s)	Takeoff Weight (LBS)	Liftoff Distance (m)	Liftoff Time (s)	Take-off Time (s)	Take-off Speed (Knots)	Catapult Force (Nm)
1	0	0	23000	52.79	1.61	1.94	153.35	268455.37
2	0	0	36970	62.14	1.49	1.65	179.39	782382.54
3	0	0	51900	66.53	1.35	1.45	205.64	1562279.65
4	30	0	23000	49.90	1.24	1.61	156.32	268455.37
5	30	0	36970	59.95	1.22	1.41	182.39	782382.54
6	30	0	51900	65.51	1.15	1.26	207.81	1562279.65
7	20	0	23000	51.91	1.37	1.71	154.54	268455.37
8	20	0	36970	61.13	1.31	1.49	181.39	782382.54
9	20	0	51900	65.54	1.21	1.32	206.62	1562279.65
10	30	5	23000	47.93	1.12	1.51	158.11	268455.37
11	30	5	36970	58.32	1.13	1.34	184.48	782382.54
12	30	5	51900	64.16	1.08	1.2	209.01	1562279.65
13	20	5	23000	49.90	1.24	1.61	156.32	268455.37
14	20	5	36970	59.95	1.22	1.41	182.39	782382.54
15	20	5	51900	65.51	1.15	1.26	207.81	1562279.65
16	30	10	23000	45.34	1	1.42	160.68	268455.37
17	30	10	36970	56.26	1.04	1.27	186.57	782382.54
18	30	10	51900	62.47	1.01	1.15	211.62	1562279.65
19	20	10	23000	47.93	1.12	1.51	158.11	268455.37
20	20	10	36970	58.32	1.13	1.34	184.48	782382.54
21	20	10	51900	64.16	1.08	1.2	209.01	1562279.65

According to the scenarios established, various simulations have been conducted. As a result of these simulations, graphs have been obtained under four different fundamental headings.

The graph titled "Aircraft Takeoff Distance Graph" illustrates the distance-time relationship from the moment the aircraft begins its takeoff. Additionally, annotations on the graph denote specific instances: "Liftoff Time" indicates the moment when the aircraft generates enough lift force, with the assistance of catapult and jet engines, to overcome its own weight while running on the runway. "End of Carrier Time" signifies the time at which the aircraft departs from the carrier (Takeoff Time). "Distance" denotes the distance covered by the aircraft at liftoff.

The graph titled "Aircraft Takeoff Speed Graph" presents the speed of the aircraft as a function of time from the moment of takeoff initiation. Additionally, annotations on the graph indicate the "Takeoff Time," marking the instance when the aircraft departs from the carrier. The parameter "Airspeed" denotes the airspeed of the aircraft as it separates from the carrier.

In the graph labeled "Pitch Angle Graph," the Pitch Angle of the aircraft is depicted as a function of time from the moment of takeoff initiation. Here, an oscillation in the aircraft's angle is observed from the onset of takeoff until the moment of departure. This oscillation represents the motion resulting from the acceleration applied to the aircraft during takeoff. Furthermore, annotations on the graph specify the "End of Carrier Time," denoting the moment when the aircraft separates from the carrier. Beyond this point, the oscillation ceases, and the pitch angle of the aircraft is provided.

The graph titled "Aircraft Altitude Graph" tracks the altitude of the aircraft from the moment of takeoff initiation. It is assumed that the altitude value on the carrier is 20 ft. At takeoff, the Rate of Climb (RoC) is taken as 5000 ft/min. The dashed red line on the graph represents the point at which the aircraft separates from the carrier.

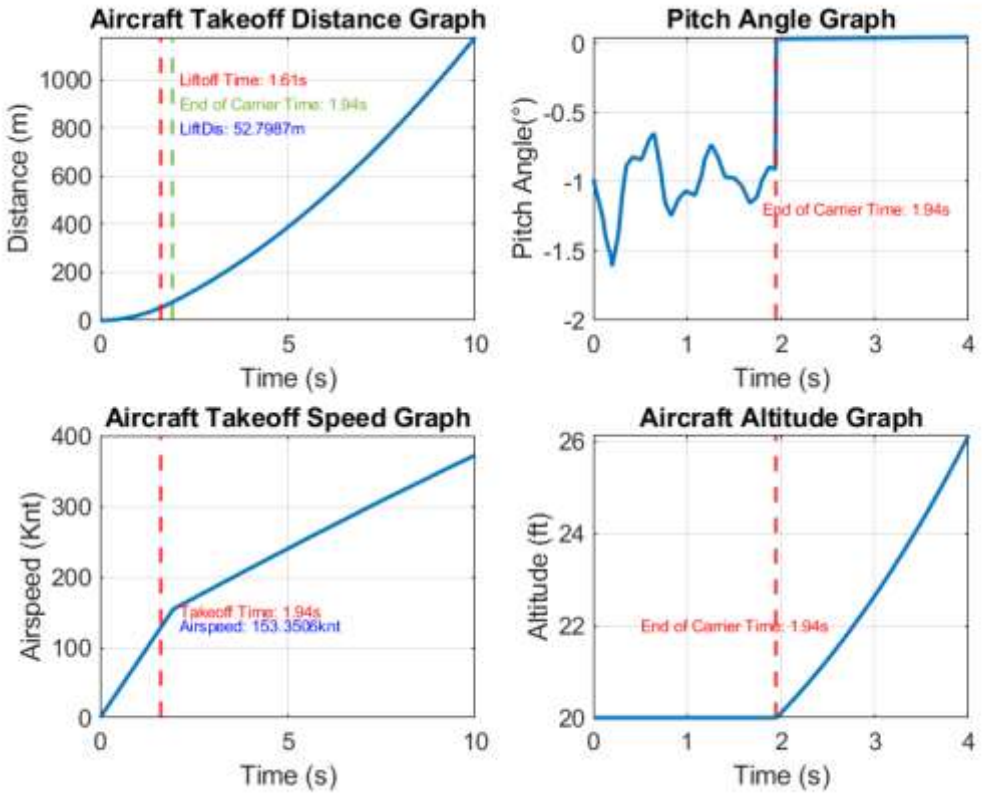

Figure 4. 14: Results of Simulation Number ID:1.

Within the scope of scenario ID:1, the C-13-0 catapult type was employed, with an aircraft weight of 23000lbs assumed, and no carrier or wind velocity considered. In the conducted simulation, upon examination of the "Aircraft Take-off Distance Graph," the Liftoff Time was calculated as 1.61 seconds, while the Take-off Time was determined to be 1.94 seconds. Upon reviewing the results, it was observed that the aircraft was able to reach lift force before departing from the carrier, successfully achieving take-off. It covered a lift off distance 52.79 meters upon reaching the specified lift value. Further analysis of the "Aircraft Take-off Speed Graph" revealed that the aircraft's speed at take-off was calculated to be 153.35 knots.

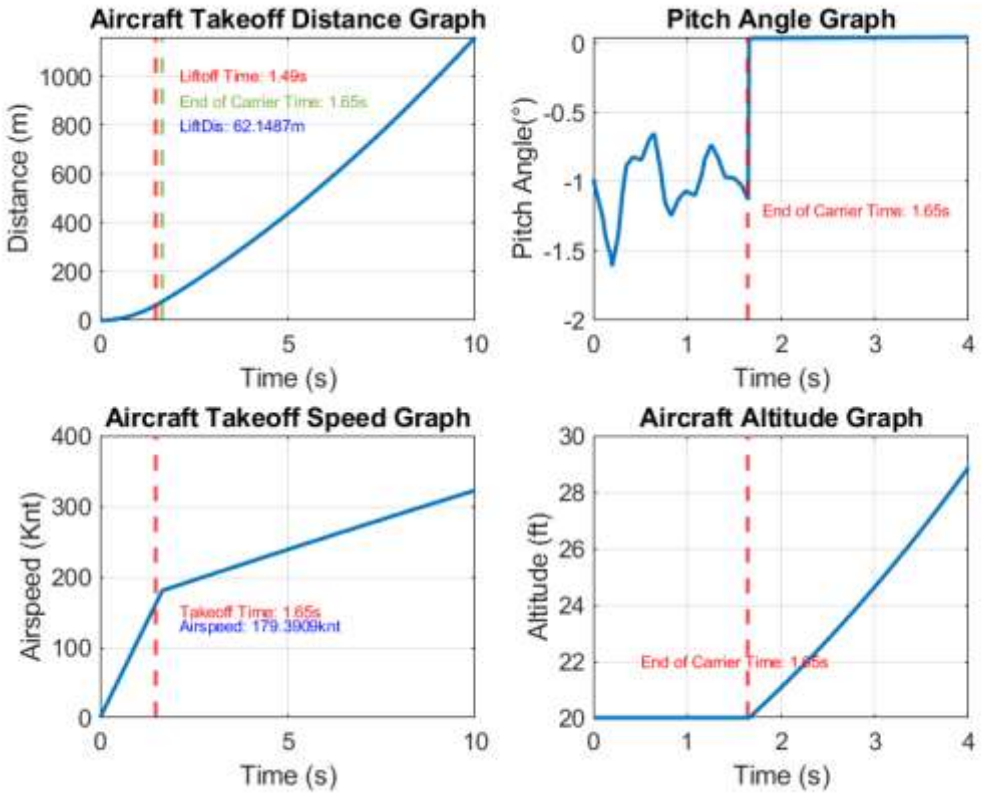

Figure 4. 15: Results of Simulation Number ID:2.

Within the scope of scenario ID:2, the C-13-0 catapult type was employed, with an aircraft weight of 36970lbs assumed, and no carrier or wind velocity considered. In the conducted simulation, upon examination of the "Aircraft Take-off Distance Graph," the Liftoff Time was calculated as 1.49 seconds, while the Take-off Time was determined to be 1.65 seconds. Upon reviewing the results, it was observed that the aircraft was able to reach lift force before departing from the carrier, successfully achieving take-off. It covered a distance of 62.14 meters upon reaching the specified lift value. Further analysis of the "Aircraft Take-off Speed Graph" revealed that the aircraft's speed at take-off was calculated to be 179.39 knots.

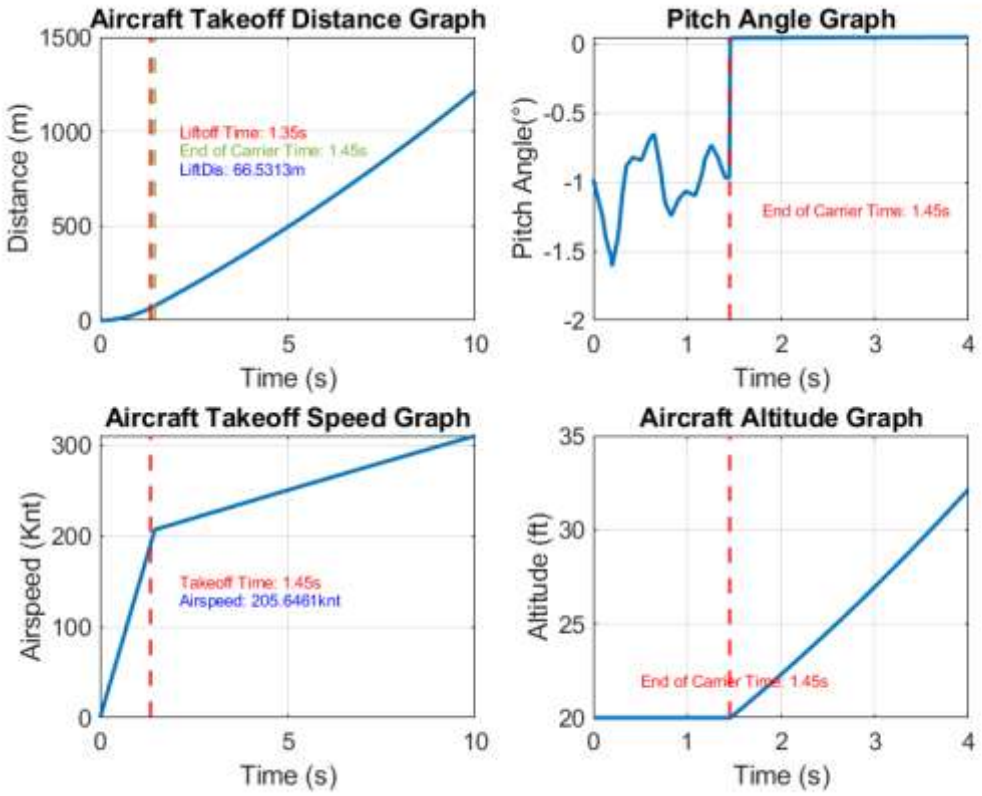

Figure 4. 16: Results of Simulation Number ID:3.

Within the scope of scenario ID:3, the C-13-0 catapult type was employed, with an aircraft weight of 51900lbs assumed, and no carrier or wind velocity considered. In the conducted simulation, upon examination of the "Aircraft Take-off Distance Graph," the Liftoff Time was calculated as 1.35 seconds, while the Take-off Time was determined to be 1.45 seconds. Upon reviewing the results, it was observed that the aircraft was able to reach lift force before departing from the carrier, successfully achieving take-off. It covered a lift off distance 66.53 meters upon reaching the specified lift value. Further analysis of the "Aircraft Take-off Speed Graph" revealed that the aircraft's speed at take-off was calculated to be 205.64 knots.

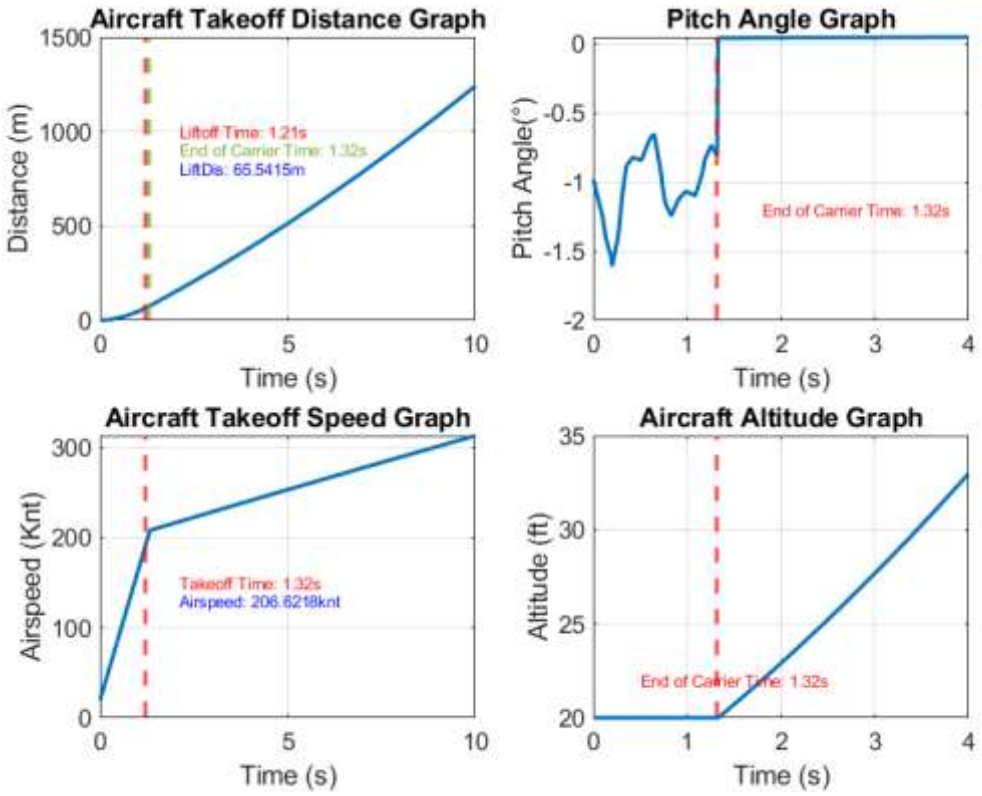

Figure 4. 17: Results of Simulation Number ID:9.

Within the scope of scenario ID:9, the C-13-0 catapult type was employed, with an aircraft weight of 51900lbs assumed, carrier is moving at a speed of 20 knots and there is no wind velocity considered. In the conducted simulation, upon examination of the "Aircraft Take-off Distance Graph," the Liftoff Time was calculated as 1.21 seconds, while the Take-off Time was determined to be 1.32 seconds. Upon reviewing the results, it was observed that the aircraft was able to reach lift force before departing from the carrier, successfully achieving take-off. It covered a lift off distance 65.54 meters upon reaching the specified lift value. Further analysis of the "Aircraft Take-off Speed Graph" revealed that the aircraft's speed at take-off was calculated to be 206.62 knots.

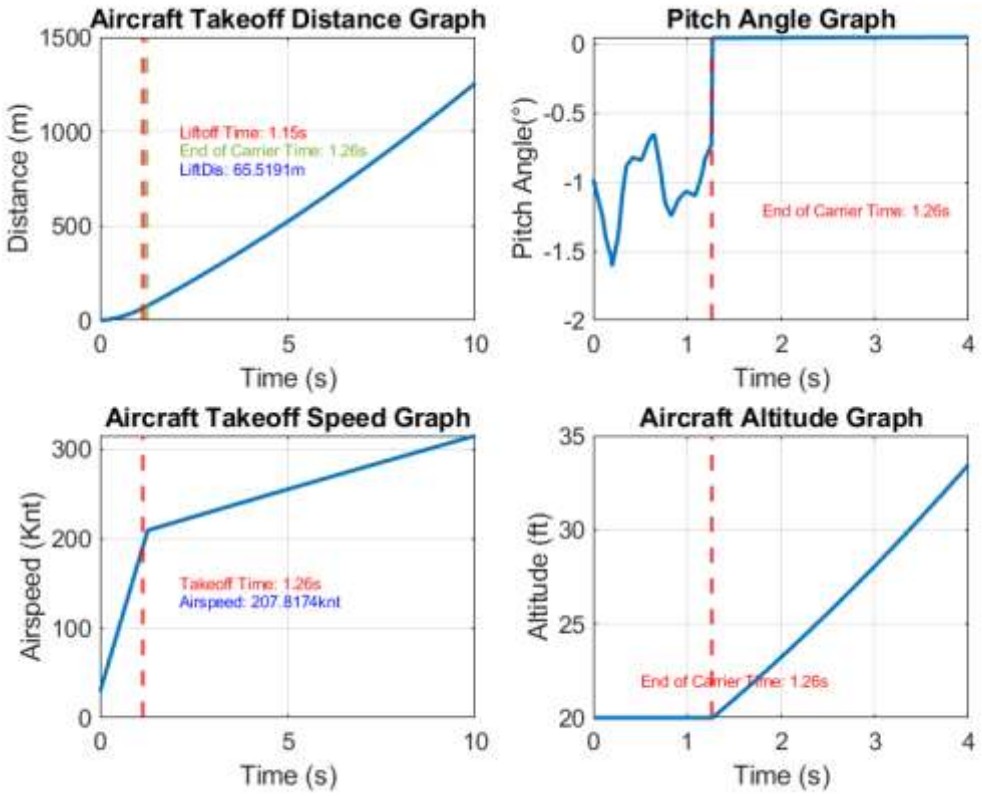

Figure 4. 18: Results of Simulation Number ID:15.

Within the scope of scenario ID:15, the C-13-0 catapult type was employed, with an aircraft weight of 51900lbs assumed, carrier moving at a speed of 20 knots and there is wind velocity at 5m/s considered. In the conducted simulation, upon examination of the "Aircraft Take-off Distance Graph," the Liftoff Time was calculated as 1.15 seconds, while the Take-off Time was determined to be 1.26 seconds. Upon reviewing the results, it was observed that the aircraft was able to reach lift force before departing from the carrier, successfully achieving take-off. It covered a lift off distance 65.51 meters upon reaching the specified lift value. Further analysis of the "Aircraft Take-off Speed Graph" revealed that the aircraft's speed at take-off was calculated to be 207.81 knots.

Table 4.4: Parameters of C/13-1 Type Catapult MATLAB Simulink Model.

Aircraft-Environmental Conditions				**Simulation Results**				
ID	Carrier Speed (Knots)	Carrier Speed (Knots)	Wind Speed (m/s)	Takeoff Weight (LBS)	Liftoff Distance (m)	Liftoff Time (s)	Take-off Time (s)	Take-off Speed (Knots)
22	0	0	0	23000	63.14	1.93	2.37	155.84
23	0	0	0	36970	75.19	1.81	2.03	180.91
24	0	0	0	51900	81.91	1.66	1.79	206.68
25	30	30	0	23000	59.96	1.49	1.96	157.93
26	30	30	0	36970	72.45	1.48	1.73	183.26
27	30	30	0	51900	79.25	1.4	1.55	208.08
28	20	20	0	23000	61.97	1.64	2.09	156.80
29	20	20	0	36970	73.91	1.59	1.83	182.47
30	20	20	0	51900	80.88	1.49	1.63	207.62
31	30	30	5	23000	57.21	1.34	1.85	160.37
32	30	30	5	36970	70.45	1.37	1.64	184.93
33	30	30	5	51900	78.17	1.32	1.48	209.70
34	20	20	5	23000	59.96	1.49	1.96	157.93
35	20	20	5	36970	72.45	1.48	1.73	183.26
36	20	20	5	51900	79.25	1.4	1.55	208.08
37	30	30	10	23000	54.38	1.2	1.74	162.81
38	30	30	10	36970	68.74	1.27	1.56	187.49
39	30	30	10	51900	76.68	1.24	1.42	212.47
40	20	20	10	23000	57.21	1.34	1.85	160.37
41	20	20	10	36970	70.45	1.37	1.64	184.93
42	20	20	10	51900	78.17	1.32	1.48	209.70

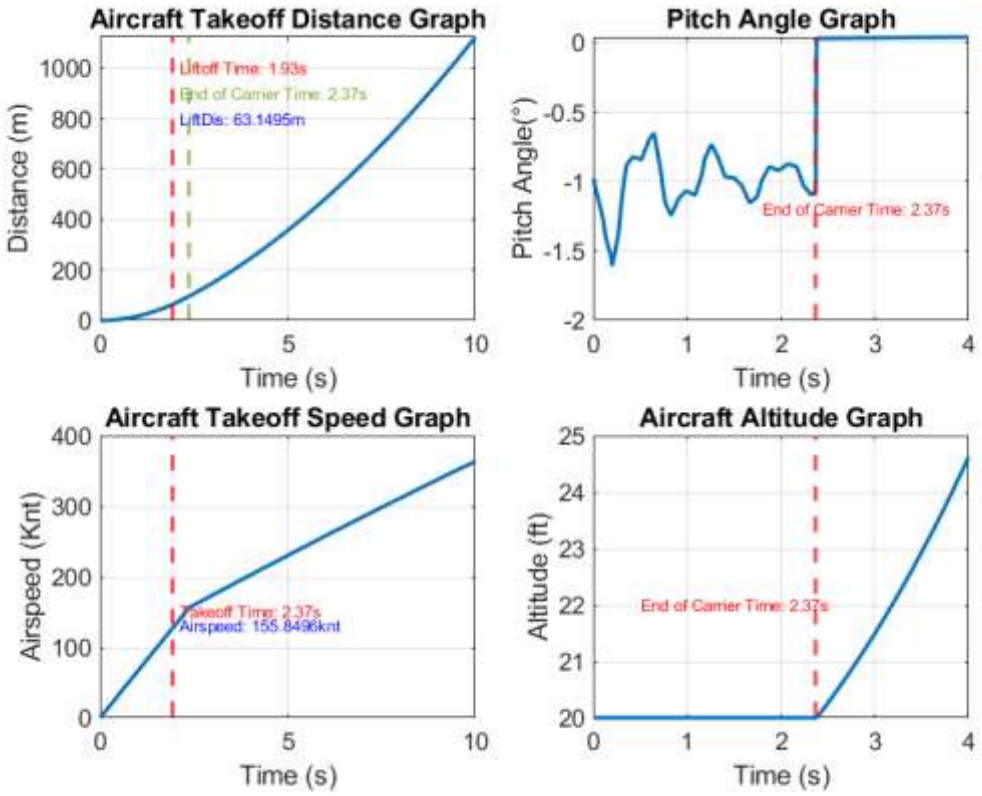

Figure 4. 19: Results of Simulation Number ID:22.

Within the scope of scenario ID:22, the C-13-1 catapult type was employed, with an aircraft weight of 23000lbs assumed, and no ship or wind velocity considered. In the conducted simulation, upon examination of the "Aircraft Take-off Distance Graph," the Liftoff Time was calculated as 1.93 seconds, while the Take-off Time was determined to be 2.37 seconds. Upon reviewing the results, it was observed that the aircraft was able to reach lift force before departing from the carrier, successfully achieving take-off. It covered a lift off distance 63.14 meters upon reaching the specified lift value. Further analysis of the "Aircraft Take-off Speed Graph" revealed that the aircraft's speed at take-off was calculated to be 155.84 knots.

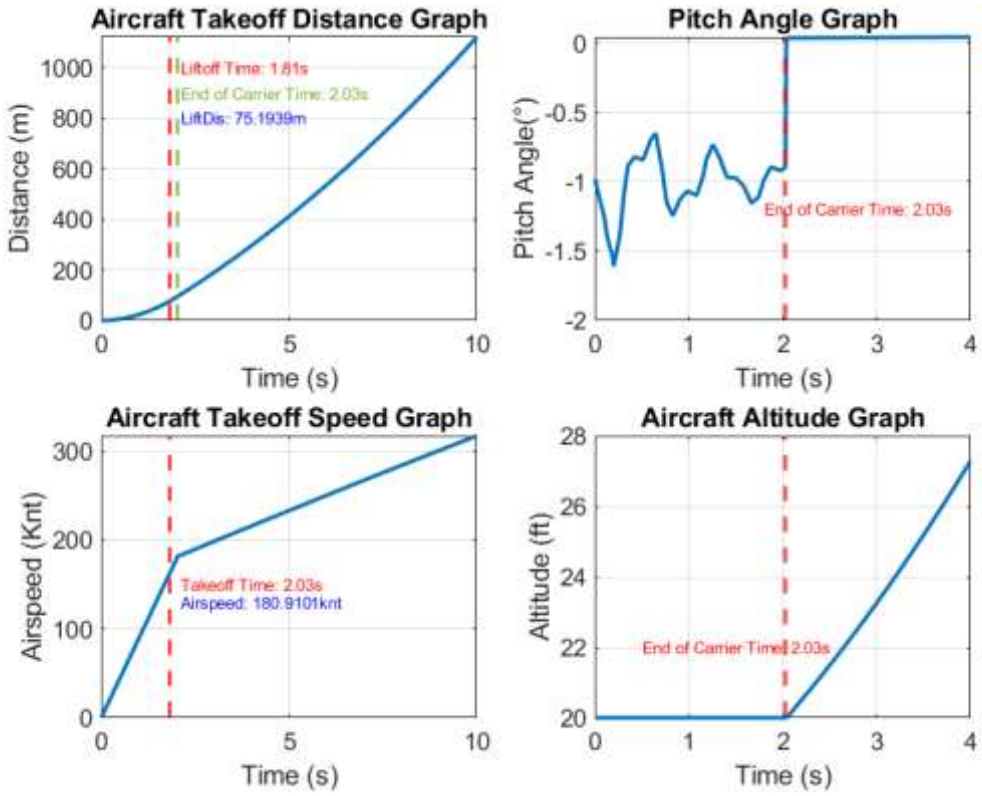

Figure 4. 20: Results of Simulation Number ID:23.

Within the scope of scenario ID:23, the C-13-1 catapult type was employed, with an aircraft weight of 36970lbs assumed, and no carrier or wind velocity considered. In the conducted simulation, upon examination of the "Aircraft Take-off Distance Graph," the Liftoff Time was calculated as 1.81 seconds, while the Take-off Time was determined to be 2.03 seconds. Upon reviewing the results, it was observed that the aircraft was able to reach lift force before departing from the carrier, successfully achieving take-off. It covered a lift off distance 75.19 meters upon reaching the specified lift value. Further analysis of the "Aircraft Take-off Speed Graph" revealed that the aircraft's speed at take-off was calculated to be 180.91 knots.

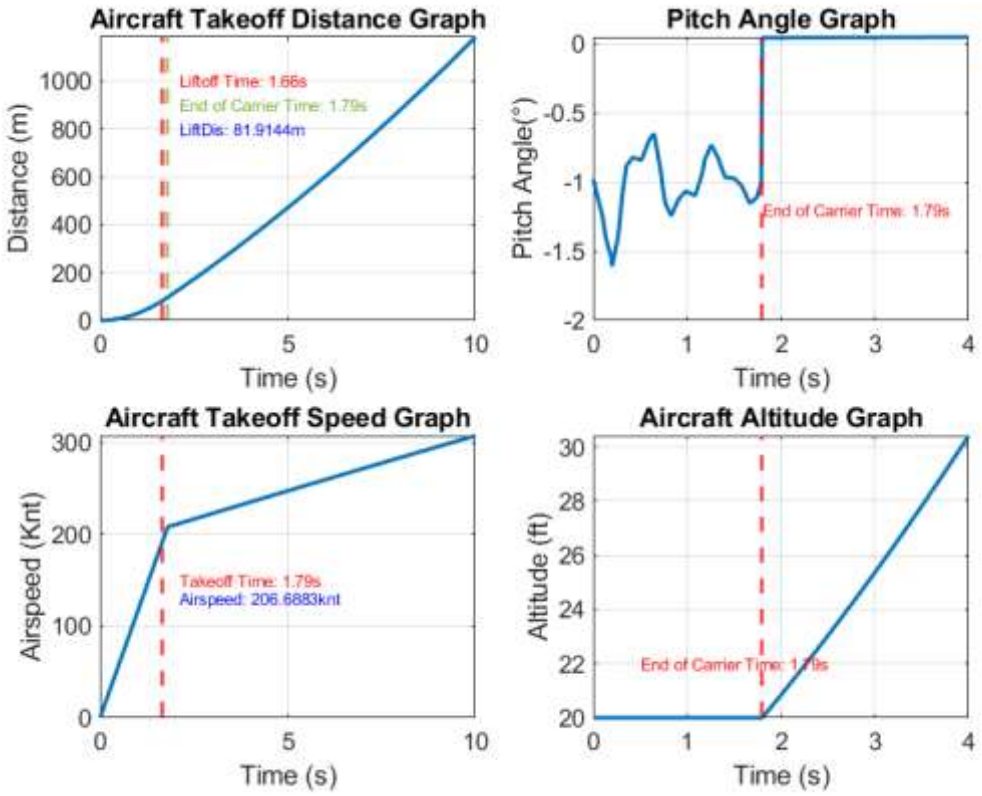

Figure 4. 21: Results of Simulation Number ID:24.

Within the scope of scenario ID:24, the C-13-1 catapult type was employed, with an aircraft weight of 51900lbs assumed, and no carrier or wind velocity considered. In the conducted simulation, upon examination of the "Aircraft Take-off Distance Graph," the Liftoff Time was calculated as 1.66 seconds, while the Take-off Time was determined to be 1.79 seconds. Upon reviewing the results, it was observed that the aircraft was able to reach lift force before departing from the carrier, successfully achieving take-off. It covered a lift off distance 81.91 meters upon reaching the specified lift value. Further analysis of the "Aircraft Take-off Speed Graph" revealed that the aircraft's speed at take-off was calculated to be 206.68 knots.

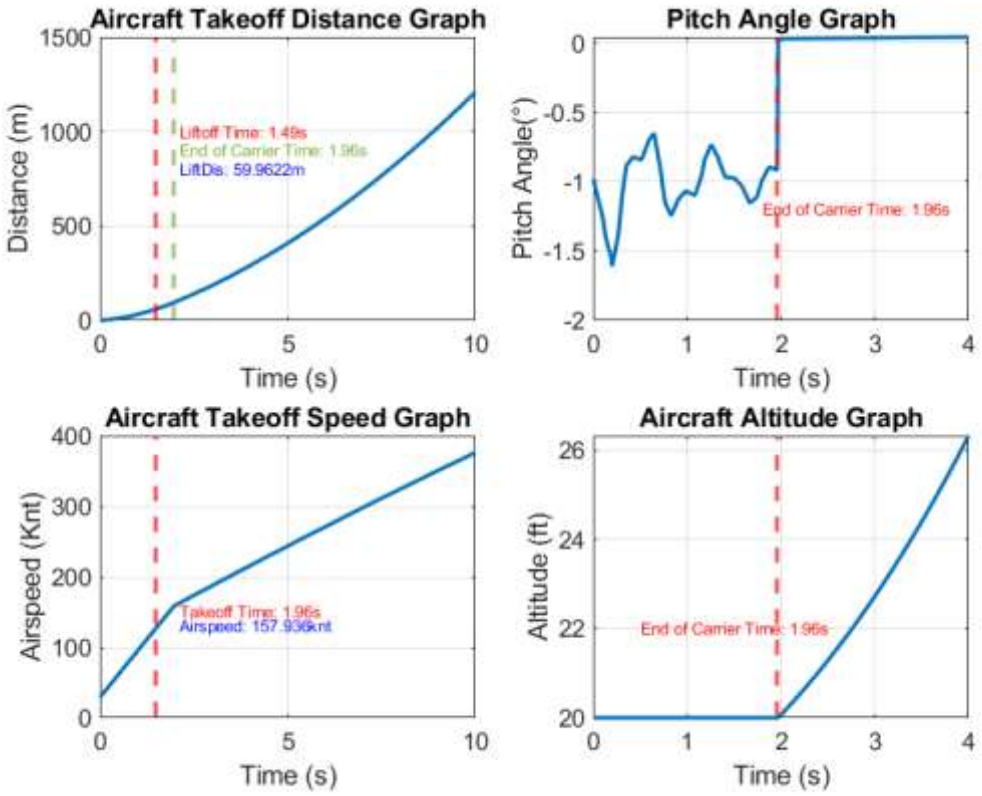

Figure 4. 22: Results of Simulation Number ID:30.

Within the scope of scenario ID:30, the C-13-1 catapult type was employed, with an aircraft weight of 51900lbs assumed, carrier is moving at a speed of 20 knots and there is no wind velocity considered. In the conducted simulation, upon examination of the "Aircraft Take-off Distance Graph," the Liftoff Time was calculated as 1.49 seconds, while the Take-off Time was determined to be 1.63 seconds. Upon reviewing the results, it was observed that the aircraft was able to reach lift force before departing from the carrier, successfully achieving take-off. It covered a lilt off distance 80.88 meters upon reaching the specified lift value. Further analysis of the "Aircraft Take-off Speed Graph" revealed that the aircraft's speed at take-off was calculated to be 207.62 knots.

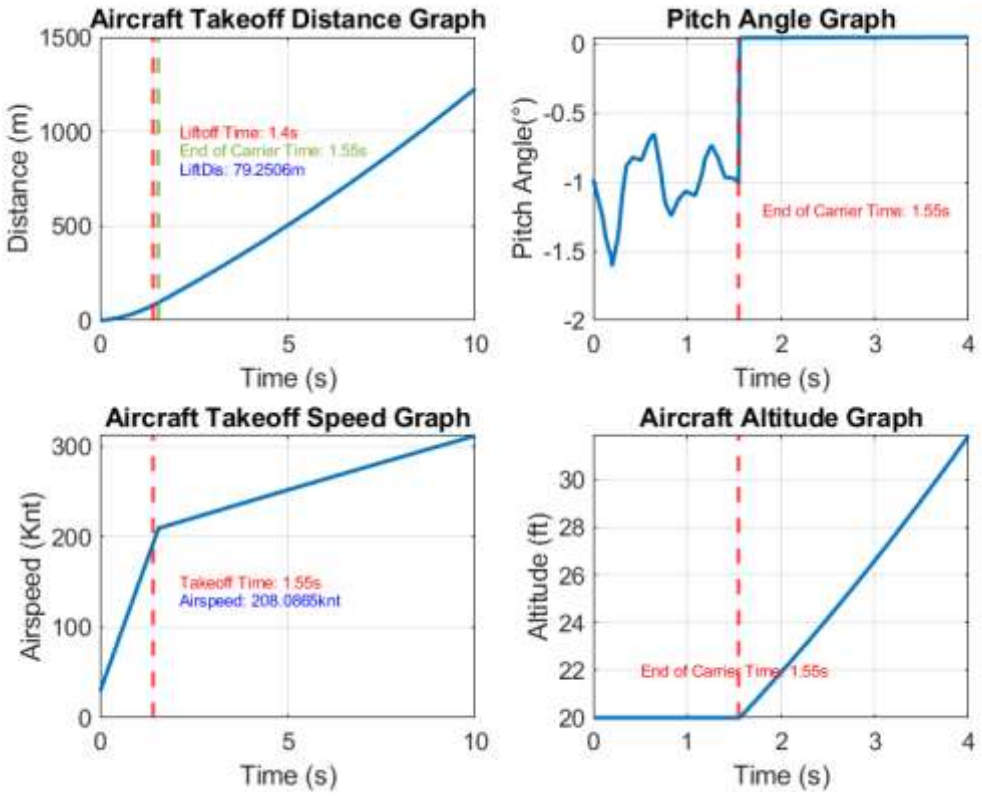

Figure 4. 23: Results of Simulation Number ID:36.

Within the scope of scenario ID:36, the C-13-1 catapult type was employed, with an aircraft weight of 51900lbs assumed, carrier moving at a speed of 20 knots and there is wind velocity at 5m/s considered. In the conducted simulation, upon examination of the "Aircraft Take-off Distance Graph," the Liftoff Time was calculated as 1.4 seconds, while the Take-off Time was determined to be 1.55 seconds. Upon reviewing the results, it was observed that the aircraft was able to reach lift force before departing from the carrier, successfully achieving take-off. It covered a lift off distance 79.25 meters upon reaching the specified lift value. Further analysis of the "Aircraft Take-off Speed Graph" revealed that the aircraft's speed at take-off was calculated to be 208.08 knots.

Table 4.5: Parameters of C/13-2 Type Catapult MATLAB Simulink Model.

Aircraft-Environmental Conditions				**Simulation Results**				
ID	Carrier Speed (Knots)	Carrier Speed (Knots)	Wind Speed (m/s)	Takeoff Weight (LBS)	Liftoff Distance (m)	Liftoff Time (s)	Take-off Time (s)	Take-off Speed (Knots)
43	0	0	0	23000	63.00	1.92	2.34	155.12
44	0	0	0	36970	74.19	1.79	2.01	180.71
45	0	0	0	51900	80.68	1.64	1.77	206.25
46	30	30	0	23000	59.60	1.48	1.95	158.31
47	30	30	0	36970	72.06	1.47	1.72	183.72
48	30	30	0	51900	78.79	1.39	1.54	208.56
49	20	20	0	23000	61.03	1.62	2.07	156.59
50	20	20	0	36970	73.59	1.58	1.81	182.12
51	20	20	0	51900	80.49	1.48	1.61	207.01
52	30	30	5	23000	56.80	1.33	1.83	160.04
53	30	30	5	36970	70.00	1.36	1.63	185.32
54	30	30	5	51900	77.66	1.31	1.47	210.10
55	20	20	5	23000	59.60	1.48	1.95	158.31
56	20	20	5	36970	72.06	1.47	1.72	183.72
57	20	20	5	51900	78.79	1.39	1.54	208.56
58	30	30	10	23000	53.91	1.19	1.73	163.08
59	30	30	10	36970	67.40	1.25	1.55	187.82
60	30	30	10	51900	76.11	1.23	1.4	211.65
61	20	20	10	23000	56.80	1.33	1.83	160.04
62	20	20	10	36970	70.00	1.36	1.63	185.32
63	20	20	10	51900	77.66	1.31	1.47	210.10

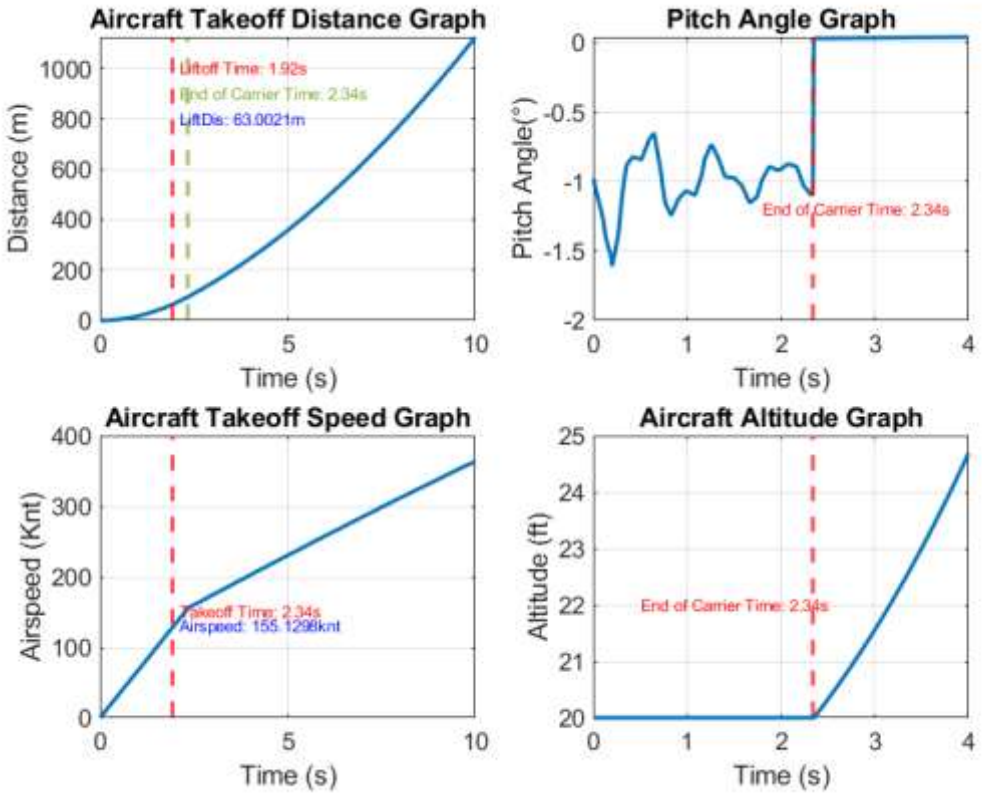

Figure 4. 24: Results of Simulation Number ID:43.

Within the scope of scenario ID:43, the C-13-2 catapult type was employed, with an aircraft weight of 23000lbs assumed, carrier is not moving and there is no wind velocity considered. In the conducted simulation, upon examination of the "Aircraft Take-off Distance Graph," the Liftoff Time was calculated as 1.92 seconds, while the Take-off Time was determined to be 2.34 seconds. Upon reviewing the results, it was observed that the aircraft was able to reach lift force before departing from the carrier, successfully achieving take-off. It covered a lift off distance 63 meters upon reaching the specified lift value. Further analysis of the "Aircraft Take-off Speed Graph" revealed that the aircraft's speed at take-off was calculated to be 155.12 knots.

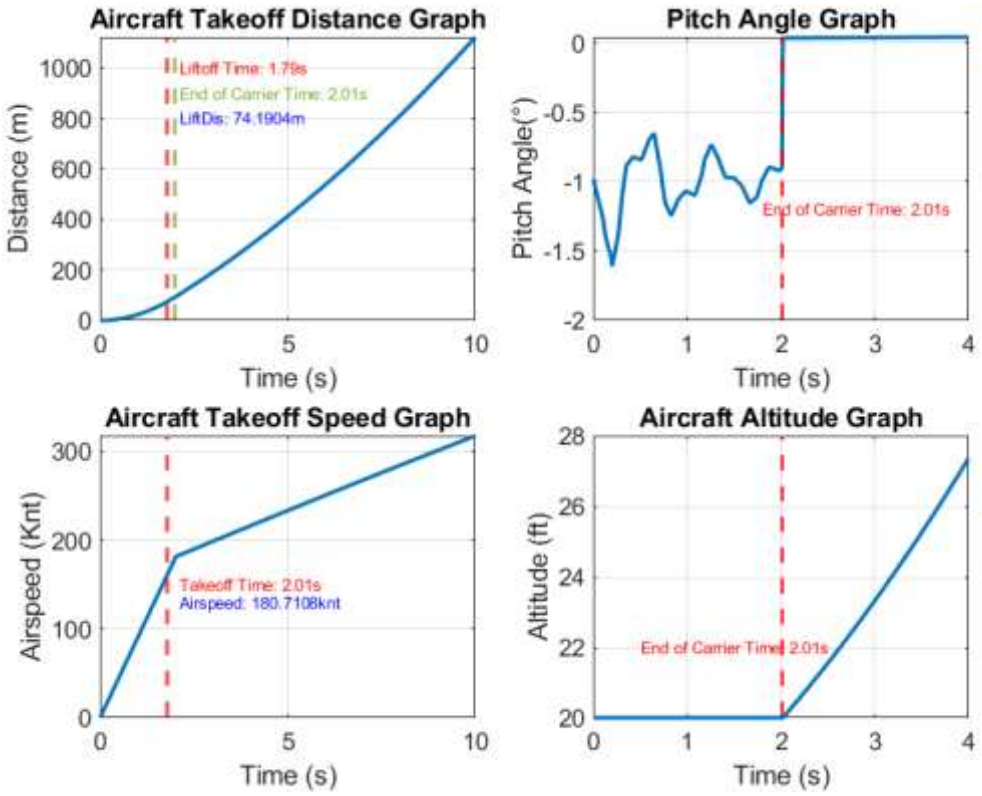

Figure 4. 25: Results of Simulation Number ID:44.

Within the scope of scenario ID:44, the C-13-2 catapult type was employed, with an aircraft weight of 36970lbs assumed, carrier is not moving and there is no wind velocity considered. In the conducted simulation, upon examination of the "Aircraft Take-off Distance Graph," the Liftoff Time was calculated as 1.79 seconds, while the Take-off Time was determined to be 2.01 seconds. Upon reviewing the results, it was observed that the aircraft was able to reach lift force before departing from the carrier, successfully achieving take-off. it covered a distance of 74.19 meters upon reaching the specified lift value. Further analysis of the "Aircraft Take-off Speed Graph" revealed that the aircraft's speed at take-off was calculated to be 180.71 knots.

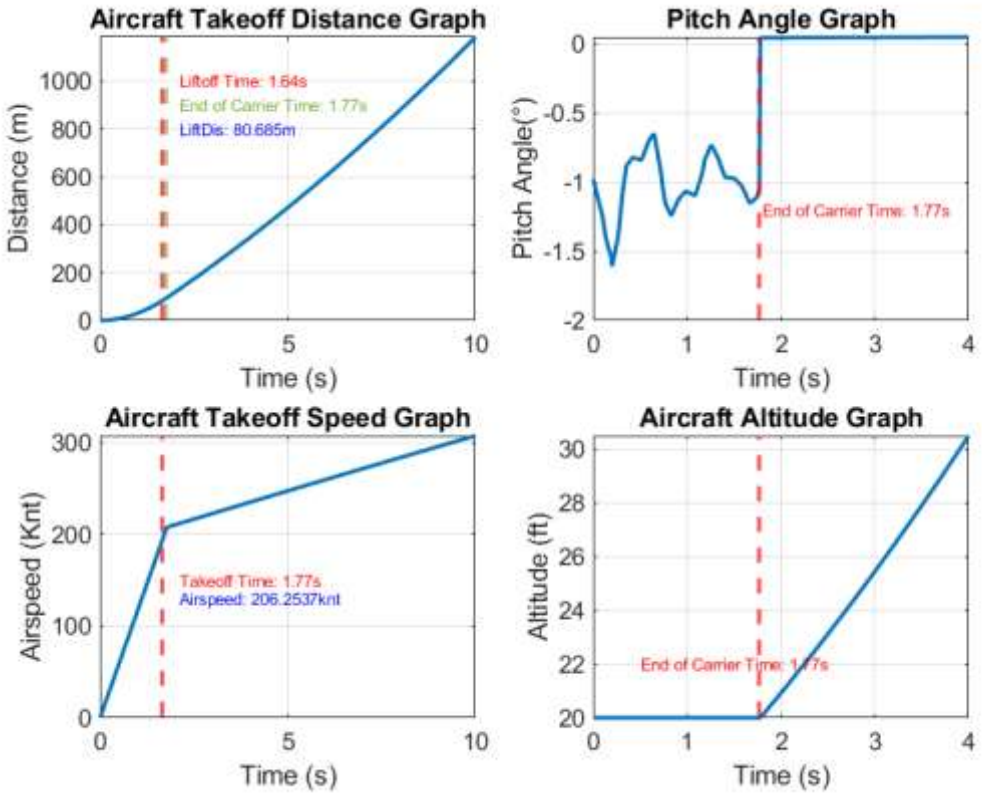

Figure 4. 26: Results of Simulation Number ID:45.

Within the scope of scenario ID:45, the C-13-2 catapult type was employed, with an aircraft weight of 51900lbs assumed, carrier is not moving and there is no wind velocity considered. In the conducted simulation, upon examination of the "Aircraft Take-off Distance Graph," the Liftoff Time was calculated as 1.64 seconds, while the Take-off Time was determined to be 1.77 seconds. Upon reviewing the results, it was observed that the aircraft was able to reach lift force before departing from the carrier, successfully achieving take-off. It covered a distance of 80.68 meters upon reaching the specified lift value. Further analysis of the "Aircraft Take-off Speed Graph" revealed that the aircraft's speed at take-off was calculated to be 206.25 knots.

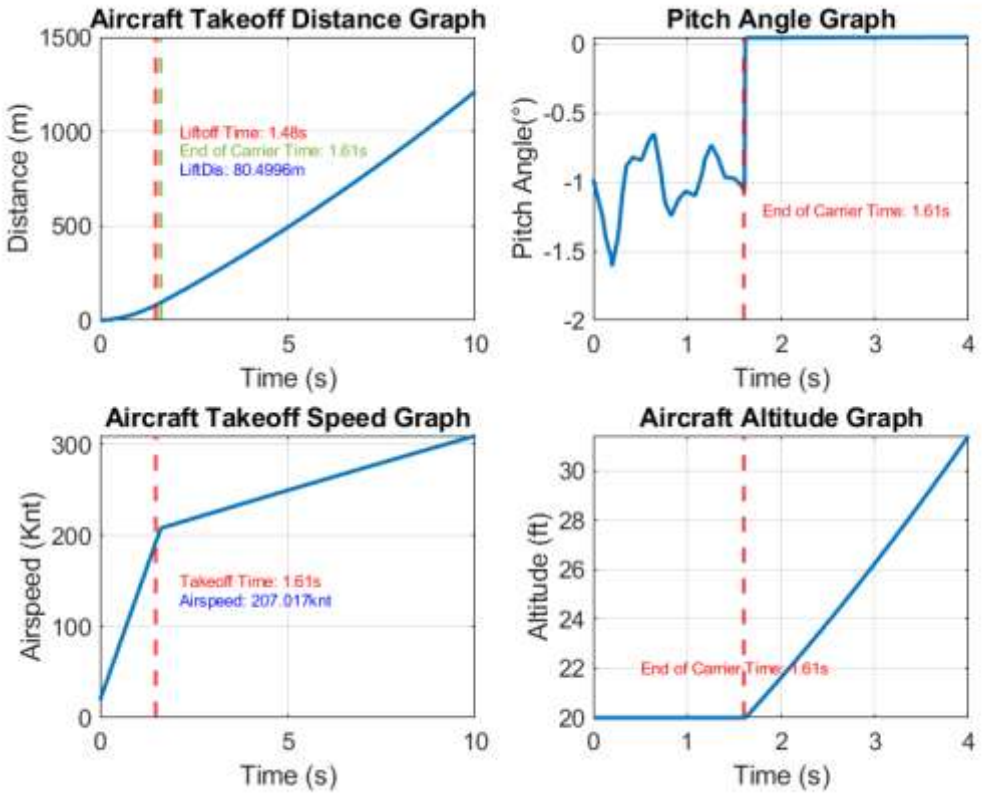

Figure 4. 27: Results of Simulation Number ID:51.

Within the scope of scenario ID:51, the C-13-2 catapult type was employed, with an aircraft weight of 51900lbs assumed, carrier is moving at a speed of 20 knots and there is no wind velocity considered. In the conducted simulation, upon examination of the "Aircraft Take-off Distance Graph," the Liftoff Time was calculated as 1.48 seconds, while the Take-off Time was determined to be 1.61 seconds. Upon reviewing the results, it was observed that the aircraft was able to reach lift force before departing from the carrier, successfully achieving take-off. It covered a distance of 80.49 meters upon reaching the specified lift value. Further analysis of the "Aircraft Take-off Speed Graph" revealed that the aircraft's speed at take-off was calculated to be 207.01 knots.

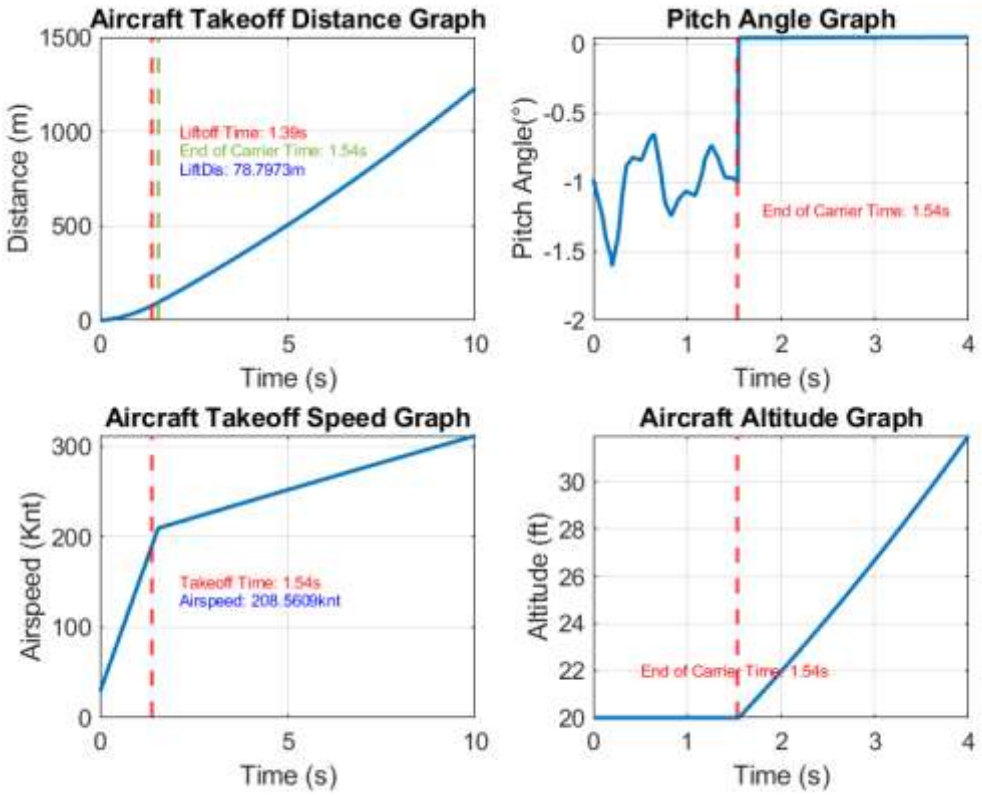

Figure 4. 28: Results of Simulation Number ID:57.

Within the scope of scenario ID:57, the C-13-2 catapult type was employed, with an aircraft weight of 51900lbs assumed, carrier moving at a speed of 20 knots and there is wind velocity at 5m/s considered. In the conducted simulation, upon examination of the "Aircraft Take-off Distance Graph," the Liftoff Time was calculated as 1.39 seconds, while the Take-off Time was determined to be 1.54 seconds. Upon reviewing the results, it was observed that the aircraft was able to reach lift force before departing from the carrier, successfully achieving take-off. It covered a distance of 78.79 meters upon reaching the specified lift value. Further analysis of the "Aircraft Take-off Speed Graph" revealed that the aircraft's speed at take-off was calculated to be 208.56 knots.

4.3 CFD ANALYSIS MODEL OF LIGHT ATTACK AIRCRAFT

In this section, the same meshing procedure applied to the F/A-18 model has been replicated. Initially, the aircraft was adjusted to a 10-degree angle of attack in the SolidWorks program, and then the part was loaded into the Ansys program for analysis purposes. Here, the initial step involved creating the wind tunnel. The parameters applied to the F/A-18 aircraft were also implemented for this model. Dimensions along the x and y axes were set to 3 meters each, while the z-axis dimension was determined to be 6 meters to form the wind tunnel.

Following this, a renaming procedure was executed to streamline the analysis process. Drawing inspiration from the naming conventions employed in the previous analysis, adjustments were made accordingly. The leading and trailing surfaces encircling the aircraft's airflow zone were designated as the "inlet" and "outlet," respectively. The "inlet" zone serves as the entry point for airflow, facilitating its ingress, while the "outlet" region marks the exit point where airflow departs the area. The lateral surfaces were denoted as "walls" to demarcate the boundaries of the airflow domain. Defining the aircraft within this framework involved concealing the faces of the airflow region and utilizing a bulk selection command within the software to encompass the entire aircraft surface, referred to subsequently as the "plane." This renaming protocol enhances the delineation of specific regions throughout the analysis and contributes to a more precise interpretation of the analysis outcomes.

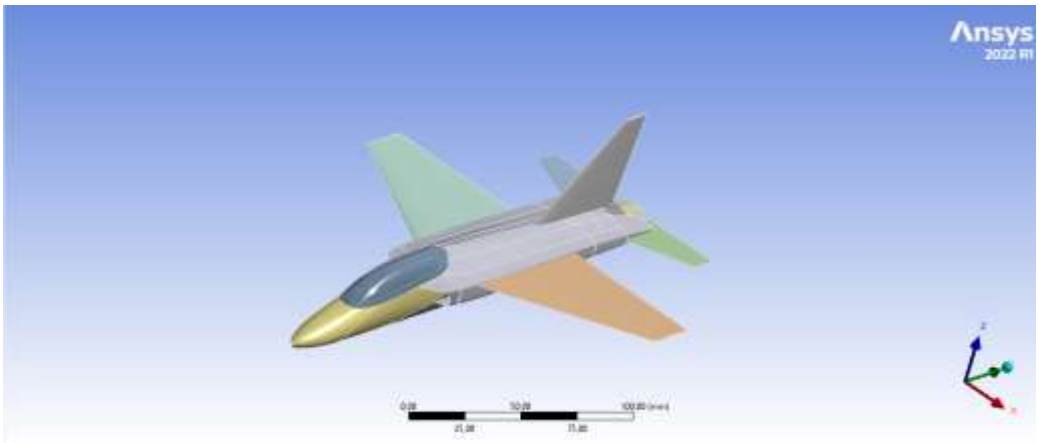

Figure 4. 29: Light Attack Aircraft at 10-Degree Angle of Attack.

In the mesh generation stage, creating a mesh structure that aligns with the aircraft's geometry is a critical step. The quality and detail of the mesh directly influence the accuracy and reliability of the results obtained. In our model, mesh settings were primarily set to tetrahedron, but in certain specialized areas dictated by the aircraft's geometry, a multi/zone mesh type was assigned for mesh generation. Other parameters in the Details of Mesh tab were entered consistent with the analysis of the F/A-18 model. Following the completion of mesh generation, we evaluated the quality of the generated mesh. These assessments provide insights into the homogeneity and geometric conformity of the mesh, thereby enhancing the reliability of the analysis results. The target skewness value was left at the default of 0.9 (very good) to ensure higher orthogonal quality values.

Throughout the analysis process, the determination of the aircraft's lift coefficient involved assigning a velocity of 92.6 m/s, equivalent to 180 knots, at the entrance section of the wind tunnel. Furthermore, after thorough research, appropriate reference values were inputted in the Reference Values and Solution Methods section, deemed suitable for the analysis.

The analysis results indicated that the lift coefficient of the aircraft ranged between 0.480 and 0.560. The graph of the lift coefficient, as shown in Figure 4.30 below, illustrates this variation.

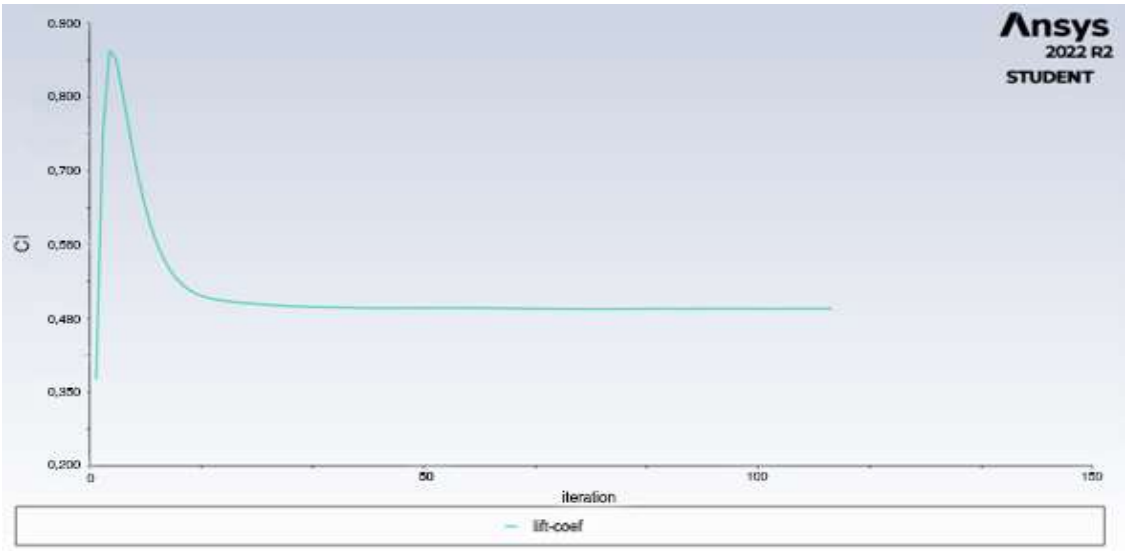

Figure 4. 30: Lift Coefficient Value for LCA at 10-Degree Angle of Attack.

4.4 MATLAB SIMULINK RESULTS OF LIGHT ATTACK AIRCRAFT

In this section, Simulink analyses of a lightweight attack aircraft, with the specified weights, were conducted. The analysis commenced with a simulation of take-off from an aircraft carrier in Section 4.2, focusing on the performance of the F/A-18 aircraft. Subsequently, to facilitate comparative analysis, modifications were made to the model to center the investigation on the lightweight attack aircraft. These modifications encompassed adjustments to parameters such as the engine specifications, aircraft weight, and lift coefficient (CL value), tailored to the characteristics of the lightweight attack aircraft. Following these adjustments, a similar simulation was executed to analyze the performance of the lightweight attack aircraft. The objective of this study is to contribute to the design and operational decision-making process by comparing the take-off performance of different aircraft. The detailed results of the model simulations for the lightweight attack aircraft have been thoroughly analysed, and the obtained data is comprehensively elucidated in the subsequent section. These findings provide crucial insights for identifying the most suitable aircraft for take-off from an aircraft carrier and enhancing operational efficiency.

Table 4.6: Estimated Values for Light Attack Aircraft.

Empty weight	9500 lbs
Loaded weight	12825 lbs
Max. takeoff weight	18825 lbs
Wing Area	35 m^2
Wingspan	9.5 m
Angle of attack	10°
Coefficient of Drag	0.025
Length	13.6 m

Table 4.7: Parameters of C/13-0 Type Catapult MATLAB Simulink Model.

Aircraft-Environmental Conditions				**Simulation Results**				
ID	Carrier Speed (Knots)	Carrier Speed (Knots)	Wind Speed (m/s)	Takeoff Weight (LBS)	Liftoff Distance (m)	Liftoff Time (s)	Take-off Time (s)	Take-off Speed (Knots)
1	0	0	0	9500	41.63	1.7	2.31	128.78
2	0	0	0	12825	47.12	1.65	2.1	140.86
3	0	0	0	18825	54.27	1.57	1.86	158.91
4	30	30	0	9500	37.72	1.18	1.84	131.53
5	30	30	0	12825	43.46	1.21	1.71	143.71
6	30	30	0	18825	51.74	1.23	1.56	162.33
7	20	20	0	9500	40.22	1.36	1.99	130.24
8	20	20	0	12825	45.59	1.36	1.83	142.09
9	20	20	0	18825	52.92	1.34	1.65	160.34
10	30	30	5	9500	34.86	1.01	1.72	134.47
11	30	30	5	12825	41.18	1.07	1.6	145.99
12	30	30	5	18825	49.99	1.12	1.47	164.32
13	20	20	5	9500	37.72	1.18	1.84	131.53
14	20	20	5	12825	43.46	1.21	1.71	143.71
15	20	20	5	18825	51.74	1.23	1.56	162.33
16	30	30	10	9500	31.13	0.84	1.6	137.41
17	30	30	10	12825	38.19	0.93	1.5	148.94
18	30	30	10	18825	46.99	1	1.38	166.31
19	20	20	10	9500	34.86	1.01	1.72	134.47
20	20	20	10	12825	41.18	1.07	1.6	145.99
21	20	20	10	18825	49.99	1.12	1.47	164.32

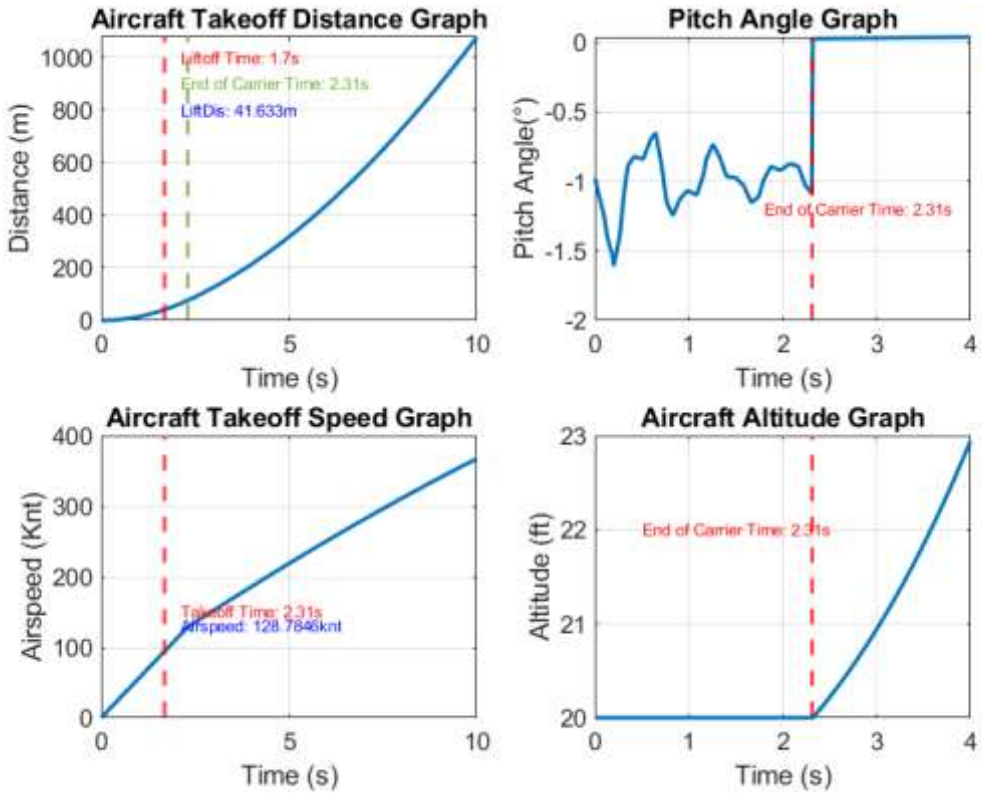

Figure 4. 31: Results of Simulation Number ID:1.

Within the scope of scenario ID:1, the C-13-0 catapult type was employed, with an aircraft weight of 9500lbs assumed, carrier is not moving and there is no wind velocity considered. In the conducted simulation, upon examination of the "Aircraft Take-off Distance Graph," the Liftoff Time was calculated as 1.7 seconds, while the Take-off Time was determined to be 2.31 seconds. Upon reviewing the results, it was observed that the aircraft was able to reach lift force before departing from the carrier, successfully achieving take-off. It covered a distance of 41.63 meters upon reaching the specified lift value. Further analysis of the "Aircraft Take-off Speed Graph" revealed that the aircraft's speed at take-off was calculated to be 128.78 knots.

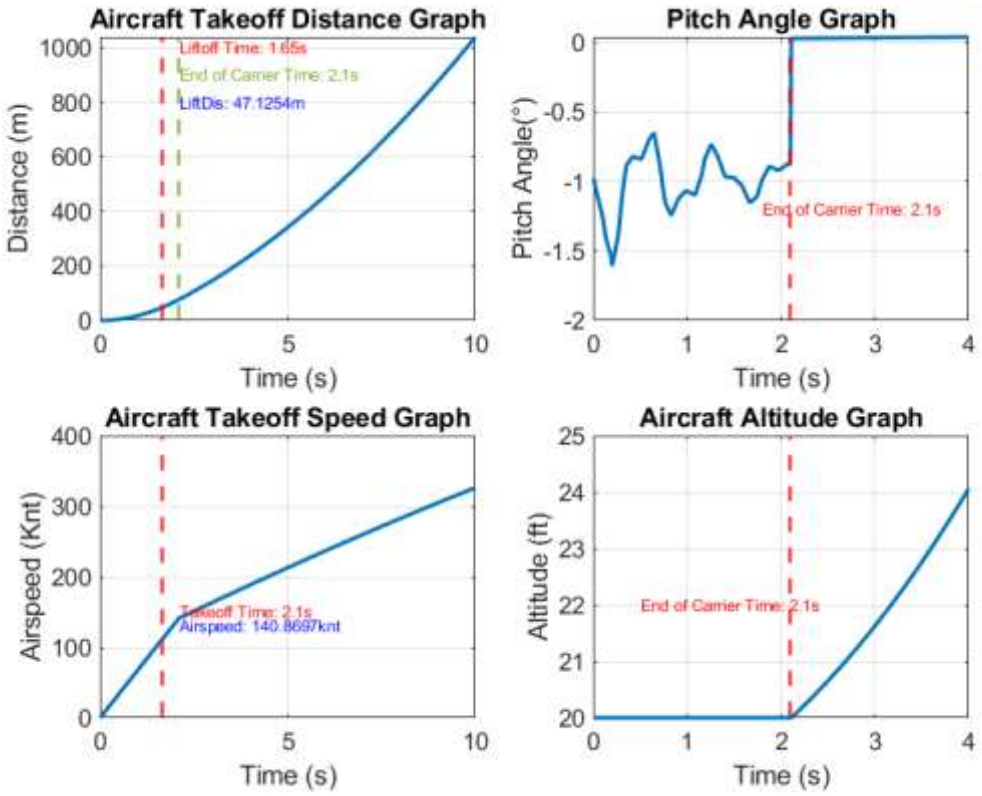

Figure 4. 32: Results of simulation number ID:2.

Within the scope of scenario ID:2, the C-13-0 catapult type was employed, with an aircraft weight of 12825lbs assumed, carrier is not moving and there is no wind velocity considered. In the conducted simulation, upon examination of the "Aircraft Take-off Distance Graph," the Liftoff Time was calculated as 1.65 seconds, while the Take-off Time was determined to be 2.1 seconds. Upon reviewing the results, it was observed that the aircraft was able to reach lift force before departing from the carrier, successfully achieving take-off. It covered a distance of 47.12 meters upon reaching the specified lift value. Further analysis of the "Aircraft Take-off Speed Graph" revealed that the aircraft's speed at take-off was calculated to be 140.86 knots.

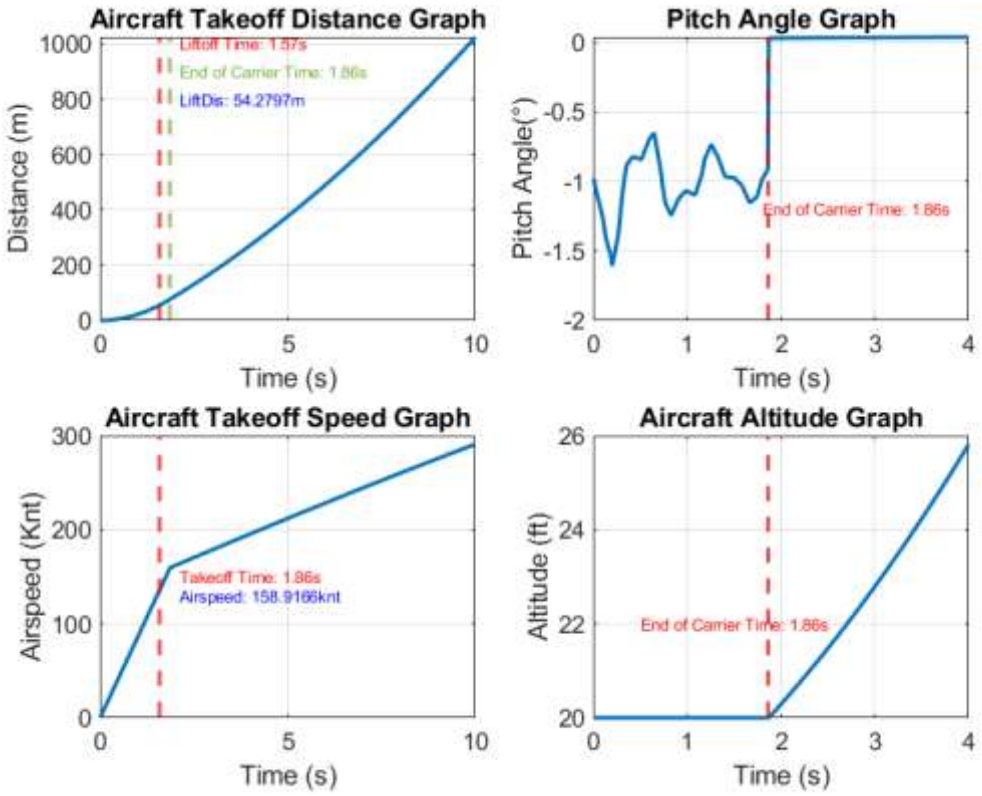

Figure 4. 33: Results of simulation number ID:3.

Within the scope of scenario ID:3, the C-13-0 catapult type was employed, with an aircraft weight of 18825lbs assumed, carrier is not moving and there is no wind velocity considered. In the conducted simulation, upon examination of the "Aircraft Take-off Distance Graph," the Liftoff Time was calculated as 1.57 seconds, while the Take-off Time was determined to be 1.86 seconds. Upon reviewing the results, it was observed that the aircraft was able to reach lift force before departing from the carrier, successfully achieving take-off. It covered a distance of 54.27 meters upon reaching the specified lift value. Further analysis of the "Aircraft Take-off Speed Graph" revealed that the aircraft's speed at take-off was calculated to be 158.91 knots.

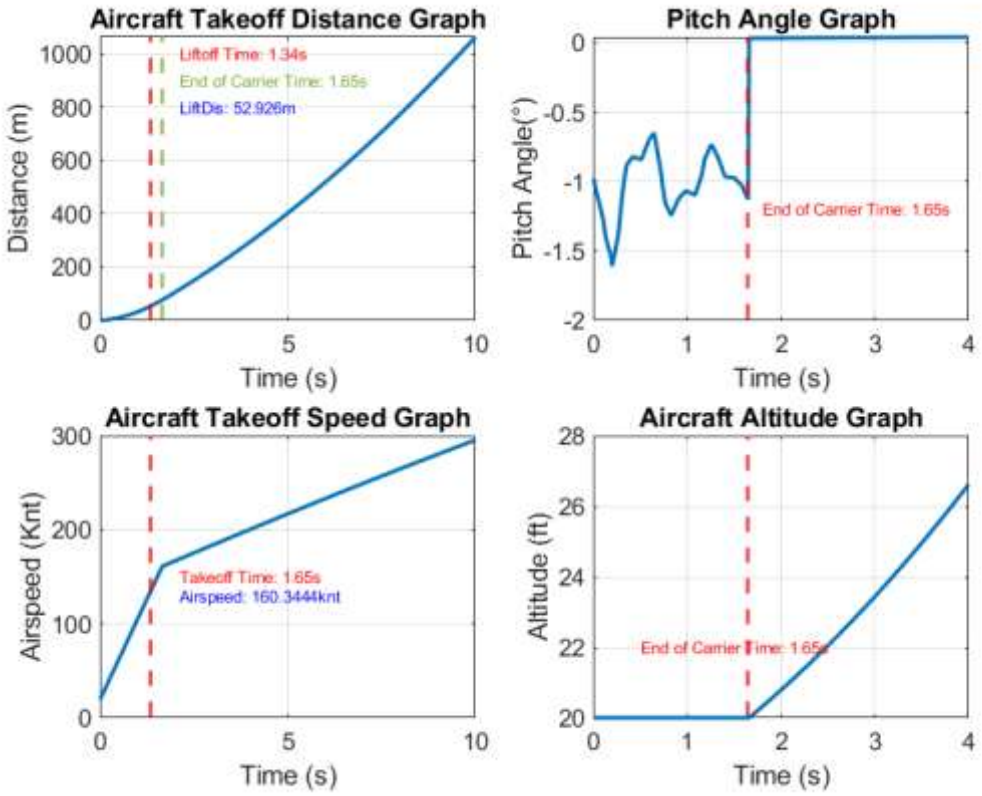

Figure 4. 34. Results of Simulation Number ID:9.

Within the scope of scenario ID:9, the C-13-0 catapult type was employed, with an aircraft weight of 18825lbs assumed, carrier is moving at a speed of 20 knots and there is no wind velocity considered. In the conducted simulation, upon examination of the "Aircraft Take-off Distance Graph," the Liftoff Time was calculated as 1.34 seconds, while the Take-off Time was determined to be 1.65 seconds. Upon reviewing the results, it was observed that the aircraft was able to reach lift force before departing from the carrier, successfully achieving take-off. It covered a distance of 52.92 meters upon reaching the specified lift value. Further analysis of the "Aircraft Take-off Speed Graph" revealed that the aircraft's speed at take-off was calculated to be 160.34 knots.

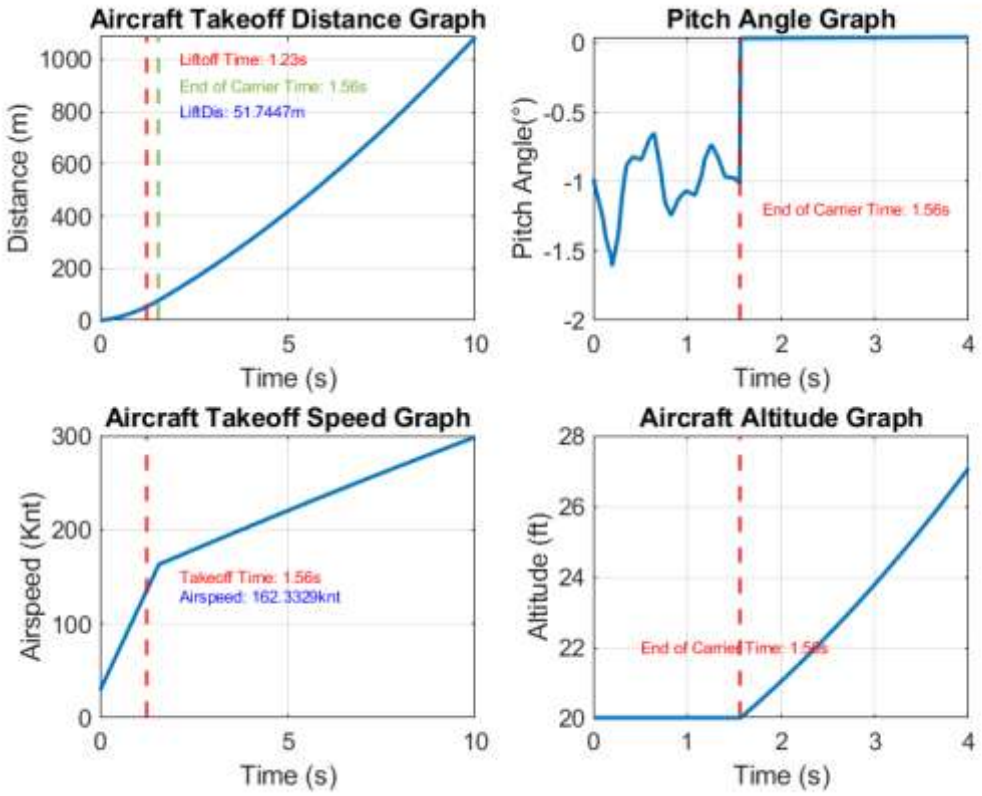

Figure 4. 35. Results of Simulation Number ID:15.

Within the scope of scenario ID:15, the C-13-0 catapult type was employed, with an aircraft weight of 18825lbs assumed, carrier moving at a speed of 20 knots and there is wind velocity at 5m/s considered. In the conducted simulation, upon examination of the "Aircraft Take-off Distance Graph," the Liftoff Time was calculated as 1.23 seconds, while the Take-off Time was determined to be 1.56 seconds. Upon reviewing the results, it was observed that the aircraft was able to reach lift force before departing from the carrier, successfully achieving take-off. It covered a distance of 51.74 meters upon reaching the specified lift value. Further analysis of the "Aircraft Take-off Speed Graph" revealed that the aircraft's speed at take-off was calculated to be 162.33 knots.

Table 4.8: Parameters of C/13-1 Type Catapult MATLAB Simulink Model.

Aircraft-Environmental Conditions				**Simulation Results**				
ID	Carrier Speed (Knots)	Carrier Speed (Knots)	Wind Speed (m/s)	Takeoff Weight (LBS)	Liftoff Distance (m)	Liftoff Time (s)	Take-off Time (s)	Take-off Speed (Knots)
22	0	0	9500	50.53	2.06	2.82	129.80	24394.92
23	0	0	12825	56.57	1.99	2.58	142.72	88052.01
24	0	0	18825	65.85	1.91	2.29	160.31	230212.31
25	30	0	9500	45.75	1.43	2.26	132.92	24394.92
26	30	0	12825	52.88	1.47	2.11	145.69	88052.01
27	30	0	18825	63.08	1.5	1.91	162.74	230212.31
28	20	0	9500	48.39	1.64	2.44	131.57	24394.92
29	20	0	12825	54.79	1.64	2.25	143.78	88052.01
30	20	0	18825	64.24	1.63	2.03	161.46	230212.31
31	30	5	9500	42.07	1.22	2.11	135.63	24394.92
32	30	5	12825	49.53	1.29	1.97	147.59	88052.01
33	30	5	18825	60.55	1.36	1.81	165.40	230212.31
34	20	5	9500	45.75	1.43	2.26	132.92	24394.92
35	20	5	12825	52.88	1.47	2.11	145.69	88052.01
36	20	5	18825	63.08	1.5	1.91	162.74	230212.31
37	30	10	9500	37.35	1.01	1.96	138.34	24394.92
38	30	10	12825	45.87	1.12	1.85	150.59	88052.01
39	30	10	18825	57.33	1.22	1.7	167.37	230212.31
40	20	10	9500	42.07	1.22	2.11	135.63	24394.92
41	20	10	12825	49.53	1.29	1.97	147.59	88052.01
42	20	10	18825	60.55	1.36	1.81	165.40	230212.31

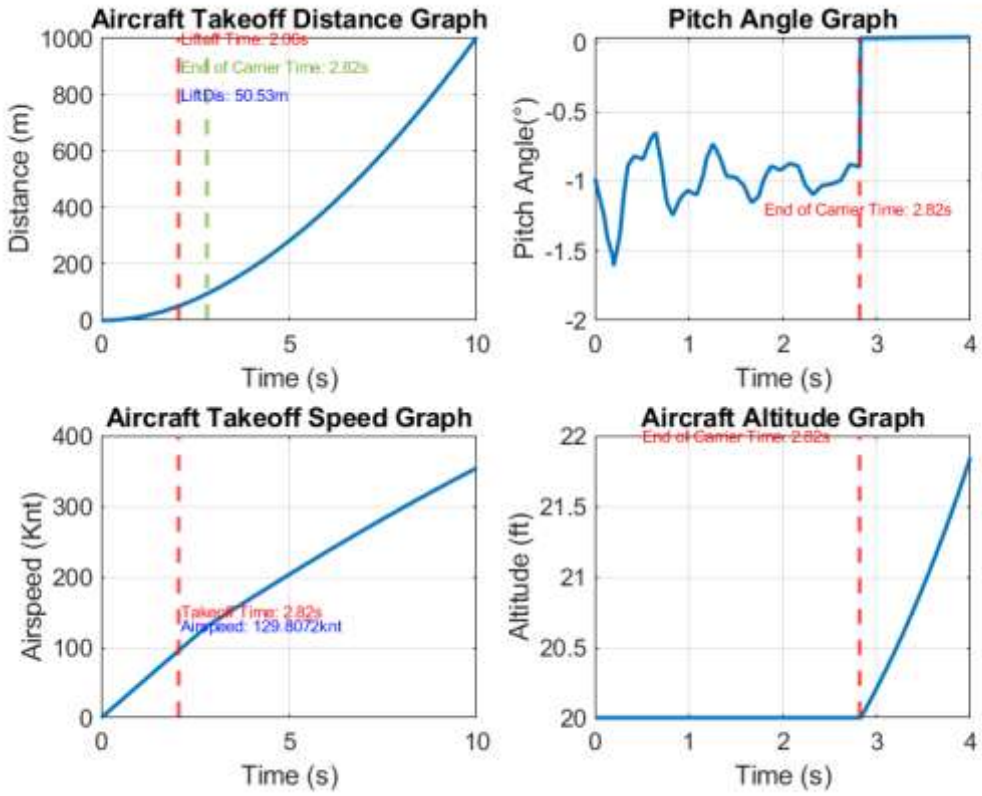

Figure 4. 36: Results of Simulation Number ID:22.

Within the scope of scenario ID:22, the C-13-1 catapult type was employed, with an aircraft weight of 9500lbs assumed, carrier is not moving and there is no wind velocity considered. In the conducted simulation, upon examination of the "Aircraft Take-off Distance Graph," the Liftoff Time was calculated as 2.06 seconds, while the Take-off Time was determined to be 2.82 seconds. Upon reviewing the results, it was observed that the aircraft was able to reach lift force before departing from the carrier, successfully achieving take-off. It covered a distance of 50.33 meters upon reaching the specified lift value. Further analysis of the "Aircraft Take-off Speed Graph" revealed that the aircraft's speed at take-off was calculated to be 129.80 knots.

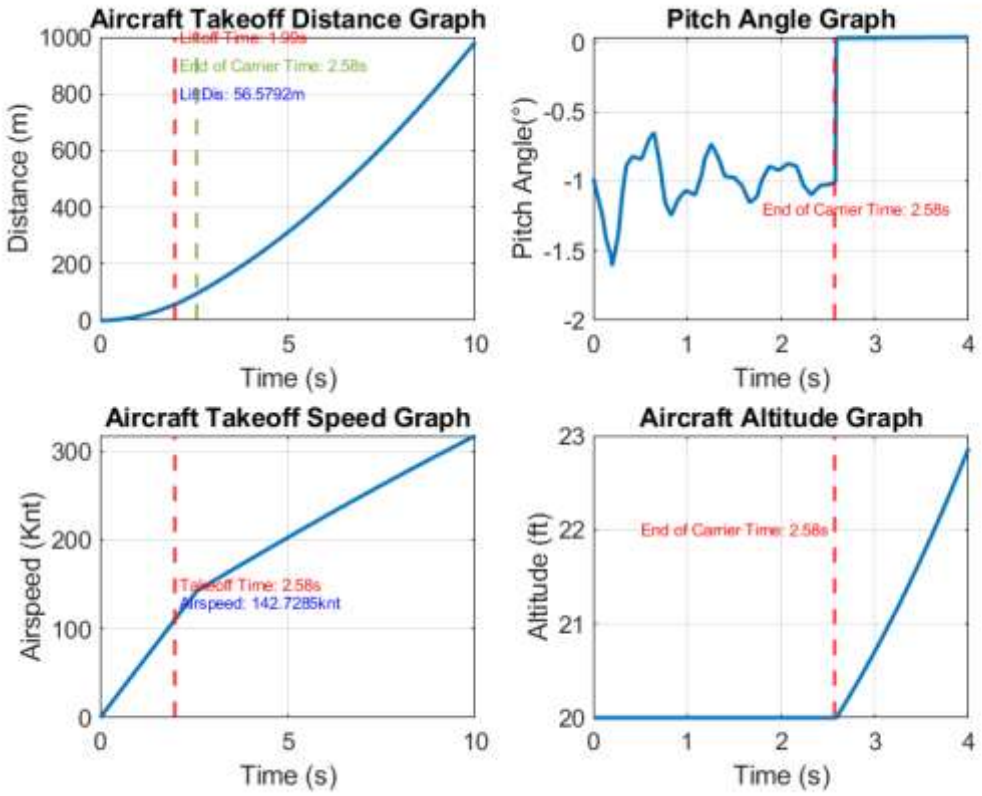

Figure 4. 37: Results of Simulation Number ID:23.

Within the scope of scenario ID:23, the C-13-1 catapult type was employed, with an aircraft weight of 12825lbs assumed, carrier is not moving and there is no wind velocity considered. In the conducted simulation, upon examination of the "Aircraft Take-off Distance Graph," the Liftoff Time was calculated as 1.99 seconds, while the Take-off Time was determined to be 2.58 seconds. Upon reviewing the results, it was observed that the aircraft was able to reach lift force before departing from the carrier, successfully achieving take-off. It covered a distance of 56.57 meters upon reaching the specified lift value. Further analysis of the "Aircraft Take-off Speed Graph" revealed that the aircraft's speed at take-off was calculated to be 142.72 knots.

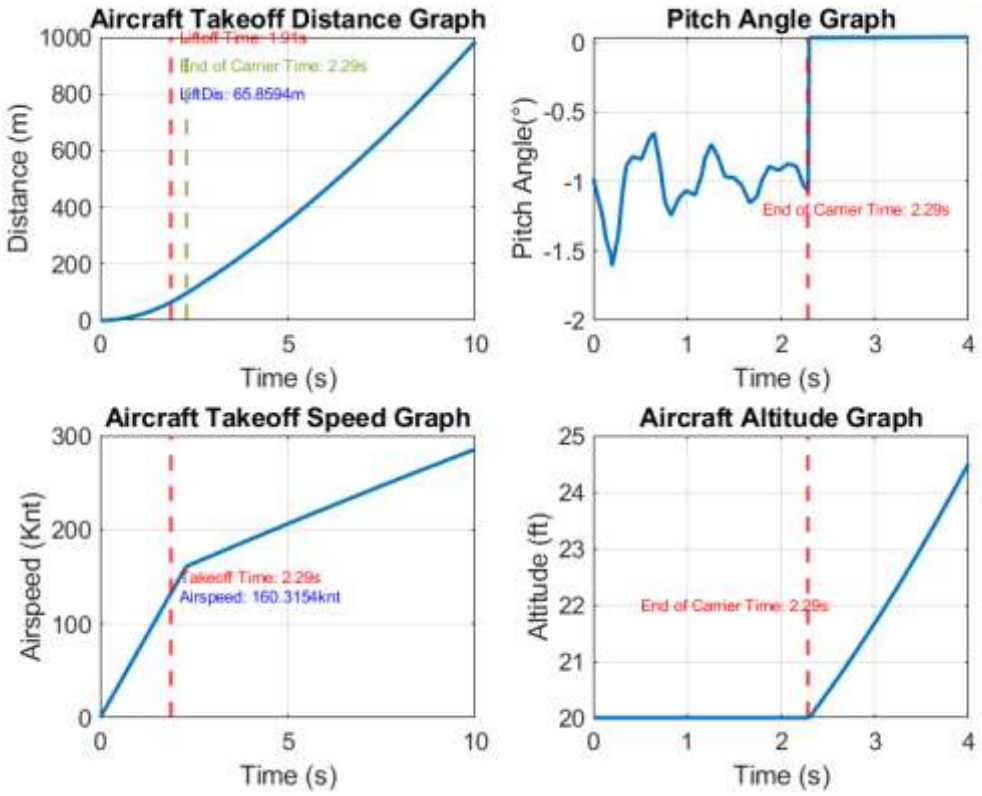

Figure 4. 38: Results of Simulation Number ID:24.

Within the scope of scenario ID:24, the C-13-1 catapult type was employed, with an aircraft weight of 18825lbs assumed, carrier is not moving and there is no wind velocity considered. In the conducted simulation, upon examination of the "Aircraft Take-off Distance Graph," the Liftoff Time was calculated as 1.91 seconds, while the Take-off Time was determined to be 2.29 seconds. Upon reviewing the results, it was observed that the aircraft was able to reach lift force before departing from the carrier, successfully achieving take-off. It covered a distance of 65.85 meters upon reaching the specified lift value. Further analysis of the "Aircraft Take-off Speed Graph" revealed that the aircraft's speed at take-off was calculated to be 160.31 knots.

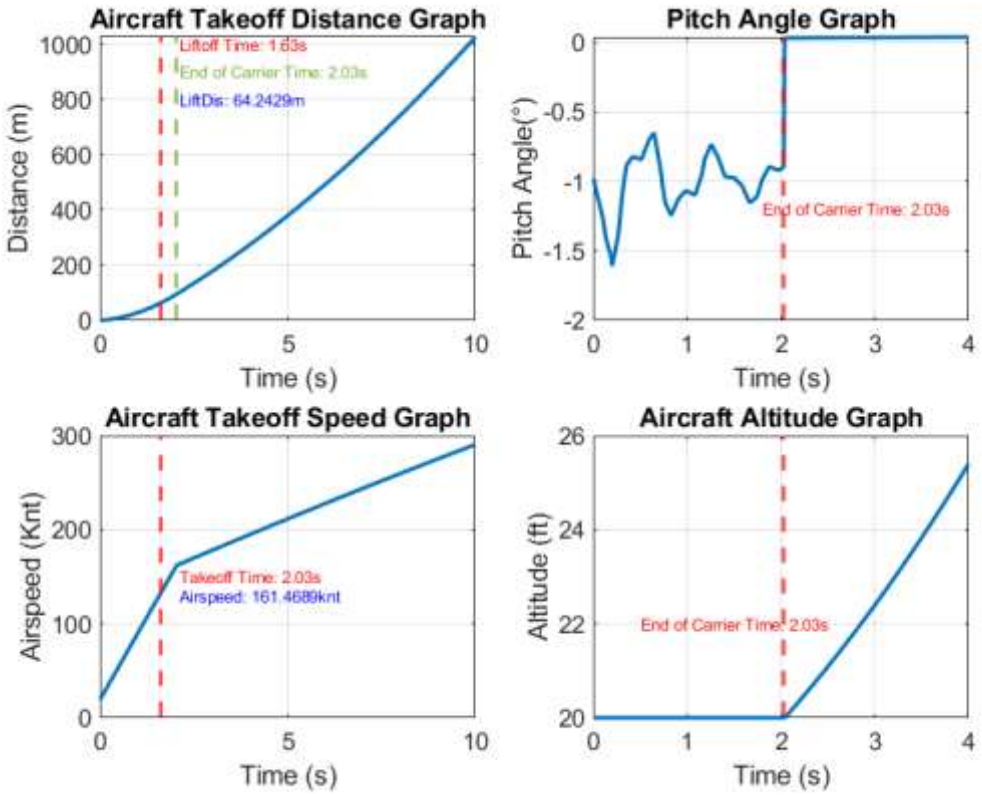

Figure 4. 39: Results of Simulation Number ID:30.

Within the scope of scenario ID:30, the C-13-1 catapult type was employed, with an aircraft weight of 18825lbs assumed, carrier moving at a speed of 20 knots and there is no wind velocity considered. In the conducted simulation, upon examination of the "Aircraft Take-off Distance Graph," the Liftoff Time was calculated as 1.63 seconds, while the Take-off Time was determined to be 2.03 seconds. Upon reviewing the results, it was observed that the aircraft was able to reach lift force before departing from the carrier, successfully achieving take-off. It covered a distance of 64.24 meters upon reaching the specified lift value. Further analysis of the "Aircraft Take-off Speed Graph" revealed that the aircraft's speed at take-off was calculated to be 161.46 knots.

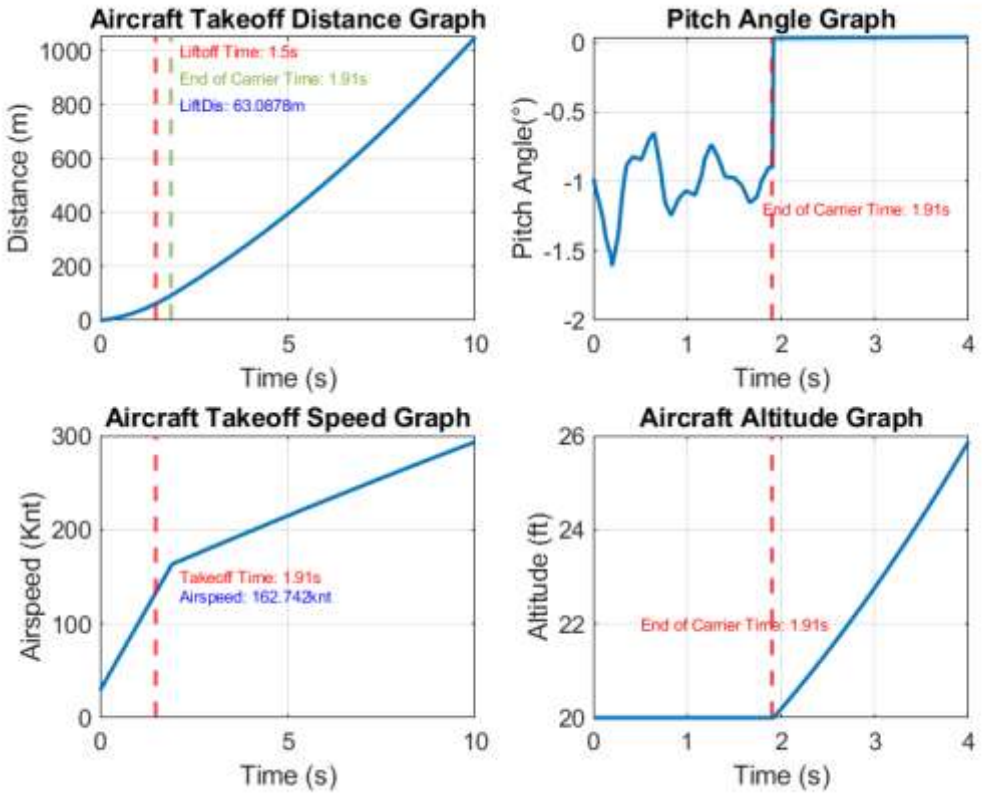

Figure 4. 40: Results of Simulation Number ID:36.

Within the scope of scenario ID:36, the C-13-1 catapult type was employed, with an aircraft weight of 18825lbs assumed, carrier moving at a speed of 20 knots and there is wind velocity at 5m/s considered. In the conducted simulation, upon examination of the "Aircraft Take-off Distance Graph," the Liftoff Time was calculated as 1.5 seconds, while the Take-off Time was determined to be 1.91 seconds. Upon reviewing the results, it was observed that the aircraft was able to reach lift force before departing from the carrier, successfully achieving take-off. It covered a distance of 63.08 meters upon reaching the specified lift value. Further analysis of the "Aircraft Take-off Speed Graph" revealed that the aircraft's speed at take-off was calculated to be 162.74 knots.

Table 4.9: Parameters of C/13-2 Type Catapult MATLAB Simulink Model.

Aircraft-Environmental Conditions				**Simulation Results**				
ID	Carrier Speed (Knots)	Carrier Speed (Knots)	Wind Speed (m/s)	Takeoff Weight (LBS)	Liftoff Distance (m)	Liftoff Time (s)	Take-off Time (s)	Take-off Speed (Knots)
43	0	0	9500	49.97	2.04	2.8	129.97	25259.36
44	0	0	12825	56.48	1.98	2.55	142.27	89463.78
45	0	0	18825	65.05	1.89	2.27	160.32	232932.91
46	30	0	9500	45.46	1.42	2.24	132.88	25259.36
47	30	0	12825	52.57	1.46	2.09	145.57	89463.78
48	30	0	18825	62.06	1.48	1.9	163.21	232932.91
49	20	0	9500	48.16	1.63	2.41	131.14	25259.36
50	20	0	12825	54.55	1.63	2.23	143.73	89463.78
51	20	0	18825	63.97	1.62	2.01	161.31	232932.91
52	30	5	9500	41.73	1.21	2.09	135.53	25259.36
53	30	5	12825	49.16	1.28	1.95	147.41	89463.78
54	30	5	18825	60.15	1.35	1.79	165.11	232932.91
55	20	5	9500	45.46	1.42	2.24	132.88	25259.36
56	20	5	12825	52.57	1.46	2.09	145.57	89463.78
57	20	5	18825	62.06	1.48	1.9	163.21	232932.91
58	30	10	9500	36.96	1	1.95	138.64	25259.36
59	30	10	12825	45.45	1.11	1.83	150.35	89463.78
60	30	10	18825	56.87	1.21	1.69	167.72	232932.91
61	20	10	9500	41.73	1.21	2.09	135.53	25259.36
62	20	10	12825	49.16	1.28	1.95	147.41	89463.78
63	20	10	18825	60.15	1.35	1.79	165.11	232932.91

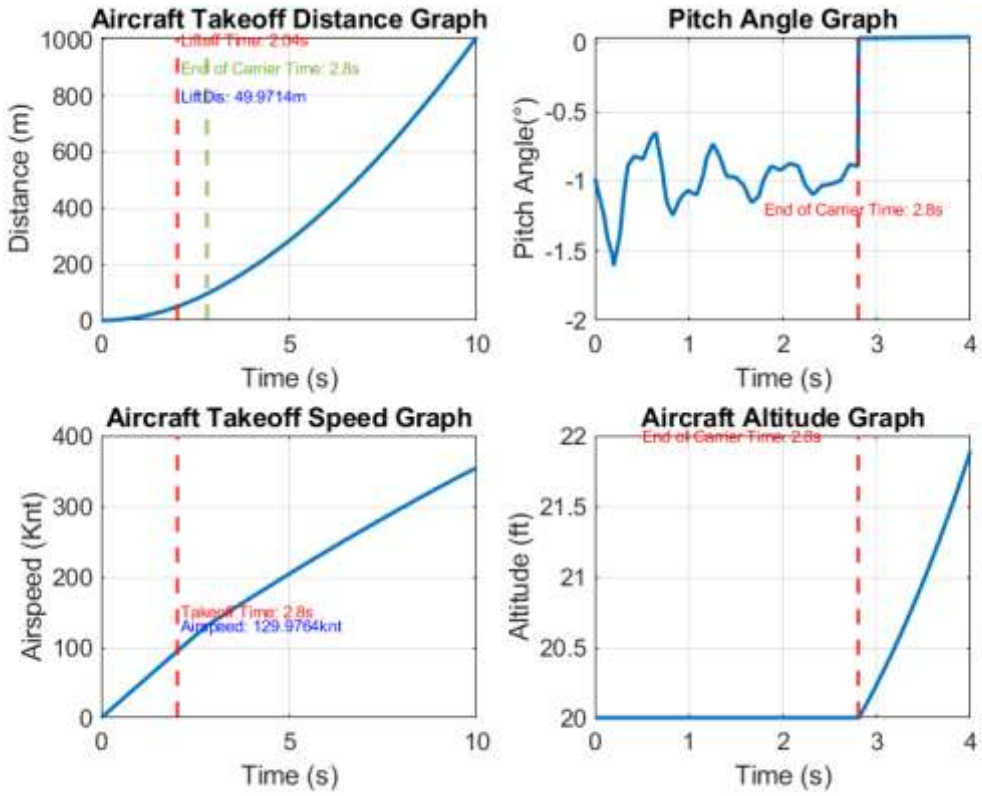

Figure 4. 41: Results of Simulation Number ID:43.

Within the scope of scenario ID:43, the C-13-2 catapult type was employed, with an aircraft weight of 9500lbs assumed, carrier is not moving and there is no wind velocity considered. In the conducted simulation, upon examination of the "Aircraft Take-off Distance Graph," the Liftoff Time was calculated as 2.04 seconds, while the Take-off Time was determined to be 2.8 seconds. Upon reviewing the results, it was observed that the aircraft was able to reach lift force before departing from the carrier, successfully achieving take-off. It covered a distance of 49.97 meters upon reaching the specified lift value. Further analysis of the "Aircraft Take-off Speed Graph" revealed that the aircraft's speed at take-off was calculated to be 129.97 knots.

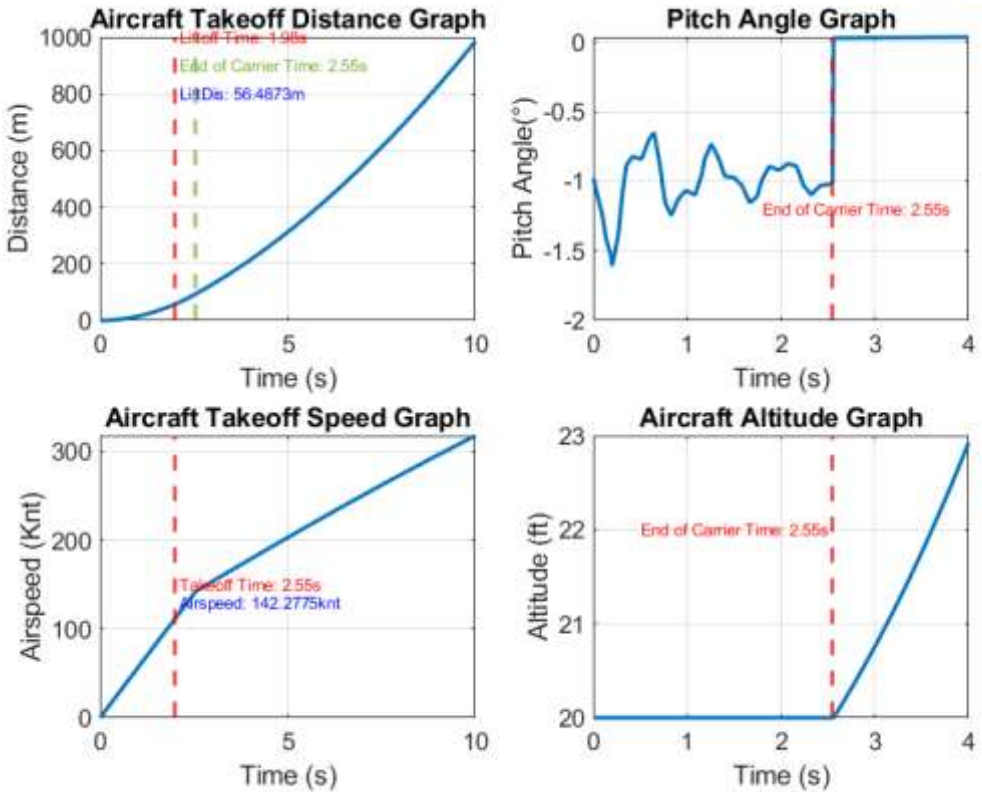

Figure 4. 42: Results of Simulation Number ID:44.

Within the scope of scenario ID:44, the C-13-2 catapult type was employed, with an aircraft weight of 12825lbs assumed, carrier is not moving and there is no wind velocity considered. In the conducted simulation, upon examination of the "Aircraft Take-off Distance Graph," the Liftoff Time was calculated as 1.98 seconds, while the Take-off Time was determined to be 2.55 seconds. Upon reviewing the results, it was observed that the aircraft was able to reach lift force before departing from the carrier, successfully achieving take-off. It covered a distance of 56.48 meters upon reaching the specified lift value. Further analysis of the "Aircraft Take-off Speed Graph" revealed that the aircraft's speed at take-off was calculated to be 142.27 knots.

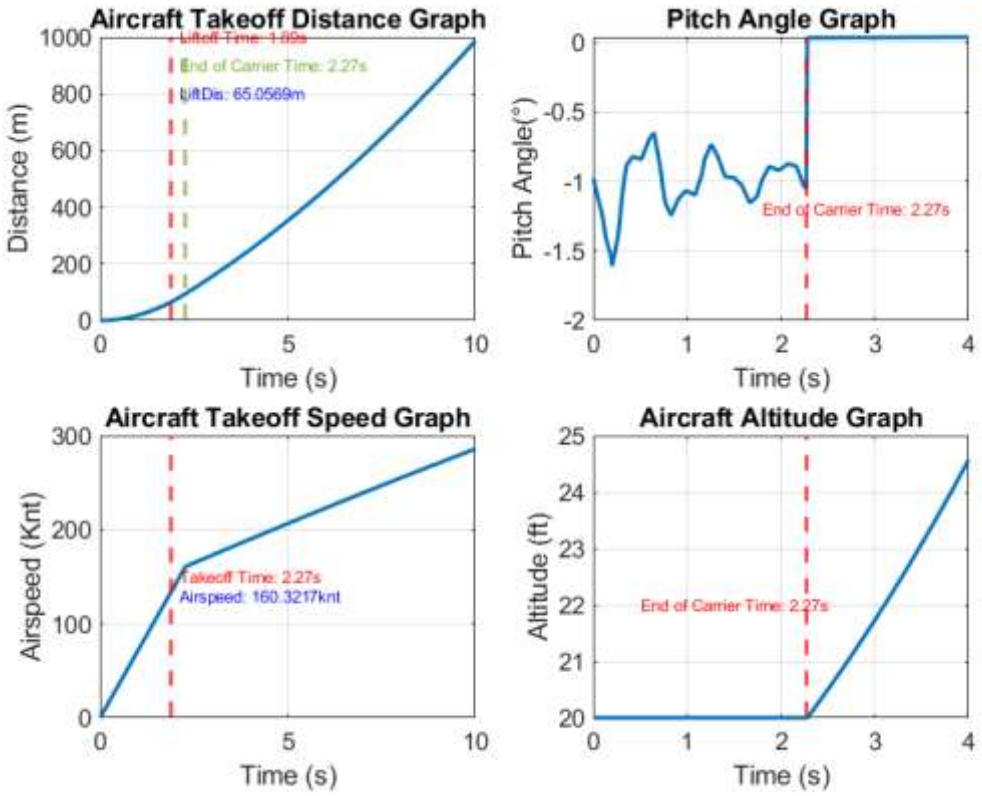

Figure 4. 43: Results of Simulation Number ID:45.

Within the scope of scenario ID:45, the C-13-2 catapult type was employed, with an aircraft weight of 18825lbs assumed, carrier is not moving and there is no wind velocity considered. In the conducted simulation, upon examination of the "Aircraft Take-off Distance Graph," the Liftoff Time was calculated as 1.89 seconds, while the Take-off Time was determined to be 2.27 seconds. Upon reviewing the results, it was observed that the aircraft was able to reach lift force before departing from the carrier, successfully achieving take-off. It covered a distance of 65.05 meters upon reaching the specified lift value. Further analysis of the "Aircraft Take-off Speed Graph" revealed that the aircraft's speed at take-off was calculated to be 160.32 knots.

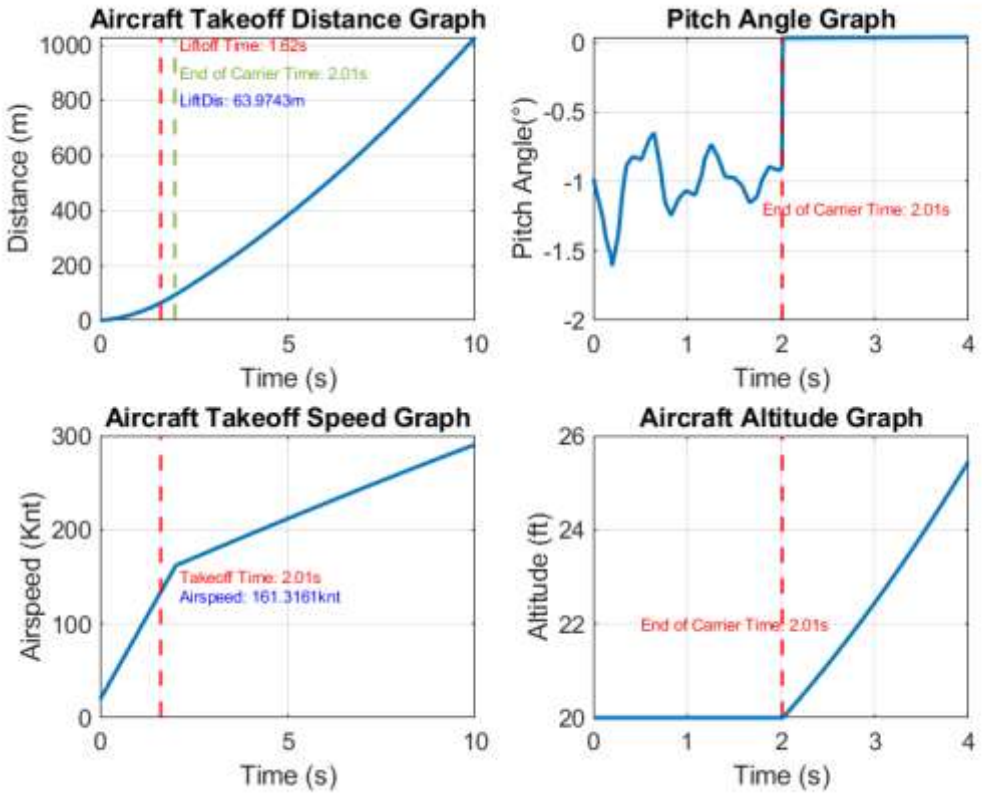

Figure 4. 44: Results of Simulation Number ID:51.

Within the scope of scenario ID:51, the C-13-2 catapult type was employed, with an aircraft weight of 18825lbs assumed, carrier moving at a speed of 20 knots and there is no wind velocity considered. In the conducted simulation, upon examination of the "Aircraft Take-off Distance Graph," the Liftoff Time was calculated as 1.62 seconds, while the Take-off Time was determined to be 2.01 seconds. Upon reviewing the results, it was observed that the aircraft was able to reach lift force before departing from the carrier, successfully achieving take-off. It covered a distance of 63.97 meters upon reaching the specified lift value. Further analysis of the "Aircraft Take-off Speed Graph" revealed that the aircraft's speed at take-off was calculated to be 161.31 knots.

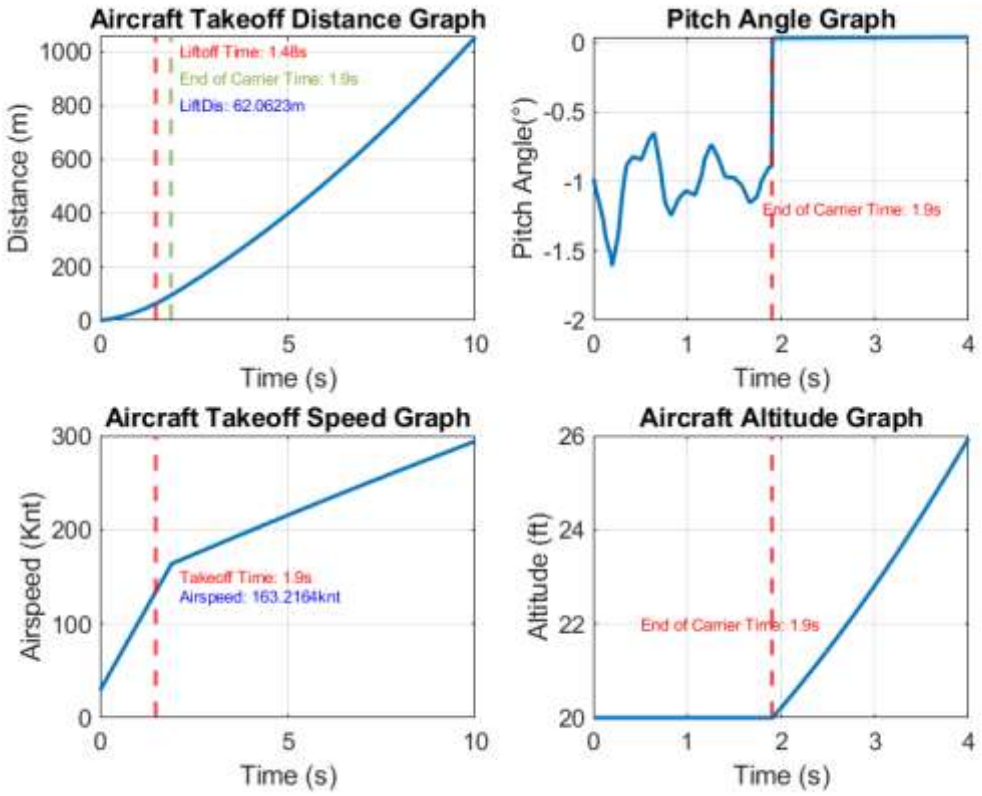

Figure 4. 45: Results of Simulation Number ID:57.

Within the scope of scenario ID:57, the C-13-2 catapult type was employed, with an aircraft weight of 18825lbs assumed, carrier moving at a speed of 20 knots and there is wind velocity at 5m/s considered. In the conducted simulation, upon examination of the "Aircraft Take-off Distance Graph," the Liftoff Time was calculated as 1.48 seconds, while the Take-off Time was determined to be 1.9 seconds. Upon reviewing the results, it was observed that the aircraft was able to reach lift force before departing from the carrier, successfully achieving take-off. It covered a distance of 62.06 meters upon reaching the specified lift value. Further analysis of the "Aircraft Take-off Speed Graph" revealed that the aircraft's speed at take-off was calculated to be 163.21 knots.

5. CONCLUSION AND ADVICE

The simulation results presented above are intended to compare several instances. According to the table provided, an aircraft weighing 18,825 lbs achieves a liftoff distance of 54.27m without wind speed and carrier velocity, with a liftoff time of 1.57s and a takeoff time of 1.86s. Additionally, the takeoff speed of the aircraft is observed to be 158.91 knots. When a carrier velocity of 20 knots is added to the aircraft taking off from the aircraft carrier of the same weight, it is noted that the added carrier velocity reduces the liftoff distance by 2.6%, decreases the liftoff time by 17.2%, and reduces the takeoff time by 12.7%. Moreover, the takeoff speed increases by 0.9% as indicated in the table above. Subsequently, by introducing a wind speed of 5m/s in addition to the carrier velocity, it is observed that the combined effect of carrier velocity and wind speed reduces the liftoff distance by 4.9%, decreases the liftoff time by 27.6%, and reduces the takeoff time by 19.2%. Furthermore, the takeoff speed increases by 2.1% as seen in the table above.

Table 5.1: Simulink Values of A C-13-0 Catapult Type Aircraft.

ID	Catapult Distance (m)	Carrier Speed (Knots)	Wind Speed (m/s)	Takeoff Weight (LBS)
1	76.1492	0	0	18825
2	76.1492	20	0	18825
3	76.1492	20	5	18825
4	76.1492	30	10	18825

Table 5.2: Comparison of Simulation Results of the C-13-0 Catapult Type Aircraft.

ID	Liftoff Distance (m)	Difference (%)	Liftoff Time (s)	Difference (%)	Take-off Time (s)	Difference (%)	Take-off Speed (Knots)	Difference (%)	Catapult Force (Nm)
1	54.27		1.57		1.86		158.91		297952.95
2	52.92	-2,6%	1.34	-17,2%	1.65	-12,7%	160.34	0,9%	297952.95
3	51.74	-4,9%	1.23	-27,6%	1.56	-19,2%	162.33	2,1%	297952.95
4	46.99	-15,5%	1	-57,0%	1.38	-34,8%	166.31	4,4%	297952.95

Finally, the simulation results from MATLAB Simulink analysis are compared by adding the highest carrier velocity and wind speed. In this scenario, assuming a carrier velocity of 30 knots and a wind speed of 10m/s, the added carrier velocity and wind speed reduce the liftoff distance by 15.5%, decrease the liftoff time by 57%, and reduce the takeoff time by 34.8%. Additionally, the takeoff speed increases by 4.4%. These findings demonstrate the significant impact of carrier velocity and wind speed on the takeoff performance of the aircraft.

Table 5.3: Simulink Values of A C-13-1 Catapult Type Aircraft.

ID	Catapult Distance (m)	Carrier Speed (Knots)	Wind Speed (m/s)	Takeoff Weight (LBS)
1	94.4	0	0	18825
2	94.4	20	0	18825
3	94.4	20	5	18825
4	94.4	30	10	18825

Table 5.4: Comparison of Simulation Results of the C-13-0 Catapult Type Aircraft.

ID	Liftoff Distance (m)	Difference (%)	Liftoff Time (s)	Difference (%)	Take-off Time (s)	Difference (%)	Take-off Speed (Knots)	Difference (%)	Catapult Force (Nm)
1	65.85		1.91		2.29		160.31		230212.31
2	64.24	-2,5%	1.63	-17,2%	2.03	-12,8%	161.46	0,7%	230212.31
3	63.08	-4,4%	1.5	-27,3%	1.91	-19,9%	162.74	1,5%	230212.31
4	57.33	-14,9%	1.22	-56,6%	1.7	-34,7%	167.37	4,2%	230212.31

According to the table provided, an aircraft weighing 18,825 lbs achieves a liftoff distance of 65.85m without wind speed and carrier velocity, with a liftoff time of 1.91s and a takeoff time of 2.29s. Additionally, the takeoff speed of the aircraft is observed to be 160.31knot. When a carrier velocity of 20 knots is added to the aircraft taking off from the aircraft carrier of the same weight, it is noted that the added carrier velocity reduces the liftoff distance by 2.5%, decreases the liftoff time by 17.2%, and reduces the takeoff time by 12.8%.

Moreover, the takeoff speed increases by 0.7% as indicated in the table above. Subsequently, by introducing a wind speed of 5m/s in addition to the carrier velocity, it is observed that the combined effect of carrier velocity and wind speed reduces the liftoff distance by 4.4%, decreases the liftoff time by 27.3%, and reduces the takeoff time by 19.9%. Furthermore, the takeoff speed increases by 1,5% as seen in the table above. Finally, the simulation results from MATLAB Simulink analysis are compared by adding the highest carrier velocity and wind speed. In this scenario, assuming a carrier velocity of 30 knots and a wind speed of 10m/s, the added carrier velocity and wind speed reduce the liftoff distance by 14,9%, decrease the liftoff time by 56,6%, and reduce the takeoff time by 34.7%. Additionally, the takeoff speed increases by 4.2%. These findings demonstrate the significant impact of carrier velocity and wind speed on the takeoff performance of the aircraft.

Table 5.5: Simulink Values of A C-13-2 Catapult Type Aircraft.

ID	Catapult Distance (m)	Carrier Speed (Knots)	Wind Speed (m/s)	Takeoff Weight (LBS)
1	93.5	0	0	18825
2	93.5	20	0	18825
3	93.5	20	5	18825
4	93.5	30	10	18825

Table 5.6: Comparison of Simulation Results of the C-13-2 Catapult Type Aircraft.

ID	Liftoff Distance (m)	Difference (%)	Liftoff Time (s)	Difference (%)	Take-off Time (s)	Difference (%)	Take-off Speed (Knots)	Difference (%)	Catapult Force (Nm)
1	65.05		1.89		2.27		160.32		232932.91
2	63.97	-1,7%	1.62	-16,7%	2.01	-12,9%	161.31	0,6%	232932.91
3	62.06	-4,8%	1.48	-27,7%	1.9	-19,5%	163.21	1,8%	232932.91
4	56.87	-14,4%	1.21	-56,2%	1.69	-34,3%	167.72	4,4%	232932.91

The simulation results presented above are intended to compare several instances. According to the table provided, an aircraft weighing 18,825 lbs. achieves a liftoff distance of 65.05m without wind speed and carrier velocity, with a liftoff time of 1.89s and a takeoff time of 2.27s. Additionally, the takeoff speed of the aircraft is observed to be 160.32knot. When a carrier velocity of 20 knots is added to the aircraft taking off from the aircraft carrier of the same weight, it is noted that the added carrier velocity reduces the liftoff distance by 1.7%, decreases the liftoff time by 16.7%, and reduces the takeoff time by 12.9%. Moreover, the takeoff speed increases by 0.6% as indicated in the table above. Subsequently, by introducing a wind speed of 5m/s in addition to the carrier velocity, it is observed that the combined effect of carrier velocity and wind speed reduces the liftoff distance by 4.8%, decreases the liftoff time by 27.7%, and reduces the takeoff time by 19.5%. Furthermore, the takeoff speed increases by 1,8% as seen in the table above. Finally, the simulation results from MATLAB Simulink analysis are compared by adding the highest carrier velocity and wind speed. In this scenario, assuming a carrier velocity of 30 knots and a wind speed of 10m/s, the added carrier velocity and wind speed reduce the liftoff distance by 14.4%, decrease the liftoff time by 56.2%, and reduce the takeoff time by 34.3%. Additionally, the takeoff speed increases by 4.4%. These findings demonstrate the significant impact of carrier velocity and wind speed on the takeoff performance of the aircraft.

Catapult Type (C-13-0, C-13-1, C-13-2): As a result of the analyses conducted, it has been concluded that if a shorter length for the aircraft carrier is desired, a greater magnitude of catapult force is required. Conversely, if a longer length for the aircraft carrier is planned, it is inferred that a lesser magnitude of catapult force could be applied.

Carrier Speed and Wind Speed: As the carrier speed and wind speed increase, there is typically a decrease in takeoff distance and time. Particularly for the aircraft weighing 18825 lbs, these effects are pronounced. The increased carrier speed suggests that it supports the aircraft's takeoff speed, thereby reducing the liftoff time. Subsequently, scenarios examining the combined effect of increased carrier speed and added wind speed have also been evaluated. In this case, it is observed that the impact of increased carrier speed on takeoff performance varies with the influence of wind speed. Specifically, higher carrier speeds exhibit a more significant effect, especially with increasing wind speeds.

Catapult Force: The catapult force directly affects the takeoff time and speed. A higher catapult force generally supports faster takeoff. Overall, the examination of different configurations demonstrates that various factors influence the aircraft's takeoff performance. A detailed analysis of this data can aid in determining optimal takeoff conditions and improving takeoff performance. However, excessively high wind speeds or carrier speeds can pose challenges to control and jeopardize safety. These conditions require careful evaluation. Additionally, the catapult type emerges as a significant factor affecting takeoff performance. For example, variations in catapult types lead to changes in takeoff time and speed. These analyses provide a valuable guide for understanding and optimizing the effects of different parameters on takeoff performance.

In conclusion, significant differences in performance may exist among aircraft of different weights. Heavier aircraft typically require longer takeoff distances, lower takeoff speeds, and higher catapult forces. These factors should be considered in takeoff planning and operations.

To enhance takeoff performance, it is crucial to select the appropriate catapult type and distance. These findings underscore the importance of considering factors such as carrier velocity and wind speed when planning aircraft operations. Additionally, the critical significance of takeoff weight and speed should not be overlooked. For a safe and efficient takeoff, it is imperative for pilots and operational teams to continuously monitor and assess these factors. Such analyses can aid in optimizing operational decisions and ensuring safe execution. Furthermore, for future research, conducting more comprehensive experiments to examine the effects of various weather conditions and carrier velocities on takeoff performance in greater detail is recommended.

REFERENCES

[1] Y. S. Taşay, "Aircraft Basic Construction," Jul. 2000.

[2] "Chapter 1: Aircraft Engines," *Federal Aviation Administration (FAA)*.

[3] M. Andersson, *Plane Wave Spectrum in Radome Applications*. 2019 International Conference on Electromagnetics in Advanced Applications (ICEAA), 2019.

[4] M. S. Dinçer, "Information Based Decision Making Process of Pilots in Flight Operations in Civil Aviation," *Information Management*, vol. 6, no. 1, pp. 75–90, Jun. 2023, doi: 10.33721/by.1294548.

[5] "Parts of an Airplane," *National Aeronautics and Space Administration (NASA)*, Jun. 2023, [Online]. Available: www.nasa.gov

[6] X. Lu, X. Liu, Y. Li, Y. Zhang, and H. Zuo, "Simulations of Airborne Collisions Between Drones and an Aircraft Windshield," *Aerosp Sci Technol*, vol. 98, p. 105713, Mar. 2020, doi: 10.1016/j.ast.2020.105713.

[7] A. Y. Patil, S. S. Gad, S. C. Policepati, S. Patil, and S. N. Mathad, "Design and Analysis of Alternative Material for Bird Strike on Aircraft Windshield," *Technological Engineering*, vol. 15, no. 2, pp. 5–10, Dec. 2018, doi: 10.1515/teen-2018-0011.

[8] O. Das, H. Battal, E. Kurt, and M. Yilmaz, *The Free Vibration Characteristics of Canadair NF-5 Aircraft Canopy*. 2023 10th International Conference on Recent Advances in Air and Space Technologies (RAST), 2023. doi: 10.1109/RAST57548.2023.10197879.

[9] S. Singh, *Airframe And Aircraft Components*. L.N.V.M. Society Group of Institutes H-974, Palam Extn., Part-1, Sec-7, Dwarka, New Delhi-77.

[10] Ira Herbert Abbott and Albert E. Von Doenhoff, *Theory of Wing Sections: Including a Summary of Air foil Data*. Dover Publications, 1959.

[11] J. D. Anderson and M. L. Bowden, *Introduction to Flight*, 8th ed., vol. 582. McGraw-Hill Higher Education New York, NY, USA, 2005.

[12] M. Frederick, E. C. Kerrigan, and J. M. R. Graham, "Gust alleviation using rapidly deployed trailing-edge flaps," *Journal of Wind Engineering and Industrial Aerodynamics*, vol. 98, no. 12, pp. 712–723, Dec. 2010, doi: 10.1016/j.jweia.2010.06.005.

[13] "Flight Controls," *Federal Aviation Administration*, Jul. 2023.

[14] O. Mohamed Alazomui, "On the development of computer code for aircraft flight dynamics analysis," Universiti Tun Hussein Onn Malaysia, 2014.

[15] F. I. Petrescu and R. Petrescu, "Aircraft Carriers," *Articles Factory*, Mar. 2017.

[16] R. C. Rubel, "The future of aircraft carriers.," *Naval War College Review*, vol. 64, no. 4, pp. 12–27, 2011.

[17] N. Li and C. Weuve, "China's Aircraft Carrier Ambitions," *Source: Naval War College Review*, vol. 63, no. 1, pp. 12–32, 2010, doi: 10.2307/26397075.

[18] K. Koo, "Aircraft Carriers," vol. MS27, no. 8861304, 1883.

[19] R. Doughty, I. Gruber, R. Flint, M. Grimsley, and G. Herring, *American Military History and the Evolution of Warfare in the Western World*. 1996.

[20] A. Güngör, "Denizlerin Efendileri: Farklı Savaş Gemisi Çeşitleri ve Özellikleri," May 2023.

[21] H. J. C. Harper, "The development of the aircraft carrier," *Royal United Services Institution. Journal*, vol. 80, no. 519, pp. 505–513, 1935, doi: 10.1080/03071843509420884.

[22] William Gurstelle, *The Art of the Catapult: Build Greek Ballistae, Roman Onagers, English Trebuchets, And More Ancient Artillery*. 2004.

[23] Future Scientists and Engineers of America (FSEA), "Science Content," 1997.

[24] C. B. Lucas, “Catapult Criteria for a Carrier—Based Airplane,” 1968.

[25] H. Shao, D. Li, Z. Kan, S. Zhao, J. Xiang, and C. Wang, “Analysis of Catapult-Assisted Take-off of Carrier-Based Aircraft Based on Finite Element Method and Multibody Dynamics Coupling Method,” *Aerospace*, vol. 10, no. 12, Dec. 2023, doi: 10.3390/aerospace10121005.

[26] T. Lawrence, “Milestones and Developments in US Naval Carrier Aviation Part II,” in *AIAA Atmospheric Flight Mechanics Conference and Exhibit*, Reston, Virigina: American Institute of Aeronautics and Astronautics, Aug. 2005. doi: 10.2514/6.2005-6120.

[27] G. Garay and D. Woodbury, “F/A-18 single engine minimum control airspeed ((Vmc)),” in *2000 IEEE Aerospace Conference. Proceedings (Cat. No.00TH8484)*, IEEE, pp. 43–48. doi: 10.1109/AERO.2000.878212.

[28] A. S. Erickson, A. M. Denmark, and G. Collins, “Beijing’s ‘Starter Carrier’ and Future Steps: Alternatives and Implications,” 2012.

[29] Y. Ġöhret and T. H. Karakoç, “Gaz Türbinli Uçak Motorlarının Termodinamik Modellenmesi Thermodynamic Modeling of Gas Turbine Aero-Engines,” 2014. [Online]. Available: http://edergi.bilecik.edu.tr/index.php/fbd

[30] T. James, “Back to propellers,” *Engineering & Technology*, vol. 4, no. 10, pp. 63–65, Jun. 2009, doi: 10.1049/et.2009.1014.

[31] G. C. Avantkar, “Turbojet Engines,” 2010.

[32] P. P. Walsh and P. Fletcher, *Gas turbine performance*. Blackwell Science, 2004.

[33] D. Klein and C. Abeykoon, “Modelling of a turbojet gas turbine engine,” in *2015 internet technologies and applications (ITA)*, 2015, pp. 200–206. [Online]. Available: http://man.ac.uk/04Y6Bo]

[34] C. Fan, R. Jiang, and S. Zhang, “Current Status and Future Prospects of Jet Engines,” 2023.

[35] Thomas R. Yechout, Steven L. Morris, David E. Bossert, Wayne F. Hallgren, and James K. Hall, *Introduction to aircraft flight mechanics: Performance, static stability, dynamic stability, and classical feedback control*. American Institute of Aeronautics and Astronautics, 2003.

[36] Arthur H. Lefebvre and Dilip R. Ballal, "Alternative fuels and emissions," *CRC Press, Boca Raton, FL, USA*, vol. 304, 2010.

[37] P. Singh Virdi St Joseph Engineering College, M. Saahil Khan, P. Singh Virdi, N. Pereira, S. K. V, and R. S. D, "Design and Fabrication of Major Components of Turbojet Engine," vol. 7, no. 5, pp. 130–135, 2017, doi: 10.5923/j.ep.20170705.02.

[38] J. D. Mattingly, *Elements of propulsion : gas turbines and rockets*. American Institute of Aeronautics and Astronautics, 2006.

[39] J. L. Kerrebrock, *Aircraft Engines and Gas Turbines*. MIT press, 1992.

[40] "Animated Turbofan Thrust," National Aeronautics and Space Administration (NASA). Accessed: Mar. 28, 2024. [Online]. Available: https://web.archive.org/web/20000816191039/https:/www.grc.nasa.gov/www/k-12/airplane/aturbf.html

[41] John D. Anderson, "Introduction to Flight".

[42] V. Fornlöf, "Improved remaining useful life estimations for on-condition parts in aircraft engines," University of Skövde, 2016.

[43] M. A. Imran, K. P. Ratin, K. M. Ahmed, M. A. Siddiq, and M. S. Hossain, "A Study on Turbofan engine for Knowing the Working Principle and to Recognize the Different parts.," Sonargoan University (SU), 2022.

[44] L. S. Langston, "Turbines Gas," in *Reference Module in Earth Systems and Environmental Sciences*, Elsevier, 2014. doi: 10.1016/b978-0-12-409548-9.09044-8.

[45] H. I. H. Saravanamuttoo, “Modern turboprop engines,” *Progress in Aerospace Sciences*, vol. 24, no. 3, pp. 225–248, Jan. 1987, doi: 10.1016/0376-0421(87)90008-X.

[46] A. Cengiz and Z. Utlu, “Analysis of Different Engine Types in Aircrafts with Exegetic Approach,” *International Journal of Engineering and Natural Sciences (IJENS)*, vol. 2, no. 2, pp. 1–6, 2019.

[47] X. Zhao, X. Huang, T. Zhang, and Y. Wang, “Integrated speed/synchrophasing control of turboprop engine,” *The Aeronautical Journal*, vol. 122, no. 1253, pp. 1038–1050, Jul. 2018, doi: 10.1017/aer.2018.44.

[48] Y. Şöhret, Y. Lisans, T. Sivil, and H. A. Dalı, “Deneysel bir turbojet motorunun yanma veriminin motor emisyonlarıyla belirlenmesi.,” Anadolu University (Turkey), 2013.

[49] O. Turan, H. Aydın, T. H. Karakoc, and A. Midilli, “Some Exergetic Measures of a JT8D Turbofan Engine,” *Journal of Automation and Control Engineering*, vol. 2, no. 2, pp. 110–114, 2014, doi: 10.12720/joace.2.2.110-114.

[50] H. Aygun, “Thermodynamic, environmental and sustainability calculations of a conceptual turboshaft engine under several power settings,” *Energy*, vol. 245, p. 123251, Apr. 2022, doi: 10.1016/j.energy.2022.123251.

[51] Ö. Turan and H. Aydın, “Numerical calculation of energy and exergy flows of a turboshaft engine for power generation and helicopter applications,” *Energy*, vol. 115, pp. 914–923, Nov. 2016, doi: 10.1016/j.energy.2016.09.070.

[52] Anonim, “Beginnings (1898-1913)”.

[53] P. E. Fontenoy, “Aircraft Carriers An Illustrated History of Their Impact.”

[54] J. Hendrix, “The Rise and Fall of Carrier Aviation, Washington: Center for a New American Security,” 2015.

[55] P. Bhatt, “Locating the role for aircraft carriers in the indo-pacific,” 2017. [Online]. Available: www.capsindia.org

[56] D. Warren, R. Church, and R. Davey, “Discovering HMS Ark Royal,” *Hydro Int*, vol. 8, no. 7, pp. 26–29, 2004.

[57] K. Emin, “Çanakkale Savaşı’nda Bir Uçak Gemisi: Ark Royal (17 Şubat 1915-18 Mart 1915).,” *SAVSAD Savunma ve Savaş Araştırmaları Dergisi* , vol. 32, no. 2, pp. 305–344, 2022.

[58] C. Özgen, G. Üniversitesi, İ. ve İdari Bilimler Fakültesi, and S. Bilimi ve Kamu Yönetimi Bölümü, “Türk Deniz Kuvvetleri Açısından Uçak Gemisi Tedarikinin İncelenmesi,” *Savunma Bilimleri Dergisi The Journal of Defense Sciences Kasım*, vol. 17, no. 2, pp. 21–59, 2018.

[59] Liddell Hart and Basil Henry, “History of the second world war.,” 1970.

[60] G. Tıll, *Seapower: A guide for the twenty-first century*, Second., vol. 25. Routledge, 2013.

[61] W. Kong, D. Firat, and T. Behler, “Unconventional Take-off and Landing Methods,” 2019. [Online]. Available: http://cppcms.com/files/skijump,

[62] J.-L. Hernando and Rodrigo Martínez-Val, “Carrier suitability of land-based aircraft,” in *28th International congress of the aeronautical sciences (ICAS)*, 2012.

[63] C. H. Sodhi, “Electromagnetic Aircraft Launch System,” *Centre for air power studies (CAPS)*, May 2015, [Online]. Available: http://www.capsindia.org

[64] A. Singh Kahlon, T. Gupta, P. Dahiya, and S. K. Chaturvedi, “A Brief Review on Electromagnetic Aircraft Launch System,” *International Journal of Mechanical And Production Engineering*, vol. 5, no. 6, pp. 2320–2092, Jun. 2017, [Online]. Available: http://iraj.in

[65] “ELECTRO MAGNETIC AIRCRAFT LAUNCH SYSTEM Captain HPS Sodhi Senior Fellow, CAPS,” 2015. [Online]. Available: http://www.capsindia.org

[66] A. Doddi, “Vertical Take-off and Landing (VTOL).,” *American Institute of Aeronautics and Astronautics*, pp. 1–8, 2016.

[67] S. SUZUKI *et al.*, “Attitude Control of Quad Rotors QTW-UAV with Tilt Wing Mechanism,” *Journal of System Design and Dynamics*, vol. 4, no. 3, pp. 416–428, 2010, doi: 10.1299/jsdd.4.416.

[68] S. Zhang, “Review of Vertical Take-Off and Landing Aircraft,” in *2017 Second International Conference on Mechanical, Control and Computer Engineering (ICMCCE)*, IEEE, Dec. 2017, pp. 53–56. doi: 10.1109/ICMCCE.2017.9.

[69] Laskowitz I B., “Vertical Take-Off and Landing (VTOL) Aircraft. Annals of the New York Academy of Sciences,” Mar. 1963.

[70] A. Intwala and Y. Parikh, “A Review on Vertical Take Off and Landing (VTOL) Vehicles,” 2015. [Online]. Available: www.ijirae.com

[71] D. X. Qin, “Vertical take-off and landing aircraft: Categories, applications, and technology,” *Theoretical and Natural Science*, vol. 13, no. 1, pp. 126–129, Nov. 2023, doi: 10.54254/2753-8818/13/20240810.

[72] B. Liu *et al.*, “Design and Experimental Study of a Turbojet VTOL Aircraft with One-Dimensional Thrust Vectoring Nozzles,” *Aerospace*, vol. 9, no. 11, Nov. 2022, doi: 10.3390/aerospace9110678.

[73] P. Thompson, “The new Short Take Off and Vertical Landing (STOVL) F35 Joint Successful Trials New Joint Strike Fighter.” [Online]. Available: http://www.simlabs.arc.nasa.gov

[74] B. Brennan, “STOVL: The Best Future for Marine Air,” 2004.

[75] C. H. Brown, “Up, Up, and Away,” *Proceedings united states naval institute* , vol. 127, no. 8; ISSU 1182}, pp. 36–41, Aug. 2001.

[76] *F-35 Joint strike fighter (JSF) Program*. Congressional Research Service CRS Report RL 30563. 55. Washington, DC, 2014.

[77] H. B. Miller and U. S. Navy, “Shooting The Catapult,” vol. 59, no. 4, Apr. 1933.

[78] S. L. McFarland, *A concise history of the US Air Force*. Createspace Independent Publishing Platform, 1997.

[79] Campbell Douglas E. and Chant Stephen J., “Patent Diary Innovative Patents Improving the United States Navy”.

[80] Robert G. Skerrett., “Our Navy Has the Best Seaplane Catapult; New Invention of Captain Washington I. Chambers Makes It Possible to Launch Aircraft from a Warcarrier’s Deck at Sea,” Apr. 1916, Accessed: Mar. 20, 2024. [Online]. Available: https://www.nytimes.com/1916/04/02/archives/our-navy-has-the-best-seaplane-catapult-new-invention-of-captain.html

[81] Anonim, “From the Archives: May 27, 1954: Explosion rips carrier Bennington.”

[82] R. Patil, R. Sanap, S. Pawar, G. Shingane, and E. Scholar, “Electromagnetic Aircraft Launching System”, [Online]. Available: www.irjmets.com

[83] A. D. Awatade and M. V Kavade, “Feasibility study of electromagnetic aircraft launching system (EMALS),” 2018.

[84] S. Hartman, “Electromagnetic Aircraft Launching System: Do the Benefits Outweigh the Costs?,” 2010.

[85] Li Meiwu, Xue Fei, and Wei Jianzhong, “Carrier science and technology ,” 2007.

[86] S. Parwate, S. Daronde, and S. Telrandhe, “Electromagnetic Aircraft Launch System,” 2017. [Online]. Available: www.ijariie.com578

[87] “Electromagnetic Aircraft Launch System (EMALS)." General Atomics Electromagnetics,” Oct. 2009, Accessed: Mar. 21, 2024. [Online]. Available: http://atg.ga.com/EM/defense/emals/index.php

[88] C. Aviation Authority, “Take-off and landing performance.” Accessed: Mar. 20, 2024. [Online]. Available:

https://www.aviation.govt.nz/assets/publications/gaps/Take-off-and-landing-performance.pdf

[89] R. R. Narcizo, C. J. Alves, and M. Caetano, “The aircraft choice based on the aircraft take-off runway length requirement,” *Journal of Aerospace Technology and Management*, vol. 12, no. 1, pp. 1–11, 2020, doi: 10.5028/jatm.v12.1167.

[90] Anonim, “Gövde ve sistemleri,” *International Virtual Aviation Organisation (IVAO)*.

[91] Y. S. Chati and H. Balakrishnan, “Modeling of aircraft take-off weight using Gaussian processes,” *Journal of Air Transportation*, vol. 26, no. 2, pp. 70–79, 2018, doi: 10.2514/1.D0099.

[92] E. G. Tulapurkara, “Airplane design (Aerodynamic), Weight estimation,” pp. 1–5. Accessed: Apr. 22, 2024. [Online]. Available: https://nptel.ac.in/courses/101106035

[93] *Weight and Balance*. Accessed: Mar. 20, 2024. [Online]. Available: https://www.faa.gov/sites/faa.gov/files/12_phak_ch10.pdf

[94] “Structure of the Atmosphere.” Accessed: Mar. 20, 2024. [Online]. Available: https://www.faa.gov/sites/faa.gov/files/13_phak_ch11.pdf

[95] Z. Karaca, “Bir uçağın kalkış ve iniş aşamalarında etkili faktörler.” Accessed: Mar. 20, 2024. [Online]. Available: https://herkesicinhavacilik.com/2024/02/06/bir-ucagin-kalkis-ve-inis-asamalarinda-etkili-faktorler/

[96] “Density Altitude”, Accessed: Mar. 20, 2024. [Online]. Available: https://itd.idaho.gov/wp-content/uploads/2020/07/FAA_Density_Altitude_Aero.pdf

[97] R. Horonjeff, F. McKelvey, W. Sproule, and S. Young, *Planning and design of airports*. McGraw-Hill Companies, 2010.

[98] Y. Zhao and L. Sushama, “Aircraft Take-off Performance in a Changing Climate for Canadian Airports,” *Atmosphere (Basel)*, vol. 11, no. 4, p. 418, Apr. 2020, doi: 10.3390/atmos11040418.

[99] “Aerodynamic Factors.”

[100] E. D. Coffel, T. R. Thompson, and R. M. Horton, “The impacts of rising temperatures on aircraft take-off performance,” *Clim Change*, vol. 144, no. 2, pp. 381–388, Sep. 2017, doi: 10.1007/s10584-017-2018-9.

[101] E. Coffel and R. Horton, “Climate change and the impact of extreme temperatures on aviation,” *Weather, Climate, and Society*, vol. 7, no. 1, pp. 94–102, Jan. 2015, doi: 10.1175/WCAS-D-14-00026.1.

[102] J. Feng, “Analysis of aerodynamic characteristics of aircraft during take-off and landing,” *Applied and Computational Engineering*, vol. 28, no. 1, pp. 92–98, Dec. 2023, doi: 10.54254/2755-2721/28/20230133.

[103] E. Yavçin, “Uçma Hareketinin Biyomekaniğinin İncelenmesi ve Robotik Kuş Tasarımı.,” Sakarya Universitesi (Turkey), 2014.

[104] S. Delbecq, J. Fontane, N. Gourdain, H. Mugnier, T. Planès, and F. Simatos, “ISAE-SUPAERO Aviation and Climate: a literature review,” 2022, doi: 10.34849/a66a-vv58.

[105] D. G. Hull, *Fundamentals of airplane flight mechanics*. Springer, 2007.

[106] “Forces Acting on the Aircraft Aerodynamics of Flight,” *Federal aviation administration*, pp. 2–10.

[107] B. Kumari and N. Kumar, “Principle of Bernoulli’s Equation and its Applications.,” *NeuroQuantology*, vol. 20, no. 10, pp. 5078–5084, 2022, doi: 10.14704/NQ.2022.20.10.NQ55485.

[108] K. Weltner, “Misinterpretations of Bernoulli’s Law,” 2015. [Online]. Available: https://www.researchgate.net/publication/303974495

[109] H. Babinsky, “How do wings work?,” 2003. [Online]. Available: www.iop.org/journals/physed

[110] T. Benson, “Four Forces on an Airplane,” National Aeronautics and Space Administration (NASA). Accessed: Mar. 02, 2024. [Online]. Available: https://www.grc.nasa.gov/www/k-12/VirtualAero/BottleRocket/airplane/forces.html

[111] S. S. Chauhan and J. R. R. A. Martins, “Tilt-Wing eVTOL Take-off Trajectory Optimization,” *J Aircr*, vol. 57, no. 1, pp. 93–112, Jan. 2020, doi: 10.2514/1.C035476.

[112] I. Sadrehaghighi, “Aerodynamic Basics CFD Open Series,” 2023, doi: 10.13140/RG.2.2.32859.72488/14.

[113] D. Anderson and S. Eberhardt, “How Airplanes Fly: A Physical Description of Lift.”

[114] “Steam powered catapults,” vol. 14310, Global Security, pp. 1–4.

[115] “McDonnell Douglas F/A-18A Legacy Hornet,” *Property of The Hickory Aviation Museum (HAM)* , pp. 1–2.